Poster abstracts

1. Calcium phosphate from excipients to bioresorbable implants: historical milestones, processing gaps, and prospects for programmable drug delivery

A. Indurkar[1,2], G. Ernestsons[3], G. E. Ernestsons[3], J. Rumkovskis[3], J. Locs[1,2]

[1]*Institute of Biomaterials and Bioengineering, Faculty of Natural Sciences and Technology, Riga Technical University, Paula Valdena Street 3, k-1, Riga, LV-1048, Latvia*

[2]*Baltic Biomaterials Centre of Excellence, Headquarters at Riga Technical University, Riga, Latvia*

[3]*SIA UNISO, Jaunatnes 24 – 40, Valdlauci, Kekava, LV-1076, Latvia*

INTRODUCTION: Calcium phosphates (CaP) have been central to medicine for over two centuries, progressing from early chemical observations to established pharmaceutical excipients and widely used biomateial. Yet advances in CaP chemistry, pharmaceutical formulation, biomaterials science, and drug-delivery research have largely evolved independently, limiting the coordinated use of knowledge across these fields. Integrating insights from excipient science, phase chemistry, and biomineralization is increasingly important, as CaP phase composition, dissolution behaviour, and microstructural control underpin both drug-delivery performance and implant functionality. Recent developments in low-temperature processing provide an opportunity to unify these perspectives. In particular, cold sintering offers a route to produce consolidated, bioresorbable CaP constructs while preserving heat-sensitive therapeutics. This work consolidates key milestones across these disciplines and highlights the potential of cold sintering as an enabling strategy for long-term CaP-based drug-delivery implants.

METHODS: A structured literature survey was conducted across domains including: i) CaP physicochemical properties, ii) early biomedical and bone-biology studies, iii) mineralization pathways, iv) CaP as adsorbent, adjuvant, and carrier, v) pharmaceutical formulation and tableting, and vi) CaP coating and processing technologies. Information on study period, material class, processing method, and functional role was extracted and organized into thematic timelines. Cross-mapping was used to relate phase composition and processing conditions to drug-material interactions.

RESULTS: Across the literature, CaP behaviour in drug delivery is consistently governed by a structure-property relationship. Pharmaceutical science studies shows that particle size, surface area, porosity, and hydration state of CaP strongly influences drug adsorption, loading efficiency, stability and release[1]. CaP chemistry further clarifies how the solubility equilibria and substitution (ions or organic) mediated phase transformations, control dissolution and conversion-driven release under physiological conditions[2]. Biological evidence identifies amorphous calcium phosphate (ACP) as a reactive, primary precursor phase well suited for drug incorporation[3]. Recent work demonstrates that cold sintering ACP (≤150°C or room temperature), producing mechanically stable, bioresorbable constructs while preserving heat-sensitive therapeutics[4]. Collectively, these insights drawn from chemistry, pharmaceutical science, and biomaterials engineering provides an essential foundation for the rational development of CaP drug-delivery systems using cold sintering.

DISCUSSION & CONCLUSIONS: Cold sintering provides a low-temperature route for integrating amorphous and nanoscale CaP into robust, bioresorbable implants while preserving drug integrity, addressing key limitations of conventional processing. The convergence of cross-disciplinary knowledge enables the development of CaP constructs with tuneable, long-term release profiles, supporting their advancement as next-generation drug-delivery implants.

ACKNOWLEDGEMENTS: This research is funded by the European Union – Recovery and Resilience Facility (RRF), project "Synthesis of Nanoceramics and Nanoceramic Composites for Medical Applications", Project No. 5.1.1.2.i.0/4/25/A/CFLA/004. The authors acknowledge the access to the infrastructure and expertise of the BBCE – Baltic Biomaterials Centre of Excellence (European Union's Horizon 2020 research and innovation programme under the grant agreement No. 857287).

REFERENCES:

[1]Schmidt and Herzog. *Pharm World Sci.* (1993)

[2]Uskoković and Desai. *J Biomed Mater Res* (2013)

[3]Lotsari et., al. *Nature communication*s (2018)

[4]Galotta et., al. *Nanomaterials* (2024)

2. Periodic Surface Structures Suppress *E. coli* Biofilm Formation by Impairing Bacterial Surface Sensing

A, HANSSON[1,2], L. PAPA[3,4], C. GAUDIUSO, F[3]. P. MEZZAPESA[3], A. VOLPE[3,4], M. BERGLIN[2], A. ANCONA[3,4,5], A. LUNDGREN[1]

[1]Department of Chemistry and Molecular Biology, University of Gothenburg, Gothenburg, Sweden, [2]Department of Chemistry and Materials, RISE Research Institutes of Sweden, Boraås, [3]University of Bari and Polytechnic University of Bari, Italy, CH, [4] National Research Council (CNR), Institute for Photonics and Nanotechnologies (IFN), Bari, Italy, University West, Trollhättan, Sweden, [5]

INTRODUCTION: Laser-induced micro- and nanostructured surfaces are increasingly used to prevent biofilm formation on materials[1], yet to determine the underlying mechanisms are challenging since conventional methods poorly resolve critical events in the early biofilm formation process. Here, we combine single-cell live microscopy with microfluidics[2] to characterize bacterial interactions with laser-fabricated nanostructured surfaces.

METHODS: Nanostructured glass was integrated into a four-channel microfluidics chamber and functionalized with covalently attached α-mannose to promote *E. coli* adhesion (Figure 1, upper). Fluorescently labeled (green) wild-type *E. coli* strains and isogenic *E. coli* overexpressing Type 1 fimbriae (red) were allowed to bind to and grow into biofilm under controlled flow and temperature conditions.

RESULTS: Biofilm formation on nanostructured surfaces was significantly reduced and displayed a less compact organization compared to unstructured surfaces. Single-call analysis revealed that *E. coli* on nanostructured surfaces experienced less Rcs membrane stress than on flat surfaces. In competition experiments where WT and fimbriae overexpressing E. coli were injected together, overfimbriaeted strains outcompeted wild-type bacteria on unstructured surfaces. In contrast, on nanostructured surfaces, WT bacteria formed microcolonies while overfimbriated strains adhered but failed to progress beyond initial attachment (Figure 1, lower).

DISCUSSION & CONCLUSIONS: These findings suggest that early biofilm formation in *E. coli* depends on mechanosensing-induced stress which is not triggered by adhesion alone. Nanostructures impair surface recognition by inducing lower activation of the Rcs mechanosensing system then do flat surfaces, likely due to smaller contact area between the bacterial outer membrane and the underlying surface. This prevents progression from adhesion to biofilm formation.

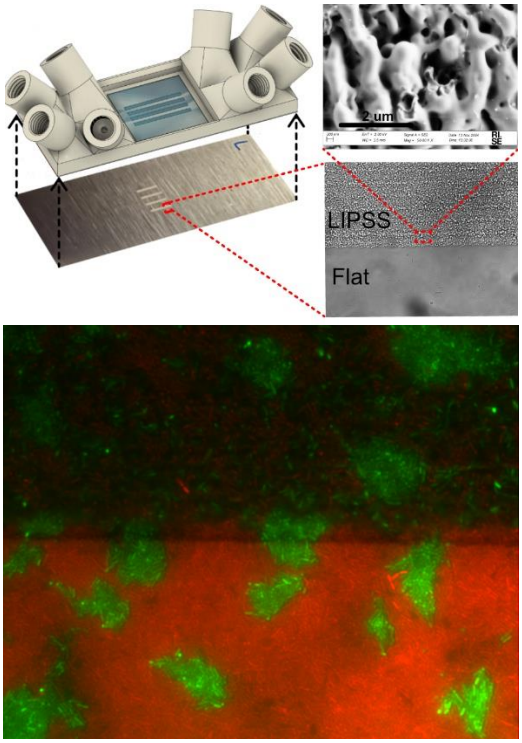

Figure 1. Schematic representation of the microfluidics system and nanostructures (upper). Fluorescence microscopy image of overnight biofilm (lower).

ACKNOWLEDGEMENTS:
SSF (grant no. FID22-0053) and RISE are acknowledged for their funding.

REFERENCES:

(1)Papa, L., Mezzapesa, F. P., Volpe, A., Gaudiuso, C. & Ancona, A. Bacterial adhesion eradication and biofilm inhibition through laser surface texturing. *Appl. Mater. Today* **45**, 102801 (2025).

(2)Hansson, A. *et al.* Preventing E. coli Biofilm Formation with Antimicrobial Peptide-Functionalized Surface Coatings: Recognizing the Dependence on the Bacterial Binding Mode Using Live-Cell Microscopy. *ACS Appl. Mater. Interfaces* **16**, 6799–6812 (2024).

3. Development of mycelium-based aerogels for biomedical applications

G. Pepi[1], E. R. K. B. Wijayarathna[1], M. Persson[2], A. Zamani[1]

[1] *Swedish Centre for Resource Recovery, Faculty of Textiles, Engineering and business University of Borås, Borås, SE-501 90, Sweden*

[2] *Department of Textile Technology, Faculty of Textiles, Engineering and business, University of Borås, SE-501 90 Borås, Sweden*

INTRODUCTION: Sustainable bio-based materials are essential for addressing the environmental challenges associated with petroleum-derived products. Filamentous fungi, often described as nature's recyclers, possess a remarkable ability to decompose organic waste and return valuable nutrients to the environment. During growth, filamentous fungi form microfibrillar networks known as mycelium. Mycelium-based materials have attracted increasing attention across diverse application areas due to their renewability, low environmental impact, and tunable properties. Furthermore, the fungal cell wall contains biopolymers such as chitin and chitosan, which represent promising building blocks for the development of circular and sustainable materials, particularly in biomedical applications. This research explores the potential of food-waste-derived mycelium materials for use in biomedical applications.

METHODS: Two fungal species belonging to the Ascomycota and Mucoromycota phyla were cultivated on food waste (bread residues) in bubble column bioreactors, and the process was subsequently scaled up. The harvested biomass was subjected to alkaline treatment to isolate fungal cell wall materials containing chitin–glucan (Ascomycota) and chitin–chitosan (Mucoromycota), respectively. Aerogels were fabricated from the extracted cell wall materials via acid-assisted gelation, followed by freezing and freeze-drying. The resulting aerogels were evaluated for cytotoxicity toward fibroblasts at different concentrations using a leachate-based MTT assay. Antibacterial activity was assessed against both Gram-positive and Gram-negative bacteria.

RESULTS: Both fungal strains were successfully cultivated under submerged conditions, resulting in well-dispersed fungal biomass. Alkali-insoluble fractions corresponding to fungal cell wall materials were efficiently recovered and subsequently used for aerogel fabrication. Cytotoxicity assessment revealed greater than 80% cell viability relative to the control when fibroblasts were exposed to aerogel leachates at concentrations up to 2500 µg/mL for 48 h. Furthermore, the addition of aerogels at this concentration to Müller–Hinton broth significantly inhibited the growth of Escherichia coli (Gram-negative) and Bacillus megaterium (Gram-positive).

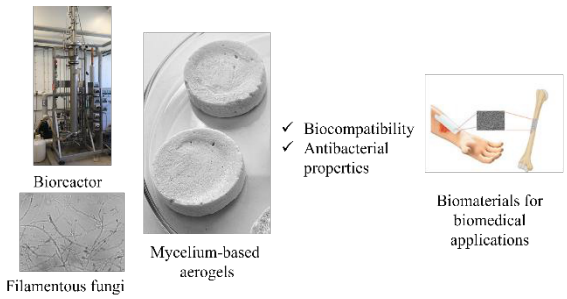

Figure 1: Food waste derived mycelium-based aerogels for biomedical applications

DISCUSSION & CONCLUSIONS: Aerogels were successfully fabricated from fungal cell wall materials derived from food-waste-grown fungal biomass. The resulting aerogels exhibited good biocompatibility and antibacterial activity, highlighting their potential as renewable and circular biomaterials for biomedical applications.

ACKNOWLEDGEMENTS: This work was financially supported by Vinnova and the Carl Trygger Foundation.

REFERENCES:

1. Svensson, S., et al., Valorization of Bread Waste to Fungal-Based Products for Medical Textile and Food Applications. ACS Sustainable Resource Management, 2024. 1.

4. OsteoMin: Cellular Automaton for Osteogenic Differentiation

A.A. Demir[1], T. Combriat[1,2], C.A. Heyward[3], A. Carlier[4], H. Tiainen[5], D.K. Dysthe[1,2]

[1] NJORD Centre, University of Oslo, NO, [2] Hybrid Technology Hub, University of Oslo, NO [3] Clinical Oral Research Laboratory, University of Oslo, NO, [4] MERLN Institute, Maastricht University, NL, [5] Department of Biomaterials, University of Oslo, NO

INTRODUCTION:

Standard in vitro osteogenic assays report alkaline phosphatase activity, collagen deposition, and mineralization as population-averaged endpoints, limiting the spatial and temporal resolution of differentiation. As a result, different initial conditions / perturbations can produce the same experimental outcomes, limiting interpretability across differentiation timeline. To address this, we integrate a bone biomineralization model[I] with a cellular automaton[II] to test whether distinct experimental conditions lead to similar outcomes.

METHODS:

We developed OsteoMin, a two-dimensional cellular automaton describing cell migration, proliferation, differentiation, and apoptosis. Cellular state dynamics are coupled to spatiotemporal lattice fields representing alkaline phosphatase activity (ALP), collagen I deposition (Col IF), and hydroxyapatite (HAp) deposition. Main rules were adapted from existing literature data, while kinetic parameters were calibrated against experimental endpoint measurements to resolve dynamics.

MC3T3-E1 cells were induced toward osteogenesis using ascorbic acid and β-glycerophosphate, with varying concentrations of dexamethasone (Dex) and menaquinone-4 (MK-4) to probe their reciprocal effects on differentiation. Experimental endpoints included ALP activity (day 10), collagen immuno-fluorescence (day 14) in Fig. 1, and Alizarin Red S (day 28) across eight conditions.

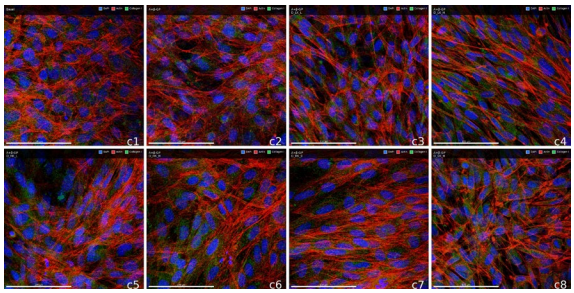

Fig. 1: Collagen I immunofluorescence (day14) overlays under Dex and MK-4 perturbations.

RESULTS:

OsteoMin reflects in vitro osteogenic assay responses by resolving cell-state trajectories (pre-osteoblast, osteoblast, apoptotic) over the differentiation timeline. The model separates the respective contributions of pre-osteoblasts and osteoblasts to alkaline phosphatase activity and collagen deposition, alongside showing the changes in mineralization patterns from day 14 to day 28, including nodule formation (Fig. 2).

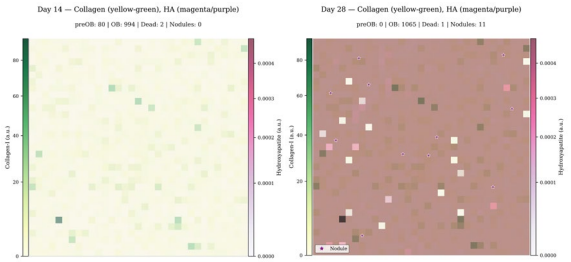

Fig. 2: Collagen matrix and mineralization patterns over 1 mm² area from day 14 to 28.

Results show multiple trajectories can converge on similar measurements, indicating limited coupling between early differentiation, matrix accumulation, and mineralization.

DISCUSSION & CONCLUSIONS:

These results highlight that variations in initial conditions and differentiation dynamics can still produce similar endpoints, which makes interpretation challenging when conclusions are based only on end-point measurements without considering details of spatiotemporal context.

ACKNOWLEDGEMENTS:

This work was funded by the EU Horizon 2020 programme (Marie Skłodowska-Curie grant No. 945371). A.A.D. acknowledges UiO:Life Science support for a research visit at MERLN Institute, Maastricht University, NL.

REFERENCES:

I. Poorhemati & Komarova, Sci Rep (2024) 14:81472
II. Van Scoy et al., Math Biosci (2017) 286:58–64

5. Gold Nanorod–Mesoporous Titania Coatings for Antimicrobial Implant Surfaces

A. Ramdén, M. Hulander, M. Andersson

Department of Chemistry and Chemical Engineering, Chalmers University of Technology, Gothenburg, Swe

INTRODUCTION: Biomaterial associated infections (BAIs) remain a major clinical challenge, largely driven by biofilm formation. Biofilms are especially hard to treat; thus it is desirable to prevent biofilm formation. Solid supported gold nanorods exhibits photothermal heating under near-IR light within the first biological window and is a promising alternative to antibiotics for preventing BAIs[1]. However, the antibacterial effect has been shown to be dependent on the substrate and is less effective on titanium surfaces, which is a common implant material. Here, we propose the use of a thin film coating of mesoporous-titania (MP-TiO_2) as an insulating layer between the AuNRs and the titanium surface to better retain the photothermal heating under near-IR (NIR) irradiation. MP-TiO_2 also represents a promising material for local drug delivery[2], thus it offers a compelling combined system that integrates photothermal heating with drug mediated effects to prevent BAIs.

METHODS: MP-TiO_2 thin films were formed by spin coating onto Si-wafers, glass slides and Ti-discs using evaporation induced self-assembly. The MP-TiO_2 films were subsequently functionalized with AuNRs through electrostatic interactions. UV-vis spectroscopy and thermal imaging was used to evaluate the photothermal heating effect of the system. The surfaces were also analysed with Scanning Electron Microscopy (SEM).

RESULTS: Figure 1A shows an SEM image of a AuNR-MP-TiO_2 surface, using a Si-wafer as substrate. Figure 1B shows a thermal image of a surface AuNR-MP-TiO_2 surface (top) and a MP-TiO_2 surface (bottom) directly after irradiation with an 808 nm laser for 30 s, using glass as the substrate. Furthermore, UV-vis measurements on the MP-TiO_2 surface shows a longitudinal plasmonic peak around 800 nm, which aligns well with the wavelength of the 808 nm laser used.

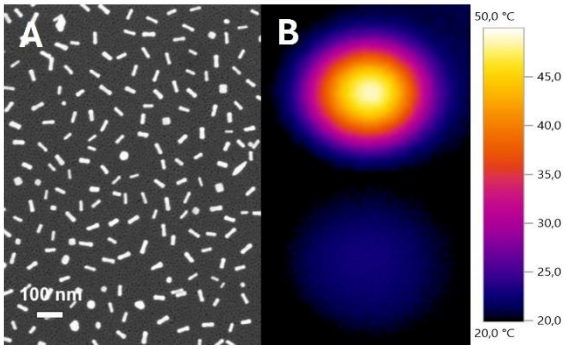

Fig. 1: A. SEM Micrograph of AuNRs functionalized onto a MP-TiO2 thin film. B. Thermal image of AuNR-MP-TiO_2 (top) and MP-TiO_2 (bottom) surfaces directly after irradiation with NIR laser (808 nm) for 30 s.

DISCUSSION & CONCLUSIONS: SEM results demonstrate that AuNRs have successfully been functionalized onto the MP-TiO_2 films, and that the pores of the MP-TiO_2 remained accessible after functionalization. The rods are evenly distributed and are mainly laying well separated, which is important for keeping the desired plasmonic behaviour of the rod. The plasmonic properties were characterized using both UV-Vis spectroscopy and thermal imaging, which together indicate that the AuNR covered surfaces exhibit a surface plasmon resonance aligned with the 808 nm laser wavelength. Future investigations will assess if this system is affective also on Ti-substrates and evaluate its antimicrobial efficacy.

REFERENCES:

(1) Uusitalo, M.; Eriksson, G.; Hulander, M.; Andersson, M. Gold Nanorods as Photothermal Antibacterial Materials. *Acs Appl Nano Mater* **2025**, *8* (7), 3661-3670. DOI: 10.1021/acsanm.5c00324.

(2) Harmankaya, N.; Karlsson, J.; Palmquist, A.; Halvarsson, M.; Igawa, K.; Andersson, M.; Tengvall, P. Raloxifene and alendronate containing thin mesoporous titanium oxide films improve implant fixation to bone. *Acta Biomater* **2013**, *9* (6), 7064-7073. DOI: 10.1016/j.actbio.2013.02.040.

6. Simulated Bioactive Glass Solution (SBGS): A Glass-free, Composition-Controlled Platform for Screening Therapeutic Ions

A. Shiralizadeh Dezfuli[1], M. Bayandori[1], M. Jafari Dargahlou[1], A. Nygård[1], G. Kohoolat[1], P. Uppstu[1]

[1] *Laboratory of Molecular Science and Engineering, Centre of Excellence in Materials-driven Solutions for Combatting Antimicrobial Resistance (MADNESS), Faculty of Science and Engineering, Åbo Akademi University, Turku, Finland*

INTRODUCTION: Doping and substituting bioactive glasses (BGs) with therapeutic ions is widely used to steer biological function. However, mechanistic ion screening typically relies on repeatedly fabricating and characterizing multiple doped-glass variants, which is time- and cost-intensive and often confounded by changes in glass structure, surface area, dissolution kinetics and solution pH. Here, we introduce Simulated Bioactive Glass Solution (SBGS) as a glass-free, composition-controlled platform that reproduces the measured ionic dissolution signature of a reference BG (first demonstrated using 45S5) in a defined biological medium, enabling rapid and interpretable screening of candidate ions without synthesizing new glasses (Fig. 1) [1–3].

METHODS: In the planned study, we will (i) quantify the dissolution products of 45S5 in a selected culture medium under standardized extraction conditions using ICP-OES and define an ion-increment vector (ΔNa, ΔCa, ΔSi, ΔP) relative to baseline medium; (ii) formulate SBGS using analytical-grade salts to match this increment profile, and verify chemical equivalence (ion concentrations, pH, osmolality) and solution stability; and (iii) benchmark SBGS against conventional 45S5 extracts in vitro. Biological readouts will include ISO-aligned cytocompatibility assays, osteogenic markers in hMSCs (e.g., ALP activity and osteogenic gene expression), and an angiogenesis module (VEGF-A secretion and HUVEC tube formation). SBGS will then be used to screen a showcase therapeutic ion (e.g., Cu^{2+}) across a defined concentration range on top of the SBGS baseline, with matched controls (ion-only, SBGS-only, extract).

RESULTS: We anticipate that SBGS will closely reproduce the ionic composition of 45S5 extracts (within predefined acceptance limits for each ion) while maintaining matched pH and osmolality over the exposure window. We further expect SBGS to recapitulate key biological outcomes observed for BG extracts in cytocompatibility and functional assays, while enabling clean dose-response and synergy mapping for added therapeutic ions under a constant background chemistry.

Fig. 1: schematic illustrating of SBGS platform

DISCUSSION & CONCLUSIONS: SBGS is designed as a front-end screening platform to accelerate therapeutic-ion discovery and improve interpretability by decoupling ion biology from glass fabrication variables. By replacing repeated doped-glass synthesis with a defined and verifiable solution recipe anchored to a reference BG (45S5), SBGS is expected to reduce experimental time and cost while increasing reproducibility. In follow-up studies, the SBGS framework will be extended to additional BG reference compositions to build a transferable library linking ionic profiles to biological outcomes.

ACKNOWLEDGEMENTS: This study is part of the activities of the Åbo Akademi University Foundation (SÅA)-funded Centre of Excellence in Research "*Materials-driven Solutions for Combatting Antimicrobial Resistance* (MADNESS)".

REFERENCES:

1 L. L. Hench, *J. Mater. Sci. Mater. Med.*, 2006, **17**, 967–978.

2 A. Hoppe, N. S. Güldal and A. R. Boccaccini, *Biomaterials*, 2011, **32**, 2757–2774.

3 P. Valerio, M. M. Pereira, A. M. Goes and M. F. Leite, *Biomaterials*, 2004, **25**, 2941–2948.

7. Tissue Informed Design of Bioinks for Urethral Tissue Engineering

Amitha Banu Shajahan[1], Stelios Alexandris[2], Nele Pien[3], Ruiqi Jing[4], Jesper de Claville Christiansen[2], Kim Lambertsen Larsen[4], Sandra Van Vlierberghe[3], Petra de Graaf[5], Cristian Pablo Pennisi[1]

[1]Department of Health Science and Technology, Aalborg University, Denmark; [2]Department of Materials and Production, Aalborg University, Denmark; [3]Department of Organic and Macromolecular Chemistry, Ghent University, Belgium; [4]Department of Chemistry and Bioscience, Aalborg University, Denmark; [5]Regenerative Medicine and Stem Cells, University Medical Center Utrecht, Netherlands

INTRODUCTION: Tissue engineering approaches for urethral reconstruction remain challenging due to the tissue's complex structure and mechanical properties. Bioprinting offers a promising strategy for engineering functional urethral tissue; however, current bioinks are limited by their inability to replicate native tissue structure. To address this, a tissue-targeted bioink design strategy is proposed, involving biomechanical and histological characterisation of healthy tissue to provide relevant benchmarks for developing hydrogel bioinks tailored for bioprinting urethral constructs (Fig.1).

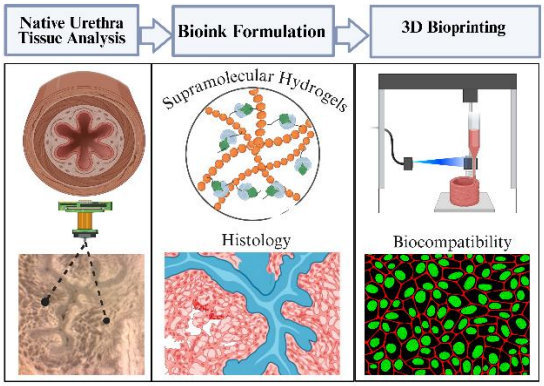

Fig 1: Tissue driven design of bioinks for urethral repair.

METHODS: Healthy rabbit urethral tissues were analysed in both cross-sectional and longitudinal orientations. Mechanical properties were assessed on 100 µm-thick sections using nanoindentation-based testing to map viscoelastic behaviour at the microscale. Histological evaluation was performed on 8 µm sections using haematoxylin and eosin for tissue morphology, fast green for collagen, and orcein for elastin distribution. To modulate mechanical performance, bioinks were prepared from dextran- and gelatine-based hydrogels, including hybrid dextran–gelatine formulations incorporating host–guest supramolecular moieties and thiol–ene crosslinking sites. Gelation kinetics and viscoelastic properties were assessed by UV-assisted photorheology. Cytocompatibility was examined using human dermal fibroblasts through elution and direct-contact assays, LDH cytotoxicity, cell proliferation, and live/dead staining.

RESULTS: Native urethral tissue exhibited heterogeneous Young's moduli ranging from approximately 2.8 to 10 kPa, reflecting spatial variability. Frequency sweep measurements indicated a viscoelastic response with a predominantly elastic contribution across the tested frequency range. Hydrogel stiffness and gelation kinetics were tuneable through polymer concentration, molecular weight, and degree of substitution. Dextran functionalised with β-cyclodextrin and complementary guest groups, combined with bifunctional gelatine derivatives, produced mechanically stable and reproducible hydrogels. These hydrogels exhibited shear-thinning behaviour suitable for extrusion-based 3D printing. Cytocompatibility tests showed low cytotoxicity, sustained cell proliferation, and high viability within the optimised formulations. Based on urethral structure and mechanics, a limited number of bioink candidates were selected for *in vivo* evaluation in a rabbit model.

DISCUSSION & CONCLUSIONS: This study establishes a tissue-informed design framework for hydrogel bioinks aimed to replicate native urethral mechanical and structural features. The developed supramolecular systems demonstrate tuneable mechanical properties, printability, and cytocompatibility, supporting their potential use in fabricating tubular scaffolds for preclinical studies in urethral tissue engineering.

ACKNOWLEDGEMENTS: This research was funded by the European Union's Horizon Europe programme (STRONG-UR, grant agreement No 101191695). Views and opinions expressed are however those of the author(s) only and do not necessarily reflect those of the European Union or HaDEA. Neither the European Union nor the granting authority can be held responsible for them.

8. Combined Chemical and Mechanical Debridement Enhances Salivary Protein Removal from Titanium While Maintaining Biological Properties

Angela De Lauretis[1,2], Marco Santacroce[1], Qiang Wang[1], Manuel Ramirez Garrastacho[3], Qianli Ma[1], Ståle Petter Lyngstadaas[1], Jan Eirik Ellingsen[4], Dirk Linke[3], Håvard Jostein Haugen[1]

[1] *Department of Biomaterials, Institute of Clinical Dentistry, Faculty of Dentistry, University of Oslo Norway*

[2] *Corticalis AS, Oslo Science Park, Gaustadalléen 21, 0349, Oslo, Norway*

[3] *Department of Biosciences, University of Oslo, 0316, Oslo, Norway*

[4] *Department of Prosthetics and Oral Function, Institute of Clinical Dentistry, University of Oslo, 0455, Oslo, Norway*

INTRODUCTION: Effective decontamination of dental implants is essential for managing peri-implant diseases, yet its impact on the salivary pellicle and cell response remains unclear. As the pellicle mediates bacterial and host cell interactions, investigating how decontamination alters its composition is key to understanding the effects on biological outcomes. Accordingly, we examined how a Poloxamer 407 (P407) hydrogel, a P407 + hydrogen peroxide (H_2O_2) hydrogel, a titanium brush, and their combinations influence the adsorbed salivary proteins and cell adhesion on OsseoSpeed®-like titanium surfaces.

METHODS: Surfaces with salivary proteins were treated with different decontamination methods and re-exposed to saliva. Protein quantity was measured using the BCA assay, while the proteomic composition and molecular functions of the adsorbed proteins were determined by liquid chromatography-mass spectrometry and gene ontology analysis. Human bone marrow mesenchymal stem cell (hBMMSC) adhesion was assessed on the surfaces, and cytotoxicity was evaluated using an LDH assay. Protein-coated and protein-free surfaces served as controls

RESULTS: Although protein levels were consistent across groups after either decontamination or recontamination, each treatment produced a different proteomic profile. Mechanical decontamination, alone or combined with chemicals, enhanced protein removal efficiency. Combined treatments yielded reduced protein diversity following recontamination and enriched adhesion-related proteins. None of the treatments compromised hBMMSCs adhesion nor made the surfaces cytotoxic.

DISCUSSION & CONCLUSIONS: Decontamination methods selectively modify the proteomic profile. Combined chemical and mechanical decontamination enhances the removal of salivary proteins and limits their re-adsorption while preserving cytocompatibility, supporting their relevance to peri-implant health.

ACKNOWLEDGEMENTS: This work was supported by The Research Council of Norway (grant numbers 331752, 332148, 359679) and (grant number 346292 to A.D.L.). Mass spectrometry-based proteomic analyses were performed by the Proteomics Core Facility, Department of Biosciences, University of Oslo. This facility is a member of the National Network of Advanced Proteomics Infrastructure (NAPI), which is funded by the Research Council of Norway INFRASTRUKTUR-program (project number: 295910).

CONFLICT OF INTEREST STATEMENT: A.D.L., J.E.E. and S.P.L. are the inventors of the technology behind PeriBrush™ (patent number: EP 2142036; patent application "MEDICAL IMPLANT CLEANING OR DEBRIDEMENT TOOL") assigned to Corticalis AS. A.D.L. and S.P.L. are the inventors of the technology behind MucoPrep™ (patent application "A NOVEL CLEANING AND/OR DEBRIDEMENT COMPOSITION") assigned to Corticalis AS. S.P.L. and H.J.H. are the inventors of the technology behind PeriPrep™ (patent number WO2011073194) assigned to Corticalis AS. A.D.L., J.E.E., S.P.L., and H.J.H. are shareholders in Corticalis AS. A.D.L. is an Industrial PhD Candidate at the University of Oslo in collaboration with Corticalis AS.

9. Mesoporous bioactive glass as a platform for plant-derived active compound delivery

A.M. Vaisla[1], O. Demir[1,2], D. Loca[1,2]

[1] *Institute of Biomaterials and Bioengineering, Faculty of Natural Sciences and Technology, Riga Technical University, Riga, Latvia,*

[2] *Baltic Biomaterials Centre of Excellence, Headquarters at Riga Technical University, Riga, Latvia*

INTRODUCTION: Invasive surgical procedures for bone fixation and replacement carry a high risk of postoperative infection. Therefore, there is an increasing demand for biomaterials that simultaneously promote bone regeneration and enable localized drug delivery. Mesoporous bioactive glass (MBG) is a promising substitute for the inorganic phase of bone tissue, offering a highly porous structure and a large specific surface area for controlled, localized drug delivery [1]. Furthermore, plant-derived bioactive agents, such as rosmarinic acid (RosAc), possess anti-inflammatory, antioxidant, and anticancer properties, and show promising potential as alternative antimicrobial agents to combat growing antibiotic resistance [2]. Accordingly, this study aimed to prepare mesoporous bioactive glass/rosmarinic acid (MBG/RosAc) composite materials and evaluate their potential for controlled drug delivery.

METHODS: 58S MBG (58 mol% SiO_2, 33 mol% CaO, 9 mol% P_2O_5) was prepared by *sol-gel* synthesis method, using tetraethyl orthosilicate, triethyl phosphate, and calcium nitrate tetrahydrate. The mouse preosteoblast MC3T3-E1 cell line was used to evaluate the effects of sintered MBG on cell viability and to determine the IC_{50} of RosAc. MBG/RosAc composite materials were prepared by adsorbing RosAc onto MBG particles. UV–Vis spectroscopy at 326 nm was used to analyse RosAc loading efficiency and release kinetics. Physicochemical properties of MBG and MBG/RosAc were assessed by X-ray diffraction, Fourier transform infrared spectroscopy and scanning transmission electron microscopy (STEM).

RESULTS: Amorphous 58S MBG were obtained using *sol-gel* synthesis method. Prepared MBGs were not cytotoxic below 1 mg MBG/mL, where the highest cell viability was observed with 0.5 mg MBG/mL sample concentration. The incorporation efficiency of RosAc increased with the active compound content used for composite preparation. The highest incorporation efficiency exceeded 97%, while the RosAc content in the composite material reached 13.41±0.03%. Adsorption of RosAc onto MBG particles was found to affect their morphology and tendency to agglomerate (Fig 1). In terms of release behaviour, an initial burst release of RosAc was observed within the first 24 hours, whereas the cumulative release reached 7.9±0.4% after 21 weeks.

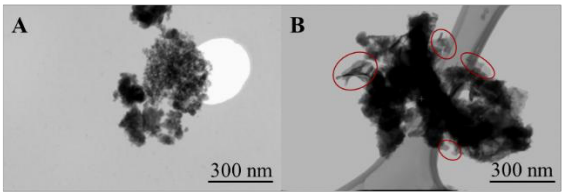

Fig. 1: STEM images of a) pure 58S MBG, b) 58S MBG/RosAc composite, changes in morphology marked with red circles.

DISCUSSION & CONCLUSIONS: Sintered MBGs were highly biocompatible with MC3T3-E1 cells, maintaining > 70% viability and promoting cell proliferation at day 3. High RosAc loading was achieved by adsorption, resulting in an initial burst release followed by sustained release over 21 weeks. Released RosAc concentrations remained below the IC_{50} for MC3T3-E1 cells, indicating no cytotoxicity toward preosteoblasts. Overall, MBG/RosAc composites represent a promising approach for localized and sustained drug delivery in bone tissue regeneration, with the potential to address infection-related challenges.

ACKNOWLEDGEMENTS: This work was supported by the European Union Cohesion Policy Programme 2021–2027 under Specific Objective 1.1.1 “Strengthening research and innovation capacity and the introduction of advanced technologies in the overall R&I system,” Measure 1.1.1.3 “Applied Research,” Project No. 1.1.1.3./1./24/A/044 (RESCUE) and infrastructure from H2020 Grant No. 857287 (BBCE).

REFERENCES: [1]O. Demir-Oguz et al. (2022) *Bioactive Materials*, **19**: 217-236. [2]H. Guan et al. (2021) *Molecules*, **27**(10): 3292.

10. 3D Cell Models of Oral Inflammation

A.E. Agger[1,2], J.Hlinkova[1,2], J.E. Reseland[1,2], A. Samara[1,2],

[1] Department of Biomaterials, Institute of Clinical Dentistry, University of Oslo, [2] FUTURE, Center for Functional Tissue Reconstruction, University of Oslo, Oslo, Norway

INTRODUCTION: This study continues from our previous work that showed that administration of inflammatory agents such as lipopolysaccharides (LPS) and interleukin-1 beta (IL-1β) induced signals that mimic chronic inflammation in human gingival fibroblasts (Agger et al., 2024) in 2D culture conditions. Now we aimed to establish and evaluate a more physiologically relevant environment in a 3D cell model with and without the introduction of hypoxia. This approach can provide a comprehensive model to investigate the interplay between inflammation and hypoxia in human tissues.

METHODS: Human gingival fibroblast cells (HGFs) cells were added to ClinoReactors on day -1 and allowed to form into spheroids for 24 h under normoxic or hypoxic conditions. At day 0, inflammatory agents were added. Media was collected at day 0, 2, 3, 7, 10 and 14 and spheroids were harvested at day 2 and 14.

RESULTS: We showed that hypoxia and inflammation, both individually and in combination, had a significant multifaceted impact on 3D fibroblast spheroids. Specifically, the combination led to the formation of smaller spheroids, alongside a marked decrease in the expression levels of selected ECM and cytoskeletal proteins, without drastic effects on cell viability. The evaluation of histological sections demonstrated that the combination of hypoxia and inflammation impacts the formation of a rim versus core area of spheroids (Fig 2). The observed increase in cytokines and chemokines associated with immune responses, such as IL-6, IL-1β, IL-1α, TNFα, and GM-CSF indicates the enhanced inflammatory signaling under the combined conditions. Aligning with previous studies on in vitro inflammatory conditions as well as in vivo inflammatory conditions, increased secretion of the angiogenic factor VEGFα, known to enhance tissue repair and neovascularization, was activated in response to inflammation.

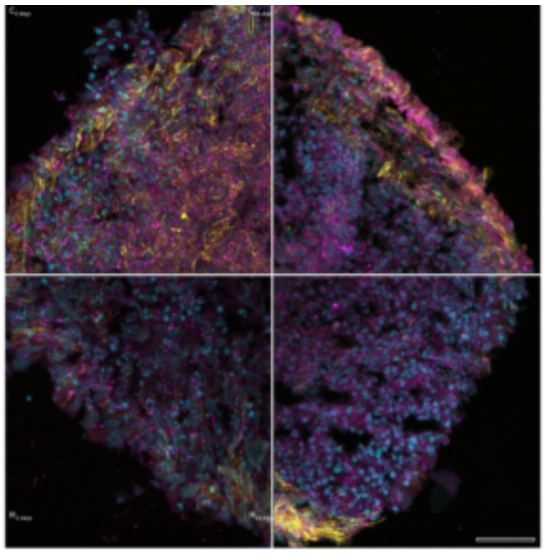

Fig 1: Spheroids fluorescent stained against actin (yellow), acetylated tubulin (pink) and co-stained with DAPI (blue) for nuclei visualization. Scale bar = 20 µm.

DISCUSSION & CONCLUSIONS: These findings suggest that the 3D model presented here effectively mimics the in vivo characteristics of inflammation by reduced expression of ECM and cytoskeletal proteins, secretion of pro-inflammatory molecules. These findings highlight the biological significance of using 3D culture systems over a traditional 2D settings in research as evaluated by the secretion of cytokines and chemokines. We show that experimental conditions impact study outcomes and that physiological levels of O_2 affect the results. Expanding in vitro work in 3D may guide the development of potential therapeutic strategies more efficiently than 2D.

REFERENCES:

Agger, A. E., Samara, A., Geng, T., Olstad, O. K. & Reseland, J. E. Mimicking and in vitro validating chronic inflammation in human gingival fibroblasts. *Arch. Oral Biol.* 106113 (2024) doi:10.1016/j.archoralbio.2024.106113.

11. A Multifunctional Levan Hydrogel Platform with CBD and IGF-1 Liposomes for Bone Regeneration

Inga Jurgelane[1,2], Karina Egle[1,2], Selay Tornaci[3], Elina Kelle[1,2], Dana Galkina[1,2], Girts Salms[2,4], Diana Solovyov[5], Ebru Toksoy Öner[3], Alejandro Sosnik[5], Arita Dubnika[1,2]

[1]Institute of Biomaterials and Bioengineering, Faculty of Natural Sciences and Technology, Riga Technical University, Riga, LV, [2] Baltic Biomaterials Centre of Excellence, Headquarters at Riga Technical University, Riga, LV, [3]IBSB, Department of Bioengineering, Marmara University, Istanbul, TUR, [4]Institute of Stomatology, Riga Stradins University, LV, [5]Laboratory of Pharmaceutical Nanomaterials Science, Department of Materials Science and Engineering, Technion-Israel Institute of Technology, ISR

INTRODUCTION: Oral bone regeneration after trauma or surgery due to periodontitis or oral cancer remains challenging because autologous grafts are limited by morbidity and availability. Levan-based hydrogels provide a biodegradable scaffold for localized delivery of bioactive compounds, while insulin-like growth factor 1 (IGF-1) and cannabidiol (CBD) offer complementary osteogenic and anti-inflammatory effects but require encapsulation for stability and efficacy. We therefore developed a levan-based hydrogel containing liposomes co-loaded with IGF-1 and CBD and evaluated it`s *in vitro* potential for oral bone regeneration.

METHODS: Liposomes composed of DSPC with or without DSPE-PEG were prepared by thin-film hydration and loaded with CBD and/or IGF-1 during the hydration step. Liposome size, surface charge, and morphology were characterized using dynamic light scattering (Anton Paar Litesizer 500) and scanning transmission electron microscopy (Verios 5 UC). Enzymatically produced and hydrolyzed levan was crosslinked with BDDE to form hydrogels, into which the prepared liposomes were incorporated. In vitro studies were performed using patient-derived gingival mesenchymal stem cells (GMSCs; ethical approval No. 6-1/12/47). Cell viability and osteogenic differentiation were evaluated.

RESULTS: The hydrodynamic diameter of liposomes decreased upon incorporation of bioactive compounds (Fig. 1; from 1167 ± 83 nm to 307 ± 21 nm). The release of CBD and IGF-1 was monitored over 14 days, reaching 34 ± 2% and 94 ± 1% release of the encapsulated amount, respectively. All levan hydrogel formulations exhibited typical gel-like behaviour within the linear viscoelastic region, with the storage modulus (G′) exceeding the loss modulus (G″). Alizarin Red S staining and alkaline phosphatase (ALP) activity assays of GMSCs cultured with liposomes and hydrogels for 28 days demonstrated significantly higher osteogenic activity compared with the positive control (up to 50 % increase).

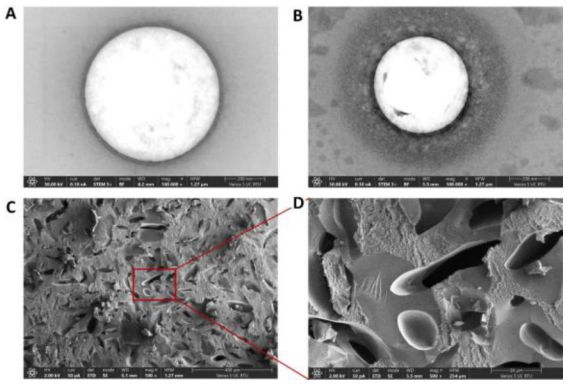

Fig. 1: STEM micrographs of (A) D_CBD/IGF-1 and (B) D-PEG_CBD/IGF-1 liposomes and (C, D) the cross-section and pore structure of swelled and then freeze-dried LH sample.

The increase in ALP activity occurred concurrently with a decrease in cell viability, suggesting a metabolic shift from glycolysis to oxidative phosphorylation as cells matured into osteoblasts during osteogenic differentiation.

DISCUSSION & CONCLUSIONS: CBD release followed the Korsmeyer–Peppas model, consistent with non-Fickian diffusion. The system maintained cell viability and significantly enhanced osteogenic differentiation, demonstrating a synergistic effect of CBD and IGF-1 within the levan hydrogel matrix.

ACKNOWLEDGEMENTS: This work was supported by Horizon 2020 BBCE (GA857287), RTU-PG-2024/1-0011, 5.2.1.1.i.0/2/24/I/CFLA/003, INJECT-BIO (ES RTD/2020/14), TUBITAK (119N756), MOST Israel (317330-3), and the Handelsman Academic Chair.

12. Nanofibrous Scaffold

Oddny Bjorgvinsdottir[1], Thorarinn Gudjonsson[2], Stephen Ferguson[3], Karin Wuertz-Kozak[4], Andrea Heinz[5], Bergthora S. Snorradottir[1]

[1]Faculty of Pharmaceutical Sciences, University of Iceland, [2] Faculty of Medicine, University of Iceland, [3] Institute for Biomechanics, ETH Zurich. [4] Department of Biomedical Engineering, Rochester Institute of Technology, USA, [5] Department of Pharmacy, University of Copenhagen.

INTRODUCTION:Cardiovascular diseases are the most common cause of death globally and will continue to rise in the coming years [1]. Medical devices, so called blood contacting devices are often used in the treatment of such diseases, like vascular grafts and ventricular assist device [2, 3]. These devices are in direct contact of the blood but can have serious side effects due to the activation of the blood coagulation cascade which leads to thrombus formation [4]. This project aims at developing fully hemocompatible biomimetic membrane for a ventricular assist device that excludes the major complications seen with devices currently on the market. The approach here is to develop a synthetic vascular basement membrane that is biomimetic in structure, coated with a bio adhesive for cellular attachment and can provide sustained release of an anti-inflammatory compound.

METHODS: Nanofibrous scaffolds were fabricated by electrospinning 20 wt% polycaprolactone and characterized by scanning electron microscope and texture analyzer. Cell morphology on coated and uncoated fibers was assessed with confocal microscopy. The concentration of released Triptolide from gelatin and silicone was quantified using ultra-performance liquid chromatography.

RESULTS A synthetic multi layered vascular basement membrane was designed and fabricated. Cells on gelatin coated fibers showed improved attachment compared to uncoated fibers. Two different drug release mechanisms showed in sustained release. The anti-inflammatory compound Triptolide was released from coating for two weeks but over a month from the silicone base membrane. However, the addition of Triptolide and its solvent also resulted in a softening of the silicone.

DISCUSSION & CONCLUSIONS: A synthetic multi-layered vascular basement membrane was fabricated that contains nanofibers, a bio-adhesive and releases an anti-inflammatory drug.

.

ACKNOWLEDGEMENTS: This project is funded by the "Stiftung PROPTER HOMINES - Vaduz / Fürstentum Liechtenstein", the "Schwyzer-Winiker Stiftung", the ETH Zurich Foundation and the pharma award fund of Bergþóra and Þorsteinn Schevings Thorsteinsson.

REFERENCES:

[1] World Health Organization. (2018, April 26, 2018). World Heart Day 2017. Available: http://www.who.int/cardiovascular_diseases/world-heart-day-2017/en/

[2] K. Werkkala et al., "Clinical Durability of the CARMEDA BioActive Surface in EXCOR Ventricular Assist Device Pumps," ASAIO J, vol. 62, no. 2, pp. 139-42, Mar-Apr 2016.

[3] P. C. Begovac, R. C. Thomson, J. L. Fisher, A. Hughson, and A. Gallhagen, "Improvements in GORE-TEX vascular graft performance by Carmeda BioActive surface heparin immobilization," *Eur J Vasc Endovasc Surg,* vol. 25, no. 5, pp. 432-7, May 2003.

[4] O. Wever-Pinzon *et al.*, "Ventricular assist devices: pharmacological aspects of a mechanical therapy," *Pharmacol Ther,* vol. 134, no. 2, pp. 189-99, May 2012.

13. From Process Parameters to Performance: Microstructural Control in Additively Manufactured Biodegradable Magnesium Alloy WE43

L. Larsson[1], H. Nilsson-Åhman[1], T. Maimaitiyili[1,2], P. Mellin[2], F. D'Elia[1], C. Persson[1]
[1]Department of Materials Science and Engineering, Uppsala University, Uppsala, Sweden;
[2]Swerim AB, Stockholm, Sweden

INTRODUCTION:

Additive manufacturing through powder bed fusion with laser beam (PBF-LB) of magnesium alloy WE43 (Mg–4 wt% Y–3 wt% RE–0.5 wt% Zr) offers the potential for patient-specific biodegradable implants. However, no additively manufactured Mg implants are currently available clinically. This work summarizes a large body of work, linking key PBF-LB parameters to microstructure, residual stress, texture, and mechanical performance to enable future reliable components implemented in the clinics [1].

METHODS:

Laser power, hatch distance, build orientation, build size, and scan rotation were systematically varied (Fig. 1 and 2). Microstructure was analysed by SEM/BSE, EBSD, and XRD; residual stresses by synchrotron X-ray diffraction; texture by neutron diffraction; and mechanical properties by tensile, compression, and hardness testing. Selected conditions were evaluated for corrosion and in vitro biocompatibility.

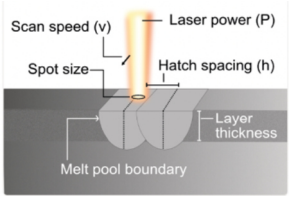

Fig. 1: Schematic of some important PBF-LB process parameters.

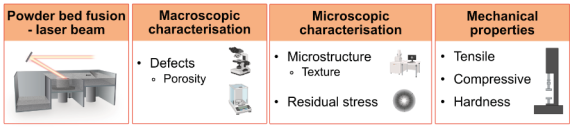

Fig. 2: Schematic illustration of the methods applied.

RESULTS:

Higher laser power promoted equiaxed-dendritic grains, increasing tensile strength but reducing corrosion resistance [1, 2]. Hatch distance tuning preserved strength at lower laser power. Horizontal builds showed ~40% higher tensile strength and ~20% higher elastic modulus than vertical builds due to basal texture alignment (Fig. 2) [3]. Scan rotation enabled texture control; segmented chessboard strategies improved compressive strength, while unidirectional scans led to poor densification.

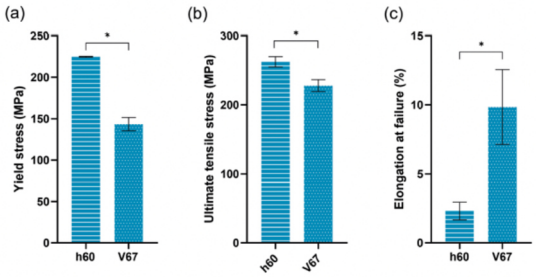

Fig. 2: The difference in tensile mechanical properties between a horizontal build (h67) and a vertical build (v67), both produced with 67 degree scan rotation between layers.

DISCUSSION & CONCLUSIONS:

The results demonstrate how coordinated selection of PBF-LB parameters enables tailoring of microstructure, texture, and performance of WE43, supporting its future application in biodegradable implants. Future work is required to further enhance the corrosion resistance.

ACKNOWLEDGEMENTS: The Swedish Foundation for Strategic Research (SSF) within the Swedish national graduate school in neutron scattering (SwedNess), and VINNOVA's Competence Centre in Additive Manufacturing for the Life Sciences AM4Life (2019-00029), are gratefully acknowledged for financial support.

REFERENCES:

1. Larsson L. Additive Manufacturing of Biodegradable Magnesium Alloy WE43. PhD Thesis, Uppsala University, 2025. 2. Nilsson-Åhman H et al. Mater Today Commun 2024;39:108979. 3. Larsson L et al. Mater Des 2025;256:114299.

14. Interplay Between Bone and Mineralized Cartilage in Rat Bone: Interface and Lacuno-Canalicular Network

Aqila Naseri, Chiara Micheletti

Department of Physics, Chalmers University of Technology, Göteborg, Sweden

INTRODUCTION: Long bones of small rodents are characterized by the presence of islands of mineralized cartilage (MC), even at considerable distances from the growth plate[1]. These features are likely remnants of endochondral ossification resulting from limited Haversian remodelling. However, their functional impact remains unclear, as they introduce both structural and compositional heterogeneity in the bone matrix. In this work, we aim to investigate the interface between bone and MC islands, with particular emphasis on the behaviour of the lacuno-canalicular network (LCN).

METHODS: Femurs from 16- and 20-week-old Sprague Dawley rats were used. Following fixation, samples were dehydrated, embedded in LR White resin, sectioned longitudinally, and polished. A multimodal approach was then employed combining two-dimensional scanning electron microscopy (SEM) and three-dimensional SEM-focused ion beam (FIB) tomography to resolve structure and pseudo-composition of the bone-MC interface. Composition was further assessed using time-of-flight secondary ion mass spectrometry (ToF-SIMS).

RESULTS: As expected, MC was more highly mineralized than the surrounding bone matrix (Fig. 1). However, the interaction between bone and MC proved more complex than suggested by prior work[1,2]. The interface between bone and MC exhibited a gradual, mineral-rich transition zone. Furthermore, although osteocyte lacunae were absent within the MC islands, canaliculi appeared to extend beyond the bone matrix.

DISCUSSION & CONCLUSIONS: The structural characteristics of the bone-MC interface closely resemble those reported for bone-ceramic biomaterial interfaces[3], suggesting similarities in mechanisms of new bone formation and mineralization. The presence of canaliculi extending beyond bone and into the MC islands potentially indicates the ability for communication across the bone matrix despite the discontinuity introduced by the MC islands. Overall, these findings highlight that a complex interplay between bone and MC may contribute to the preservation of tissue functionality in rat bone.

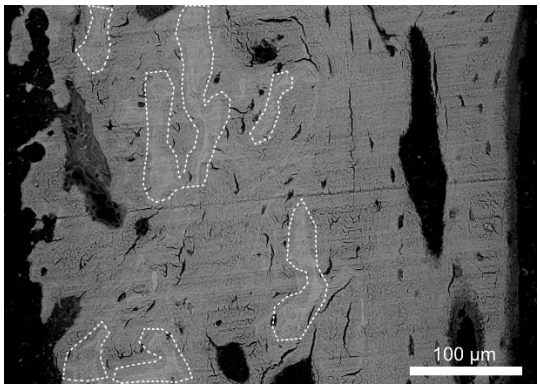

Fig. 1: SEM image showing islands of MC (contoured by dashed lines) throughout the bone matrix.

ACKNOWLEDGEMENTS: We are grateful to Furqan A. Shah, University of Gothenburg, for kindly providing the rat samples. CM is thankful to the Health Engineering and Materials Science Areas of Advance at Chalmers University of Technology for financial support. This work was performed in part at the Chalmers Materials Analysis Laboratory, CMAL.

REFERENCES:

1. FL Bach-Gansmo et al. *Bone* 92 (2013)
2. C Micheletti et al. *Bone* 172 (2023)
3. K Grandfield et al. *Clinical Implant Dentistry and Related Research* 14 (2012)

15. A framework for efficient porosity analysis and process parameter optimization in powder bed fusion with laser beam of biodegradable alloys

C. Jetton[1,2], S.R. Babu[1], J. Sjölund[3], C. Persson[1,2]

[1]Division of Biomedical Engineering, Department of Materials Science and Engineering, Uppsala University, Uppsala, SW, [2]Wallenberg Initiative Materials Science for Sustainability, Department of Materials Science and Engineering, Uppsala University, Uppsala, SW,

[3]Department of Information Technology, Uppsala University, Uppsala, SW

INTRODUCTION: WE43, a magnesium alloy, has received increasing interest for degradable biomedical implants [1]. Optimizing WE43 and other alloys requires workflows that automate as much of the research as possible to reduce the development cost and environmental impact.

To do so, this work proposes to automate the porosity calculation with a neural network (via a U-net [2]) and model the porosity with a Gaussian process [3], a machine learning model that excels with low sample sizes. The pairing of these two steps represents a novel workflow that can reduce the time required to improve WE43, other alloys for biomedical use, and additive manufacturing research as a whole.

METHODS: A WE43 alloy was printed with 73 process parameter combinations before taking microscopy images to calculate porosity. A U-net was trained using 127 manually annotated images porosity masks, which was then applied to segment pores in the remaining 611 images.

After the U-net calculated porosity, a Gaussian process modeled how the process parameters affected porosity. This interpolates between observations and infers the values at the missing datapoints. The research emphasizes transparency in model validation and includes the exploration into various model types, meaning it can also serve as a guide to other researchers looking to use Gaussian processes.

RESULTS: The U-net helped find a set of parameters that lead to a porosity percentage of 0.06%. Additionally, the use of multiple images helped identify process parameters that would be a robust choice with a lower standard deviation.

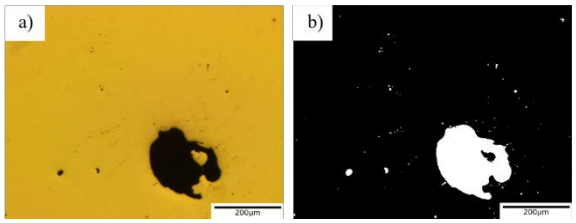

Fig. 1: Example of a microscopy image (left) with the U-net porosity segmentation (right)).

The Gaussian process model closely matched the true porosity values, especially in the low-porosity region, and could estimate the porosity values in the missing regions by using the surrounding parameter combinations.

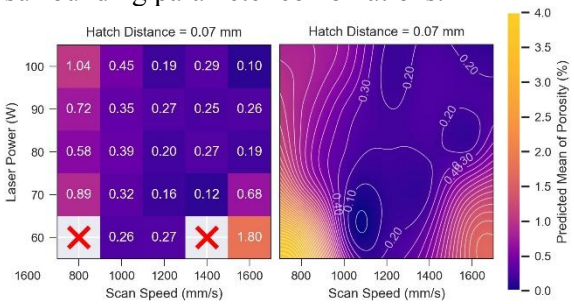

Fig. 2: Extracted (left) and predicted (right) porosity for one hatch distance. This highlights how the Gaussian process models multimodal data and interpolates values for failed prints.

DISCUSSION & CONCLUSIONS: This research demonstrated the advantage of using a U-net with the microscopy images of printed samples to decrease the analysis time. The Gaussian process model captured the porosity trends across the process parameter space with significantly less samples than other machine learning techniques. The workflow presented in this research is not limited for the purpose of analyzing porosity data, but can be applied to other materials to understand their process-structure-property relationships.

REFERENCES:

[1] Cavaliere GP, Shtender V, Mellin P, Persson C, D'Elia F. Powder reuse in powder bed fusion-laser beam of WE43 magnesium alloy: towards sustainable manufacturing of biodegradable implants. Journal of Materials Research and Technology 2025;38:5498–510.

[2] Ronneberger O, Fischer P, Brox T. U-Net: Convolutional Networks for Biomedical Image Segmentation 2015.

[3] Rasmussen CE, Williams CKI. Gaussian Processes for Machine Learning. The MIT Press; 2005.

16. BCR activation studied via antigen nanopatterns

TOS. Lehmann[1,3], A. Shahrokhtash[1,3], KS. Kastberg[2,3], S. Degn[2,3] and DS. Sutherland[1,3]

[1]iNANO Center, Aarhus University, Aarhus, DK, [2] Dept. Biomedicine, Aarhus University, Aarhus, DK, [3] Center for Cellular Signal Patterns, Aarhus University, Aarhus, DK,

INTRODUCTION: Immune responses via B cell activation occurs through the binding of antigen or processed antigen to the B cell receptor (BCR) leading to activation, ultimately leading to antibody production. The process by which BCR is activated is still not understood[1]. Reports from the T cell field have suggested a process where dynamic receptor relocalisation after antigen binding leads to signal transduction. Here we use an in vitro model for B cell interaction with antigen presented by antigen presenting cells (APCs) to understand the role of nanoscale clustering of antigen in BCR activation.

METHODS: Nanoscale chemical patterns of functionalised PEG and PMOXA polymers were generated by sparse colloidal lithography and used to localised antigen with integrated DNA force sensors[2] in a background of APC specific cell adhesion molecules (ICAM-1). Murine primary B cells were purified untouched from a mouse model with BCRs modified to bind to specific small molecule haptens (NIP or NP). The interaction of NIP/NP with BCRs were studied both by live TIRF microscopy to look at forces exerted on the antigens and after fixation and staining to look at activation through phosphorylation of Syk.

RESULTS: First we quantified the clustering state of antigen in germinal centers in lymph nodes of mice using fluorescent antigen. Antigen was present on follicular dendritic cells (FDC) in clear clusters with a distinct size scale of clusters between 100nm-500nm. In a second set of experiments Antigen patterns of NP and NIP were created with a range of pattern sizes between 80nm and 600nm in a mimic of FDC-B cell interactions. The NIP/NP was coupled to a hairpin DNA force sensor covalently attached to a PEG/PMOXA layer. Phosphonothioate-modified DNA was used to prevent degradation of the force sensors by cellular released enzymes and showed good stability. B cell interactions in the first 10 minutes showed rapid formation of contacts and opening of force sensors indicating both antigen engagement and force exerted through the BCRs on surfaces with patterned antigen but not on comparable global densities of unclustered antigen. While the level of force pulling events was comparable between pattern sizes the level of activation varied with the cluster size with a lower activation level (indicated by the level of pSyk) at 80nm patterns and increasing with cluster size. Little activation was observed at unclustered antigen surfaces. The formation of contacts between the B cell membranes and the antigen patches also resulted in exclusion of CD45 which is one of a number of regulatory transmembrane membrane phosphatases.

DISCUSSION & CONCLUSIONS: In T cell biology the exclusion of CD45 from TCR contacts results from its large size. In analogy to this process termed *kinetic segregation* in T cell receptor/ T cell activation the exclusion of CD45 and its correlation to BCR activation suggests that a similar mechanism may be in play in B cell activation.

We observe in an in vitro model of antigen presentation by FDC's that B cell activation is substantially increased at clustered antigen and that clusters in the size range 200-300nm give enhanced activation. This size range is similar to the size range of antigen clusters in vivo. The in vitro system suggest that forces exerted by the B cells correlate to both BCR activation and to CD45 exclusion. We propose that that physical separation of this regulatory phosphase from the BCRs leads to activation in a process similar to kinetic segregation in T cells.

ACKNOWLEDGEMENTS: This work was funded by the DNRF excellence center grant CellPAT (DNRF135)

REFERENCES:

1 Degn, S. E. & Tolar, P. Towards a unifying model for B-cell receptor triggering. Nat Rev Immunol (2024) doi:10.1038/s41577-024-01073-x

2 Shahrokhtash, A., Sivertsen, M. von T., Laursen, S. H. & Sutherland, D. S. Nanoscale Cellular Traction Force Quantification: CRISPR-Cas12a Supercharged DNA Tension Sensors in Nanoclustered Ligand Patterns. ACS Appl. Mater. Inter. 17, 7339–7352 (2025)

17. Electrospun silk fibroin mats for wound healing

E. Kelle[1,2], K. Egle[1,2], M. Li[3], A. Dubnika[1,2], A. R. Boccaccini[3]

[1] *Institute of Biomaterials and Bioengineering, Faculty of Natural Sciences and Technology, Riga Technical University, Riga, Latvia*

[2] *Baltic Biomaterials Centre of Excellence, Headquarters at Riga Technical University, Riga, Latvia*

[3] *Institute of Biomaterials, Department of Materials Science and Engineering, Friedrich-Alexander-Universität Erlangen-Nürnberg, Erlangen, Germany*

INTRODUCTION: Biomimetic scaffolds that replicate the structure of the extracellular matrix represent a promising strategy for enhancing wound healing by promoting cell adhesion, migration, and tissue regeneration. Silk fibroin is a biopolymer of significant interest for wound healing applications due to its biocompatibility, biodegradability, and favourable mechanical properties [1]. Electrospinning enables the fabrication of fibrous mats with controlled architecture and high surface area; however, conventional electrospinning of silk fibroin typically relies on organic solvents, which limits its biomedical translation [2]. Therefore, this study aimed to develop a water-based electrospinning approach for producing fibrous silk fibroin mats suitable for wound healing and tissue engineering applications.

METHODS: Silk fibroin was extracted from *Bombyx mori* silkworm cocoons and prepared as a 23% (w/w) aqueous solution. Electrospinning was performed under ambient conditions using an applied voltage of 18 kV, a flow rate of 0.8 mL/h, and a tip-to-collector distance of 12 cm. The aqueous stability of the resulting mats was enhanced by inducing β-sheet crystallization through post-treatment in 96% (v/v) ethanol. All prepared mats were characterized by FTIR, SEM, water contact angle, and swelling degree analyses.

RESULTS: The electrospun mats comprised smooth, randomly oriented fibres with a mean diameter of 1.82 ± 0.51 µm (Fig. 1). Ethanol treatment preserved the fibrous morphology while inducing β-sheet formation, leading to a significant improvement in aqueous stability. Treated mats retained 92.5 ± 2.8% of their original mass after immersion in water, whereas untreated mats exhibited rapid degradation. In addition, ethanol treatment reduced the swelling capacity to 406.8 ± 86.7% and increased surface wettability, as evidenced by a decrease in the water contact angle to 59.3 ± 6.7°.

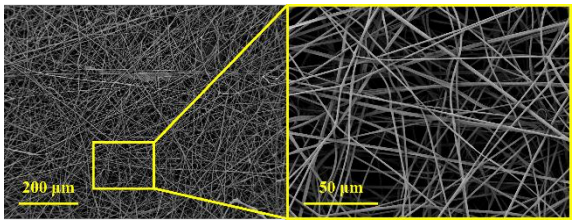

Fig. 1: Electrospun silk fibroin mats.

DISCUSSION & CONCLUSIONS: This water-based electrospinning approach enabled the fabrication of homogeneous, cylindrical silk fibroin microfibres with enhanced structural integrity and surface properties. Ethanol-induced crystallization produced moderately hydrophilic mats well suited for cell attachment and proliferation. Overall, this study demonstrates a simple yet effective, organic solvent-free strategy for manufacturing fibrous scaffolds with strong potential for wound healing and tissue engineering applications.

ACKNOWLEDGEMENTS: The authors acknowledge financial support from the European Union's Horizon 2020 research and innovation programme under the grant agreement No. 857287 (BBCE – Baltic Biomaterials Centre of Excellence) and from the Riga Technical University 2025/2026 Project for Strengthening Scientific Personnel Capacity Nr. ZM-2026/30.

REFERENCES:

1. S.-D. Wang, K. Wang, J. Yan, C. Ding, Y. Zhang, Mater. Today Commun. 50 (2026).
2. F.V. dos Santos, R.L. Siqueira, L. de Morais Ramos, S.A. Yoshioka, M.C. Branciforti, D.S. Correa, Int. J. Biol. Macromol. 254 (2024).

18. Protein corona effects on fibroblast adhesion to tannic acid-coated surfaces

E. Oreja[1], D.S. Zaytseva-Zotova[1], A. Barrantes[1], M. Sandomierski[2], H. Tiainen[1]

[1]*Deparment of Prosthetic Dentistry, University of Oslo, Norway*

[2]*Institute of Chemical Technology and Engineering, Poznan University of Technology, Poland*

INTRODUCTION: Success of implants is strongly determined by their capacity to integrate with bone and soft tissues. Upon implantation, proteins immediately absorb to the surface creating a conditioning layer that will determine the subsequent biological responses. Albumin is a globular protein present in blood plasma and forms non-specific protein-cell interactions, whilst fibrinogen (FNG) contains specific RGD domains that can interact with integrin receptors on cell surfaces. Because of their different biological functions, they serve as a model to study the adsorption and properties of the protein corona on implants. Development of functionalized surfaces that can control the formation of the protein corona have become a good strategy to achieve strong cell-biomaterial interactions. Our aim is to understand how proteins present in blood interact with tannic acid (TA)-coated titanium surfaces and how the formed protein corona affects the adhesion of human gingival fibroblasts (HGF).

METHODS: Quartz crystal microbalance with dissipation monitoring (QCM-D) was used to study protein adsorption on TA-coated surfaces. The chemical/physical properties of the formed protein corona were investigated by Fourier transform infrared (FTIR) and ultraviolet-visible (UV-vis) spectroscopy. Zeta potential and contact angle measurements were made to determine how surface properties relevant to cell adhesion were modified. QCM-D in combination with live-cell imaging was used to determine the dynamics of HGF adhesion onto TA-protein coated surfaces. Cell morphology was observed using confocal microscopy.

RESULTS: Different thickness, absorption mechanisms, orientation of proteins and changes in conformation were observed depending on the concentration and type of protein used. The interaction between TA and proteins was found to be noncovalent, as determined by FTIR and UV-vis spectroscopy, although TA altered the secondary structures of BSA and FNG. Despite the stable interaction between TA and BSA, the Vroman effect was observed when depositing FNG on a surface saturated with BSA. FTIR mapping based on the intensity of amide I band revealed different surface coverage and distribution of proteins for the studied conditions. Surface parameters relevant to cell adhesion, such as zeta potential and surface energy, were found to be comparable among the different protein-coated surfaces but different from TA-coated. Combining QCM-D and timelapse imaging showed that stronger cell adhesion was achieved in surfaces with FNG, which contains RGD domains. Surfaces containing protein delayed initial cell adhesion compared to TA-coated surfaces, although high cell density and interconnection were observed in all surfaces.

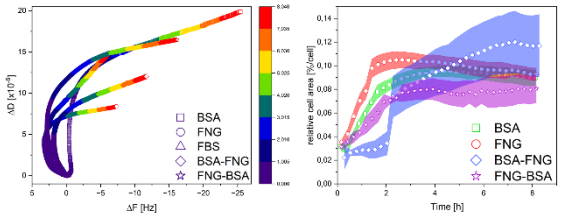

Fig. 1 Fibroblast adhesion on proteins deposited onto TA-coated surfaces. Averaged ΔD vs ΔF plots (left) and relative area occupied by fibroblasts (right).

DISCUSSION & CONCLUSIONS: The differences in protein orientation, surface coverage and layer thickness were attributed to limited mass transport in lower concentrations. Modifications of the secondary structures of proteins were attributed to the physical interaction between TA and proteins. The enhanced adhesion observed on surfaces containing the RGD sequence indicates the importance of integrin-mediated interactions in stabilizing cell attachment. In contrast, the surfaces lacking RGD sequence relied initially on weaker interactions before secreting ECM proteins that allowed the formation of integrin-mediated interactions. It was demonstrated that the presence of TA affects the properties of the protein layer and altered cell adhesion dynamics.

ACKNOWLEDGEMENTS: This work was financially supported by the Research Council of Norway (grant# 302590).

19. Bioactive Glasses with Enhanced Biological Response for Tissue Regeneration

G. Kohoolat, A. Nygård, M. Jafari, M. Bayandori, A. Shiralizadeh Dezfuli, L. Hupa, P. Uppstu

Laboratory of Molecular Science and Engineering, Centre of Excellence in Materials-driven Solutions for Combatting Antimicrobial Resistance (MADNESS), Faculty of Science and Engineering, Åbo Akademi University, Turku, Finland

INTRODUCTION: Bioactive glasses (BGs) are materials that have several favourable properties for regeneration of bone tissue [1]. After implantation, a bone-like hydroxyapatite (HA) layer forms on their surface, promoting early recruitment of bone-forming cells. As the glass dissolves, it releases ions in a controllable manner, with therapeutic effects on cells and tissues [2]. The biological effects of therapeutic ions have been researched in many studies, and several BG compositions have been developed to optimise ion release for bone growth stimulus [3]. However, despite promising *in vitro* data for BGs with added therapeutic ions, the improvements have generally been modest *in vivo* compared to conventional BGs, and the correlation between bone regeneration outcomes *in vitro* and *in vivo* has been poor [4]. Bone regeneration is a complex process that involves a variety of biological functions. Stimulation of a subset of the involved cellular processes may result in improved cell function for isolated cell lines *in vitro*, but this kind of limited stimulation may not be sufficient for improved outcomes *in vivo*. Instead of focusing on specific ions that stimulate only a subset of biological processes, it may be beneficial to stimulate a wider variety of cellular pathways for a more comprehensive bone growth stimulation. We hypothesise that bioactive glasses designed for multi-objective ion release will simultaneously promote shifting macrophages toward a pro-regenerative phenotype, enhancing vascular network formation, and promoting osteogenic differentiation, with potential to enhance bone regeneration.

METHODS: Multi-ion substituted bioactive glass frits will be prepared by mixing precursor oxides and carbonates that are melted for 3 hours at 1360 °C in quartz crucibles, followed by pouring into an ice-water bath and washed with acetone. Subsequently, the quenched frits are dried overnight at 70 °C.

RESULTS: The glass frits are milled and sieved to a narrow size fraction and analysed by XRD, FTIR, HSM, SEM, BET, and DSC. Their dissolution in simulated body fluid (SBF) will be studied by ion release (ICP-OES), pH changes, and reaction layer formation (SEM-EDX, FTIR) at multiple time points.

DISCUSSION & CONCLUSIONS: This work is expected to verify the amorphous nature of the BGs and reveal calcium phosphate layer formation on their surfaces after SBF immersion with XRD and SEM, while BET analysis will quantify their surface area. DSC analysis will be used to determine key thermal properties, including glass transition and crystallisation peak temperatures, and FTIR spectroscopy will characterise the multi-substituted borosilicate glass structure and HA layer development post-dissolution. HSM results will provide critical hot working temperatures to guide processing.

ACKNOWLEDGEMENTS: The authors would like to acknowledge the Swedish Cultural Foundation and the Finnish National Agency for Education, for financial support. This work is part of the Åbo Akademi University Foundation (SÅA)-funded Centre of Excellence in Research, MADNESS.

REFERENCES:

[1] Jones JR, et al. Bioglass and Bioactive Glasses and Their Impact on Healthcare. doi: 10.1111/ijag.12252.

[2] Hupa, et al. Bioactive Glass S53P4 – From a Statistically Suggested Composition to Clinical Success. doi: 10.1002/9781119724193.ch3.

[3] Hoppe A, et al. A review of the biological response to ionic dissolution products from bioactive glasses and glass-ceramics. doi: 10.1016/j.biomaterials.2011.01.004.

[4] Hulsart-Billström G, et al. A surprisingly poor correlation between in vitro and in vivo testing of biomaterials for bone regeneration: results of a multicentre analysis. Eur Cell Mater .doi:10.22203/ecm.v031a20.

20. Nanoemulsion-based Kappa-Carrageenan Hydrogels: A Platform for the Release of Hydrophobic Drugs

Punyashraya Mahapatra [1], Likhith K. [1], Tarun Mateti [2], Goutam Thakur [1]

[1]School of Electrical Engineering, Manipal Institute of Technology, Manipal, Karnataka, India [2] Department of Mechanical Engineering & Materials Science, Yale School of Engineering & Applied Science, Yale University, 17 Hillhouse Avenue, New Haven, Connecticut–06520, United States of America

INTRODUCTION: Nanoemulsions are thermodynamically stable, nanosized emulsions in which an emulsifying agent stabilizes two immiscible liquids, and they have been explored to improve the delivery of active biomolecules. Curcumin is a hydrophobic polyphenol with significant medicinal value. However, its application is limited because of poor pharmacokinetics and physicochemical instability. Here, we fabricate nanoemulsions based on k-carrageenan hydrogels using the ionotropic gelation method, with potassium chloride and calcium chloride serving as ionic crosslinkers. The primary goal of this nanoemulsion hydrogel is to investigate the in vitro release of hydrophobic molecules such as curcumin from the gel matrix.

METHODS: We prepared a nanoemulsion using the solvent displacement technique. Briefly, a 50 mL nanoemulsion with an aqueous and oil phase was prepared at a 9:1 ratio. A solution of 10 mg of curcumin in 10 mL of polysorbate 80 was prepared, and 1000 µL was added to the nanoemulsion under magnetic stirring at 800 rpm. Next, 1.5 g of κ-carrageenan was added and heated to 80 °C while stirring vigorously at 1600 rpm. Crosslinker solutions of KCl and $CaCl_2$ at various concentrations were prepared and used to crosslink the nanoemulsion. A combinational study was conducted using different percentages of KCl and $CaCl_2$. The effects of crosslinking were evaluated through water retention, chemical composition, and surface topography. The release behavior of curcumin was examined by immersing the hydrogels in a beaker containing 30 mL of PBS at pH 7.4 and analyzing them spectrophotometrically.

RESULTS: The characteristic peaks of K-carrageenan are at 1260 cm^{-1} and 1048 $cm^{-1,}$ and the peak of curcumin is at approximately 3000 cm-1, indicating the presence of phenolic O-H stretching. A comparison of the various crosslinked hydrogels revealed that the samples retained the characteristic peaks of κ-carrageenan (1260 and 1048), indicating their presence in the matrix. The absence of curcumin peaks represents the complete incorporation of the drug into the hydrogel matrix. The more compact and rigid surface due to cross-linking is shown in Figure 1. The control (gel without crosslinking) has a maximum swelling percentage of 550%, whereas the gel crosslinked with both KCl and $CaCl_2$ is observed to have the least swelling capacity. Furthermore, the greater release of curcumin is attributed to poor crosslinking and a wider pore size.

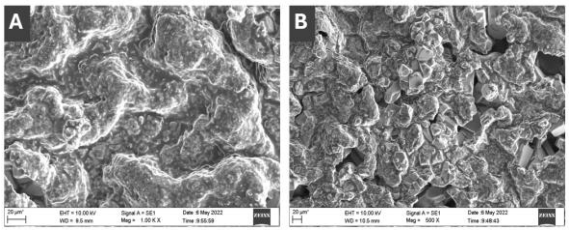

Fig. 1: (A) Dual-crosslinked k-carrageenan gel, (B) curcumin-loaded dual-crosslinked k-carrageenan gel.

DISCUSSION & CONCLUSIONS: The challenges associated with using curcumin have been successfully addressed by preparing a nanoemulsion-based k-carrageenan-crosslinked hydrogel impregnated with curcumin. The crosslinking effects of potassium chloride, calcium chloride, and their combination were used to evaluate water retention, chemical composition, and surface topography. SEM micrographs of the dual-crosslinked gels showed a compact gel structure. IR studies confirmed the successful incorporation of curcumin within the matrix. Additionally, *in vitro* drug release was tested in physiological buffer, and compared with other hydrogels, those crosslinked with both KCl and $CaCl_2$ exhibited sustained release of curcumin.

REFERENCES: [1]Adv. Healthcare. Mater., 2(6), 895–907(2022), [2]Carbohydr. Polym. Technol. Appl., 101066 (2025)

21. Spatially resolved transcriptomics maps the inflammatory-to-regenerative switch driving the osseointegration of biodegradable magnesium implants

Heithem Ben Amara[1], Furqan A. Shah[1], Anders Palmquist[1], Omar Omar[2], Peter Thomsen[1,2]

[1]Department of Biomaterials, University of Gothenburg, Sweden, [2] Department of Biomedical Dental Sciences, Imam Abdulrahman bin Faisal University, Saudi Arabia

INTRODUCTION: Despite being a mainstay for bone fracture fixation, titanium (Ti) implants may require removal after healing, leading to complications. Magnesium (Mg) degrades *in situ* and circumvents these problems (1), but how Mg influences the biological processes (2) at the bone–implant interface remains poorly understood. Using spatial transcriptomics to profile gene expression in spatially defined interfacial regions (3), this work investigates the molecular and structural dynamics underlying Mg osseointegration.

METHODS: Pure Mg and Ti screws were implanted in rat tibiae and retrieved at 3 d and 28 d (n=8/group/timepoint). Spatial transcriptomics (Bruker-NanoString GeoMx DSP) targeted regions within 20 µm of the Mg interface *versus* distant control areas, enabling direct, whole transcriptome profiling of the interfacial bone microenvironment (*Fig. 1*). Complementary analyses included histomorphometry, Raman spectroscopy, and qPCR at the interface bone–implant. Mann-Whitney test was used for comparisons between Mg and Ti. Student's t-test was used for spatial transcriptomics data. Significance was set at $p < 0.05$.

RESULTS: Spatial transcriptomics demonstrated a two-phase transcriptional program at the interface with Mg implants. At 3 d (*Fig. 1*), a transient NF-κB/IFN alarmin surge was evident, with the upregulation of the transcripts *Irgm1*, *Trpv1*, and *Il18bp*, alongside the activation of Wnt-related and mechanosensitive pathways. By 28 d, these inflammatory signatures resolved, while genes marking for osteoblast lineage, collagen remodeling, and angiogenesis were strongly upregulated (*Cntfr*, *Sp5*, and *Cxcl12*), evidencing a transition from inflammation to regeneration. qPCR corroborated these findings, showing a ~2-fold higher osteocalcin (*Bglap*) and collagen 1a1 (*Col1a1*) mRNA levels ($p < 0.05$; *Fig. 1*), as well as a ~4-fold higher expression of vascular endothelial growth factor (*Vegf*) gene ($p < 0.05$) at the interface with Mg *vs* Ti at 28 d. These molecular changes translated into differences in bone apposition: histomorphometry demonstrated 55% higher bone–implant contact for Mg (92.2 ± 7%) *vs* Ti (59.5 ± 7%) ($p = 0.002$; *Fig. 1*). Yet, Raman spectroscopy revealed a lower mineral crystallinity (*Fig. 1*) and a higher organic content near Mg, indicating a compositionally 'younger' bone matrix.

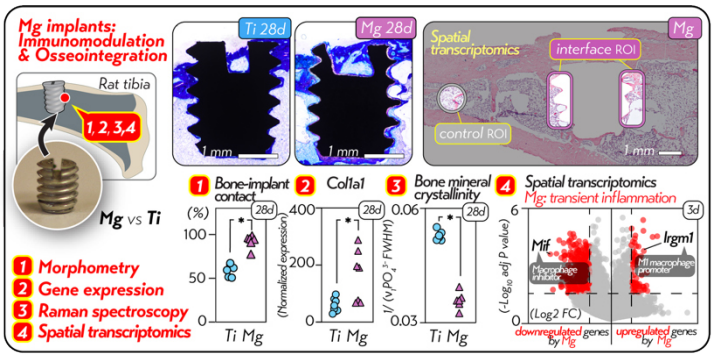

Fig. 1: Morphometry (bone–implant contact), qPCR (Col1a1), Raman spectroscopy, and spatial transcriptomics of the bone–implant interface.

DISCUSSION & CONCLUSIONS: Spatial transcriptomics demonstrates a temporally coordinated immunomodulatory program at the Mg–bone interface: an early alarmin/inflammatory surge transitions to a pro-regenerative signaling, therefore promoting new bone formation at the surface of Mg implants. Intriguingly, this enhanced bone quantity is accompanied by a lower bone age, pointing to the unique bone microenvironment around Mg implants shaped by their degradation.

ACKNOWLEDGEMENTS: Horizon 2020 Marie Skłodowska-Curie Action; The Swedish Research Council; the ALF agreement (725641); the IngaBritt and Arne Lundberg Foundation; the Sylvan Foundation; the Hjalmar Svensson Foundation, and the Area of Advance Materials of Chalmers and GU Biomaterials.

REFERENCES: 1. Zhang Y, et al. *Nat Med.* 2016;22(10):1160-9. **2.** Ben Amara H, et al. *Bioact Mater*. 2023;26:353-69. **3.** Ben Amara H, et al. *Adv Sci (Weinh)*. 2025;12(28):e2503123.

22. Combined Effect of Graphene Oxide, Serum Supplementation, and Surface Topography on Early Stages of Neural Cell Aggregation

J. Hlinkova[1], A. Samara[1,2]

[1] *Department of Biomaterials, FUTURE, Center for Functional Tissue Reconstruction, University of Oslo, Oslo, NO,* [2] *Department of Women's and Children's Health, Karolinska Institutet, Stockholm, SE*

INTRODUCTION: Understanding the early morphogenetic steps of neural cell aggregation and pseudospheroid formation is critical to model neurodevelopment and neurodegenerative disorders[1]. Graphine oxide (GO) is widely used in biomedical applications and tissue engineering for itch exceptional electronic, optical, mechanical and biological properties[2].

In this study, we investigated how combined effect of GO, serum supplementation and substrate topography influences the cell clustering using human neuroblastoma SH-SY5Y cells. To this end, we employed polycaprolactone (PCL) randomly aligned nanofiber scaffolds fabricated by solution blowspinning (SBS), mimicking an anisotropic, low-attachment microenvironment, and parafilm, mimicking rougher surface.

METHODS: The fibers were produced via SBS in-house. Fibers and parafilm (Seal-R-film) were wrapped around coverslips, UV sterilized and prewetted with cell culture media for 1.5 h at 37°C before cell seeding. The samples were characterized via scanning electron microscopy (SEM), contact angle measurement and profilometry. GO was applied overnight prior to seeding. SH-SY5Y cells were cultured at high seeding density in media supplemented with FBS or serum replacement (SR) the tested substrates as well as on glass controls and were analyzed over several early time points to capture cell dynamics. We employed confocal microscopy and quantitative PCR (qPCR) for gene expression analysis.

RESULTS: Contact angle, which was initially highly hydrophobic for both substrates, significantly decreased after prewetting, and parafilm did not differ from glass after preprocessing. Surface roughness varied among the experimental groups; however, preprocessed samples significantly differed from the original untreated material and reached values similar to glass coverslips.GO did not cause cell death in the FBS group and only induced minor changes in the SR and parafilm groups. Gene expression analysis via qPCR provided insights into key regulators of cell–cell interaction, migration, and neuronal differentiation markers.

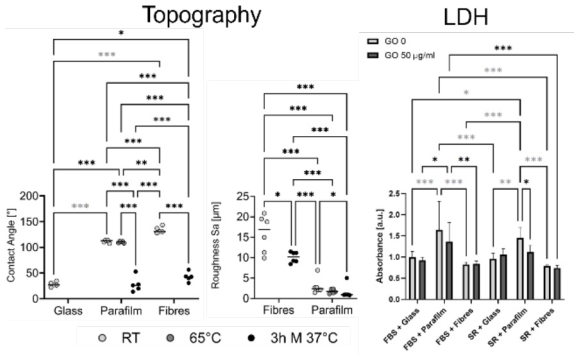

Fig. 1: Contact angle (left) and roughness (middle) of material pre-processing with heat (room temperature, RT, or 65°C) and prewetting. LDH (right) at day 3. Prewetting with cell culture media significantly altered surface and thus cell adhesion. GO did not affect LDH release in FBS, only in SR and parafilm.

DISCUSSION & CONCLUSIONS: This work demonstrates the importance of preprocessing the surfaces for cell culture and effect of media supplementation. We also proved that GO did not negatively affected cell proliferation. Future studies integrating functional assays will be instrumental in identifying the molecular players and early programs driving spheroid formation.

REFERENCES: 1 Hlinková J, Dziemidowicz K, Ullrich MM, Agger AE, Lian AM, Reseland JE, and Samara A (2025): Neural growth patterns: how random and aligned fibers guide 3D cell organization and pseudospheroid formation.

2 Sanchez VC, Jachak A, Hurt RH, Kane AB (2012). Biological interactions of graphene-family nanomaterials: an interdisciplinary review.

23. Upscaling, Rapid Synthesis, and Room-Temperature Sintering of Octacalcium Phosphate

J. Locs[1,2]

[1] *Institute of Biomaterials and Bioengineering, Faculty of Natural Sciences and Technology, Riga Technical University, Paula Valdena 3, K-1, Riga LV-1048, Latvia.*

[2] *Baltic Biomaterials Centre of Excellence, Headquarters at Riga Technical University, Riga, Latvia.*

INTRODUCTION: Octacalcium phosphate (OCP, $Ca_8(HPO_4)_2(PO_4)_4 \cdot 5H_2O$) is a metastable calcium orthophosphate considered a precursor of biological apatite due to its apatite-like layers separated by hydrated layers. Its metastability limits high-temperature processing, complicating scale-up and densification into implantable forms. Here, we combine scalable OCP powder synthesis with room-temperature densification to preserve the OCP phase.

METHODS: OCP was synthesised by (i) room-temperature hydrolysis of alpha-tricalcium phosphate (alpha-TCP), scaled from 0.1 g to 10 g, tracking phase evolution at 1-180 h [1]; and (ii) a rapid co-precipitation route tailored to tune specific surface area (SSA) [2]. Powders were characterised by X-ray diffraction (XRD), FT-IR, Raman spectroscopy, BET (SSA) and SEM. Room-temperature sintering (high-pressure consolidation) was performed by uniaxial pressing (<1500 MPa). Relative density and biaxial flexural strength were determined.

RESULTS: In the hydrolysis route, alpha-TCP transformed gradually to OCP via brushite (DCPD) as an intermediate (up to ~36%). The co-precipitation route produced reproducible OCP with SSA of 16-91 m2/g. Cold sintering preserved the OCP phase while achieving a relative density of over 90%; densification increased with compaction pressure, yielding crack-free compacts flexural strength close to conventionally sintered calcium phosphates.

DISCUSSION & CONCLUSIONS: The combined synthesis and room-temperature densification strategy offers a manufacturable pathway for OCP-based ceramics and composite feedstocks, thereby avoiding thermal decomposition. This low-temperature approach is compatible to form organic/inorganic composites with high inorganic loading and potential load-bearing resorbable properties for bone-regenerative applications.

ACKNOWLEDGEMENTS: This research is funded by the Latvian Council of Science, project "Load-Bearing Bioresorbable Nanocomposites" (LBBN), project No. Nr. lzp-2025/1-0364. The authors acknowledge the access to the infrastructure and expertise of the BBCE – Baltic Biomaterials Centre of Excellence (European Union's Horizon 2020 research and innovation programme under the grant agreement No. 857287).

REFERENCES:

1. https://doi.org/10.3390/biom13030462
2. https://doi.org/10.1021/acsomega.4c01436

24. 3D Microrheology for Microstructural Analysis of Hydrolytic Degradation of Collagen-Based Hydrogels

T. Taipale[1], K. Liimatainen[1], M. Kellomäki[1], J.T. Koivisto[1]

[1]*Biomaterials & Tissue Engineering Group, Faculty of Medicine and Health Technology, Tampere University, Tampere, Finland*

INTRODUCTION: Passive multiple particle tracking (MPT) enables the study of changes in microstructures of hydrogel biomaterials over time. In MPT, Brownian motion of tracer particles embedded in hydrogel is tracked, which reveals rigid, viscoelastic, and fluid-like areas in the hydrogel sample[1]. In our 3D version of MPT microrheology, the sample is imaged with known Z-intervals, and the data is reconstructed into a 3D visualization based on quantified viscoelastic micromechanics with the help of generalized Stokes-Einstein relation[1].

METHODS: We used Nikon Eclipse Ti2 wide field fluorescent microscope to image hydrogels filled with Ø 200 nm fluorescent tracers (Bangs Laboratories). In our proof-of-concept research, we used Geltrex™ and collagen type I from rat-tail, both in two different concentrations. For Geltrex™ concentrations were 10 mg/ml and 7 mg/ml, and for collagen I 1.5 mg/ml and 1 mg/ml. For data analysis and visualization, we used our recently developed MuRheo software.

MuRheo does particle detection and tracking based on optimized nearest neighbour algorithm[2]. When 3D data is used, different Z-levels are processed in parallel for faster computations. To study changes in 3D microstructures of hydrogels during hydrolytic degradation, we imaged focus stacks from the same locations in the samples for two weeks. The statistical overview created in MuRheo shows changes in pore volumes of hydrogels, defined by adjustable mean square displacement (MSD) threshold.

RESULTS: Our data shows that with Geltrex™ the microstructure is more heterogenous when concentration is higher, while collagen type I hydrogels are more similar between each other's. Furthermore, the difference between heterogeneities of samples was observed only during the first week of incubation.

We have found that with collagen type I apparent modulus of polymer network decreases 20% while pore volume increases 60% due to hydrolytic degradation in one week. Figure 1 shows the visualization of highly heterogenous microstructure and the quantified changes in pore volume and apparent modulus.

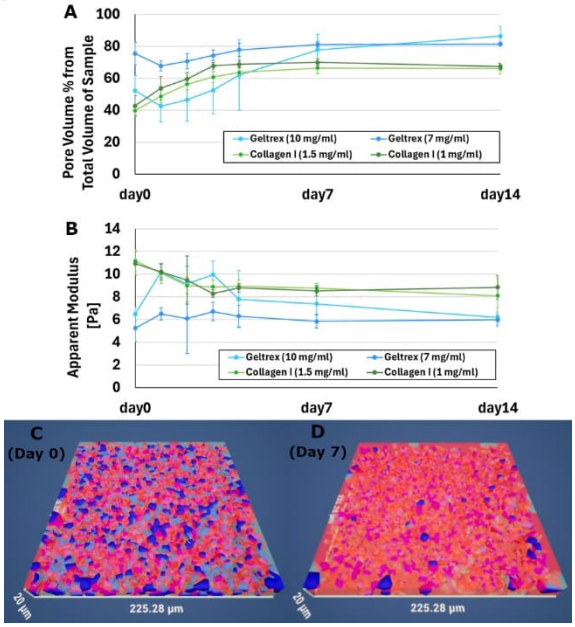

Fig. 1: (A) Change in pore volume over time based on highly mobile tracer particles. (B) Average apparent modulus measuring hydrogel network stiffness change over time. (C) & (D) Example microstructural visualizations of Geltrex™ hydrogel produced in MuRheo with red showing pores and blue molecular network.

DISCUSSION & CONCLUSIONS:
Our MPT-based 3D microrheology is shown to work in studying the effect of hydrolytic degradation on hydrogel microstructure, enable by our in-house developed analysis software MuRheo.

ACKNOWLEDGEMENTS: We thank the Tampere Imaging Facility for support with microscopy and the Centre of Excellence in Body-on-Chip Research for funding this study.

REFERENCES: [1]Zia, R. N. (2018). Active and passive microrheology: Theory and simulation. *Annu. Rev. Fluid Mech.*, *50*(1), 371-405.

[2]Crocker, J. C., & Grier, D. G. (1996). Methods of digital video microscopy for colloidal studies. *J. Colloid Interface Sci.*, *179*(1), 298-310.

25. Oxidized Polysaccharides as Templates for Green Synthesis of Anti-inflammatory Polypyrrole Biomaterials

J. Vícha, L. Münster, M. Muchová, Z. Víchová, O. Vašíček, P. Humpolíček

Centre of Polymer Systems, Tomas Bata University in Zlín, Czech Republic

INTRODUCTION: Polypyrrole (PPy) is a conductive polymer with significant potential in biomedicine due to its antioxidant and electrical properties. However, its broader application is hindered by poor processability, limited biodegradability, and the tendency of PPy to leach from composite matrices due to its lack of covalent bonding. Conventional methods to covalently anchor PPy often require toxic linkers, complex synthetic pathways, and provide minimal control over the PPy deposition. This work introduces a novel, green and versatile technology based on the spontaneous aldol condensation between pyrrole and dialdehyde polysaccharides (DAPs), demonstrated on two distinct biomaterial morphologies: electrospun nanofibers and injectable hydrogels, both exhibiting potent anti-inflammatory effects.

METHODS: The method is based on a spontaneous aldol condensation between the aldehyde groups of DAP and the pyrrole rings, covalently tethering pyrrole to the polysaccharide backbone, following its shape. This "pyrrole-decorated" template is bioactive on its own and can facilitate polymerization of added pyrrole, yielding a covalently bound DAP-PPy copolymer.

Nanofibers: Chitosan-based nanofibers were fabricated via electrospinning, utilizing DAC as a dual-function reagent that simultaneously crosslinks the chitosan via Schiff bases and anchors PPy (via aldol condensation).

Hydrogels: Injectable, shear-thinning hydrogels were formulated using soluble chitosan and DAC-anchored PPy, loaded with bone morphogenetic protein-2 (BMP-2) for bone defect regeneration.

RESULTS: The aldol condensation mechanism successfully anchored PPy to the polysaccharide matrices. The resulting covalently crosslinked chitosan/DAC/PPy nanofibers exhibited conductivities up to 11 mS/cm and enhanced mechanical and chemical stability. In vitro assays confirmed significant antibacterial activity against *S. aureus* and accelerated wound healing compared to neat chitosan nanofibers.

The composite hydrogels demonstrated excellent self-healing and shear-thinning properties, suitable for direct injection into the body. In a critical-size calvarial defect mouse model, the PPy-modified hydrogels effectively scavenged reactive oxygen species (ROS) and suppressed pro-inflammatory cytokines (IL-6), leading to reduced acute inflammation (lower CD45+ and CD68+ counts) and enhanced collagen deposition, higher early osteogenesis marker expression, and better bone regeneration.

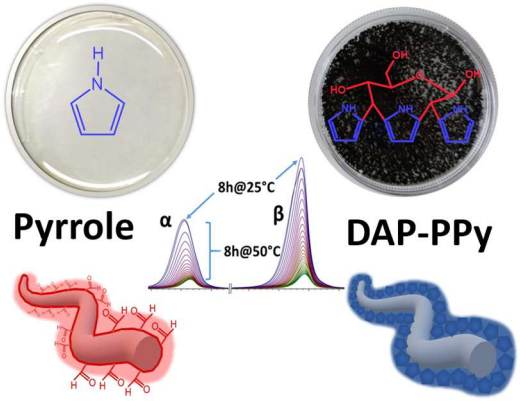

Fig. 1: Simplified scheme of the DAP-PPy reaction on the example of nanofibers.

DISCUSSION & CONCLUSIONS:
We have developed a green synthetic route to covalently bond PPy to polysaccharide matrices *via* aldol condensation. The resulting biomaterials combine the biocompatibility of polysaccharides with the conductivity and anti-inflammatory properties of PPy. Whether processed into nanofibers for wound dressings or hydrogels for bone regeneration, these composites provide a bioactive platform that modulates the immune response and accelerates tissue repair.

ACKNOWLEDGEMENTS: This work was supported by the Czech Science Foundation project 24-11534S.

REFERENCES: Vícha J, et al. ACS Sustain Chem Eng. 2025;13:8435-8446; Muchová M, et al. Int J Biol Macromol. 2025;308:142105.

26. M1 and M2 macrophage-derived extracellular vesicles differentially influence cellular and molecular responses to titanium implants *in vivo*

J. Philip[1], H. Ben Amara[1], A. Johansson Loo[1], F. Asa'ad[1,2], O. Omar[3], P. Thomsen[1]

[1]Department of Biomaterials, Institute of Clinical Sciences, Sahlgrenska Academy, University of Gothenburg, Sweden, [2]Department of Oral Biochemistry, Institute of Odontology, Sahlgrenska Academy, University of Gothenburg, Sweden, [3]Department of Biomedical Dental Sciences, College of Dentistry, Imam Abdulrahman bin Faisal University, Saudi Arabia

INTRODUCTION: Macrophages are key orchestrating cells during the tissue response to implanted biomaterials [1]. Extracellular vesicles (EVs) mediate cell-to-cell communication via transferring cargo between cells [2]. EVs have been used in the treatment of various diseases [3]; however, the role of macrophage-derived EVs during biomaterial integration or rejection has not been thoroughly investigated.

METHODS: A soft tissue model in rats was employed to investigate the effects of M1 and M2 macrophage-derived EVs on the cellular and molecular responses during titanium (Ti) implant integration. Ti discs (9 ´1.4 mm) were implanted subcutaneously with and without M1 or M2 EVs to evaluate cellular and tissue responses in three peri-implant compartments using cell counting, histomorphometry, confocal microscopy and quantitative polymerase chain reaction (qPCR) after 1 and 21 d (n = 8/group/time point). Kruskal–Wallis and Wilcoxon signed-rank tests were used for statistics ($p < 0.05$).

RESULTS: Despite similarities such as low cytotoxicity and leukocyte influx, predominantly mononuclear cells, in the Ti, M1 EV, and M2 EV groups, pronounced immunomodulatory responses were induced by both M1 and M2 EVs. M1 EVs promoted polymorphonuclear and eosinophilic cell infiltration, whereas both M1 and M2 EVs induced multinuclear giant cell formation at 21 d. PKH67-labeled M1 EVs were more efficiently internalized than M2 by implant-adherent cells (*Fig. 1*). M1 EVs promoted proinflammatory gene programs and interferon regulatory factor-7 (*Irf7)* expression. M2 EVs promoted collagen-1a1 (*Col1a1)* expression in implant-adherent and tissue cells than in the Ti group. A thicker peri-implant fibrous capsule was evident in the M2 EV group than in the Ti group after 21 d (*Fig. 2*).

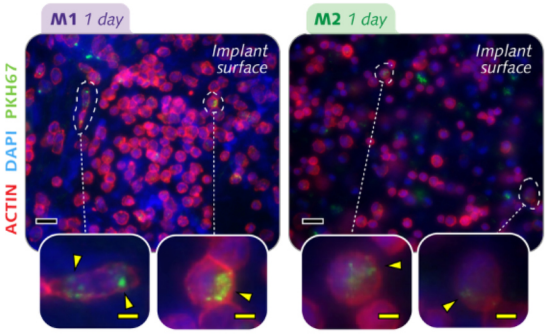

Fig. 1: Fluorescence micrographs showing implant-adherent cells in the M1 EVand M2 EV groups internalizing PKH67-labeled EVs at 1 d (Scale bars: black = 50 μm, yellow = 5 μm).

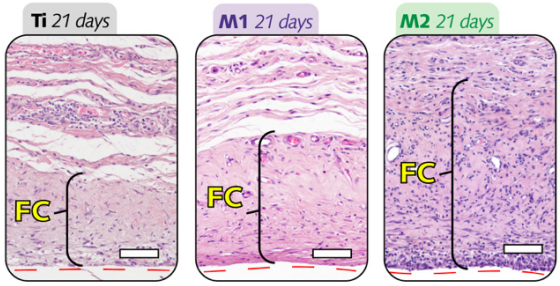

Fig. 2: Sections showing the fibrous capsules around implants in the Ti, M1 EV, and M2 EV groups at 21 d (Scale bar: 50 μm).

DISCUSSION & CONCLUSIONS: Macrophage-derived EVs could influence tissue responses around Ti implants. M1 EVs can modulate peri-implant tissue response towards a more proinflammatory state, whereas M2 EVs can induce a profibrotic tissue response. Our findings suggest that macrophage-derived EVs promote phenotype-dependent inflammation and immunomodulation around implants.

ACKNOWLEDGEMENTS: The Swedish Research Council; the ALF agreement; the IngaBritt and Arne Lundberg Foundation; the Sylvan Foundation; the Hjalmar Svensson Foundation; and the Area of Advance Materials of Chalmers and GU Biomaterials.

REFERENCES: [1]Yang et al (2023), *Nat Commun*, **14**(1):5995. [2]Valadi et al (2007), *Nat Cell Biol*, **9**(6):654-9. [3]Wang et al (2021), *Basic Clin Pharmacol Toxicol*, **128**(1):18-36.

27. Toward physiologically relevant metrics of bone mineral composition

J. Ewerman[1], F.B.G. Zambardino[1], H. Ben Amara[1], A. Palmquist[1], F.A. Shah[1]

[1]*Department of Biomaterials, Sahlgrenska Academy, University of Gothenburg, Sweden*

INTRODUCTION: Bone extracellular matrix is a nanocomposite material consisting of an organic matrix, mainly collagen type-I, and an inorganic matrix, i.e., bone mineral. The structure and chemical composition of bone mineral is a heavily debated subject and it is often incorrectly labelled as "hydroxy(l)apatite" (HAp) (1). This mislabelling complicates bone mineral characterisation since it places preconceptions on both structural and chemical properties of the mineral, e.g., that the calcium to phosphorous ratio (Ca/P) "should" be ~1.67 (i.e., the stoichiometric value of Ca/P for HAp) in mature bone. As a result, this leads to misinterpretation of experimental data as it ignores the cation and anion substitutions, such as carbonate (CO_3^{2-}) occupying trivalent anionic phosphate (PO_4^{3-}) sites in the apatite crystal lattice (also called B-type substitution) (2). Thereby, bone mineral is better described as an ion-substituted carbonated apatite (1). We present a simple approach towards a realistic measurement of elemental composition of bone mineral by accounting for cation and anion site substitutions (3).

METHODS: Bovine bone slices were commercially sourced (https://boneslices.com) and systematically deproteinised using 5 % NaOCl at 4 °C for up to 168 h. Energy-dispersive X-ray spectroscopy (EDX) was used for elemental analysis. Raman spectroscopy was used to monitor deproteinisation. Phosphorous correction was done by accounting for B-type carbonate substitution using Raman spectroscopy (1070/960 cm^{-1}) and Fourier transform infrared spectroscopy (FTIR; 872/1020 cm^{-1} and 1412/1020 cm^{-1}). Backscattered electron scanning electron microscopy (BSE-SEM) was used to image the bone slices. One-way analysis of variance (ANOVA) with post hoc Bonferroni correction was used for statistical analysis of the cation-to-anion ratios (CAR) between 0 h, 96 h, and 168 h.

RESULTS: Raman spectroscopy shows a gradual decrease in organic matrix (amide III) in relation to mineral content ($\nu_2PO_4^{3-}$) (**Fig. 1A**), going from undeproteinised (whole bone) to completely deproteinised after 168 h of NaOCl exposure, further validated by increasing atomic number (*Z*) contrast on BSE-SEM (**Fig. 1C**), and decreasing organic matrix content based on inverse mineral-to-matrix ratio (1/MMR) (**Fig. 1D-E**). EDX reveals that the CARs (Ca/P, Ca+Mg+Na/P) increase from 0 h to 96 h and 168 h ($p < 0.0001$, $p < 0.0001$), and from 96 h to 168 h ($p < 0.0001$). Additionally, phosphorus correction (P_{corr}) based on Raman and FTIR spectroscopy generally decreases the overall CAR values (**Fig. 1D-E**).

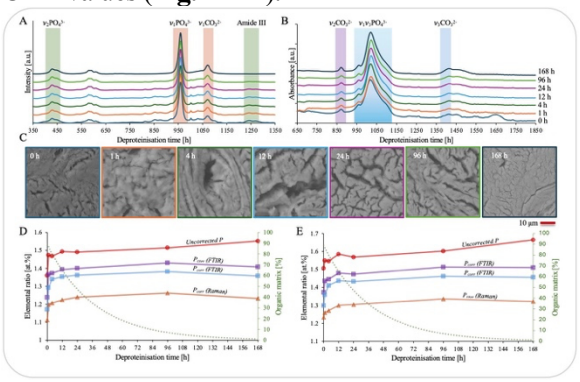

Fig.1: (A) Raman spectra. (B) FTIR spectra. (C) BSE-SEM. (D) Ca/P ratios. (E) Ca+Mg+Na/P ratios. Secondary y-axes show the organic matrix content based on inverse mineral-to-matrix ratio (1/MMR).

DISCUSSION & CONCLUSIONS: The increase in CAR values using uncorrected phosphorus values over deproteinisation time show that they are strongly influenced by the organic matrix, making whole bone inadequate to use for analysing elemental composition of bone mineral. Additionally, the decrease in CAR values obtained using corrected phosphorous values, for both Raman and FTIR spectroscopy, underscores that uncorrected CAR values are grossly overestimated as the phosphate sites occupied by carbonate ions in the apatite lattice are ignored. Correlative EDX and vibrational spectroscopy performed on completely deproteinised bone reveals a more realistic view of bone mineral elemental composition by eliminating uncertainties introduced by the organic matrix and accounting for expected cation and anion substitutions.

ACKNOWLEDGEMENTS: Funding from Svenska Sällskapet för Medicinsk Forskning (SSMF), Vetenskapsrådet, the IngaBritt and Arne Lundberg Foundation, the Hjalmar Svensson Foundation, and the Chalmers Materials Analysis Laboratory (CMAL) is acknowledged.

REFERENCES:

1. Wopenka B, Pasteris JD. Mat Sci Eng C. 2005;25.
2. Taylor EA, Mileti CJ, Ganesan S, Kim JH, Donnelly E. Calcif Tissue Int. 2021;109.
3. Shah FA. Acta Biomater. 2025;196.

28. Nanoencapsulated microRNA-31 for the Treatment of Aphthous Ulcers

PS. Yin[1], KC. Yang[1,2]

[1]School of Dental Technology, College of Oral Medicine, Taipei Medical University, Taipei, Taiwan [2] Graduate Institute of Biomedical Materials and Tissue Engineering, College of Biomedical Engineering, Taipei Medical University, Taipei, Taiwan

INTRODUCTION: Chitosan exhibits antimicrobial activity and promotes re-epithelialization and angiogenesis, making it a suitable candidate for wound management. Aphthous ulcers are common oral ulcerative lesions that can be caused by trauma and pathogen infection. However, currently available medications only relieve pain, rather than addressing the cause. miRNA-31 is reported to modulate the inflammatory response and enhance re-epithelialization, potentially accelerating the healing of ulcerative lesions in the oral cavity. Therefore, manipulation of miR-31 is proposed for treating aphthous ulcers in this research project. However, exogenous miRNAs can be degraded shortly *in vivo*. On the contrary, nanoparticle (NP)-mediated delivery can protect miRNAs against nuclease degradation and improve cell retention. Accordingly, chitosan NPs will be used for miR-31 transfection for this project.

METHODS: Human oral epithelial cells were stimulated with tumor necrosis factor-alpha (TNF-α), and the injured cells were transfected with mR-31 by chitosan NPs. The cell cycle, proliferation, viability, gene expression, and protein production for inflammatory cytokines/chemokines and extracellular components were studied. NF-κB, STAT3, and TGF-β signalling pathways were demonstrated, and the effects on wound healing and cell migration were analysed.

RESULTS: Chitosan NPs exhibited high biocompatibility. However, transfection of miR-31 decreased cell proliferation and viability. Overexpression of miR-31 downregulated the mRNA levels of inflammatory cytokines *TNFA*, *IL1B*, *IL6*, *IL6ST*, and *IL8*, while increasing *IL6R*, *COL4A1*, and *SMAD4* in cells stimulated by TNF-α. The results of the inflammatory protein array revealed that miR-31 mimic transfection decreased the secretion of IL-6, IL-6sR, and IL-8. Otherwise, the increase in TIMP-2 product may promote the remodelling of stomatitis wounds. The results of the Western blot revealed that miR-31 suppressed NF-κB/STAT3 signalling pathway in TNF-α-stimulated oral epithelial cells.

DISCUSSION & CONCLUSIONS: Modulation of miR-31 using chitosan NPs can regulate the inflammatory response and promote extracellular matrix remodelling in oral epithelial cells and has the potential to treat aphthous ulcers.

ACKNOWLEDGEMENTS: This work was supported by the National Science and Technology Council, Taiwan (NSTC 113-2813-C-038-109-B and NSTC 114-2221-E-038-017).

29. Impact of the molecular weight on the physicochemical and biological properties of hydrogel precursors for microgel formation

K.Walczak[1], K. Reczyńska-Kolman[1], E. Pamuła[1]

[1] *Faculty of Materials Science and Ceramics, AGH University of Krakow, Poland*

INTRODUCTION: Regeneration of articular cartilage remains a major clinical challenge due to its avascular and aneural nature, which limits nutrient supply and intrinsic repair [1]. Current surgical approaches, including microfracture, autologous chondrocyte implantation, and osteochondral grafting, can improve symptoms but often result in fibrocartilage formation and fail to restore long-term tissue function [2], [3]. The aim of this study was to investigate the physiochemical and biological properties of oxidized hyaluronic acid with different molecular weights and to identify materials most suitable for microgel formation.

METHODS: Hyaluronic acid (HA, Contipro) with molecular weights (MW) of 90–130 kDa, 500–750 kDa, and 1250–1500 kDa was oxidized in aqueous solution using sodium periodate at HA:$NaIO_4$ molar ratios of 1:1, 1:2, and 1:3 to introduce aldehyde functionalities along the polymer chains. The oxidation reaction was conducted under dark conditions at room temperature and terminated with ethylene glycol. Purification of oxidized HA was achieved by dialysis against distilled water using membranes with molecular weight cut-offs adjusted to the polymer size (3.5 or 10 kDa), followed by freeze-drying. At this stage, Fourier-transform infrared spectroscopy (FTIR) was performed to confirm successful oxidation, and the TNBS assay was used to quantify the degree of oxidation of the obtained materials.

Oxidized HA was subsequently dissolved at concentrations of 10 and 12% (w/v) for 90–130 kDa HA and 2, 4, and 6% (w/v) for higher MW variants. Hydrogel formation was achieved via hydrazone crosslinking with adipic acid dihydrazide (ADH) used at concentrations of 1.0, 1.5, and 2.0% (w/v). The oxi-HA and ADH solutions were mixed at a fixed volume ratio of 4:1, resulting in rapid gelation. The hydrogels were poured onto Petri dishes, punched into 12 mm discs, frozen at −80°C, and freeze-dried to obtain porous hydrogel constructs.

At this stage, the hydrogels were characterized using a combination of techniques to evaluate their structural, mechanical, and functional properties. Fourier-transform infrared spectroscopy (FTIR) was employed to confirm successful crosslinking, while rheological measurements assessed viscoelastic behavior and self-healing capacity. Degradation studies provided insight into material stability over time. Morphological analysis was performed using both optical and scanning electron microscopy to examine the microstructure and surface features of the hydrogel scaffolds. Lastly, biological evaluation (AlamarBlue assay, Live/Dead staining and LDH assay) enabled to determine the most promising combinations for microgel fabrication.

RESULTS: FTIR confirmed successful oxidation through aldehyde peaks, and TNBS assay showed higher HA:$NaIO_4$ ratios increased oxidation. The hydrogels fully recovered within 30 minutes, exhibited rapid water uptake, and had a porous structure. In vitro tests demonstrated that they were cytocompatible and non-toxic, supporting their biomedical potential.

DISCUSSION & CONCLUSIONS: The observed physicochemical and functional properties of the hydrogels were strongly dependent on both the degree of oxidation and the molecular weight of hyaluronic acid. Higher oxidation levels generally led to increased crosslinking density, enhancing structural recovery and water uptake, while molecular weight influenced network formation and porosity. These results provided valuable insights into the relationship between polymer characteristics and hydrogel behavior, guiding the optimization of formulations. Building on this understanding, we proceeded to the next stage of our study: the preparation of microgels with tailored properties for subsequent biological and mechanical evaluation.

ACKNOWLEDGEMENTS: This study was supported by the Program „Excellence initiative – research university" for the AGH University of Krakow.

REFERENCES: [1] Roseti L. et al., *J Exp Orthop*, 2022. [2] Barui S., *Regenerative Biomaterials*, 2023. [3] Zhang Y. et al., *Bioactive Materials*, 2023.

30. Polysaccharide-Based Microguards for Injectable Platelet-Rich Fibrin

K. Egle[1,2], A. G. Guex[3,4,5], E. Kelle[1,2], I. Salma[2,6,7], M. D`Este[3], A. Dubnika[1,2]

[1]Institute of Biomaterials and Bioengineering, Faculty of Natural Science and Technology, Riga Technical University, Riga, LV, [2]Baltic Biomaterials Centre of Excellence, Headquarters at Riga Technical University, Riga, LV, [3]AO Research Institute Davos, AO Foundation, Davos, CH, [4]Department Research, University Center for Dental Medicine Basel UZB, University of Basel, CH, [5]Department of Biomedicine, University of Basel, Basel, CH, [6] Institute of Stomatology, Riga Stradins University, Riga, LV, [7]Department of Oral and Maxillofacial Surgery, Riga Stradins University, Riga, LV

INTRODUCTION: Injectable platelet-rich fibrin (PRF) is a second-generation platelet concentrate consisting of fibrin enriched with autologous platelets and leukocytes. Its purpose is to accumulate platelets, immune promoters and release cytokines from the fibrin clot. A key limitation of injectable PRF is its rapid clearance from the injection site, so a delivery system that sustains growth-factor release could enhance cellular responses and improve tissue repair. The current study explores a novel approach by integrating PRF with fucoidan/chitosan microparticles (FU_CS µPs) to investigate whether this formulation can prolong the release of bioactive factors, while providing injectability and compatibility with other tissue regeneration materials.

METHODS: A 0.25% (w/v) chitosan solution in 0.1% acetic acid was mixed with 1.5% (w/v) fucoidan in water (1:1) under stirring to form FU_CS µPs. The particles were neutralized in water, then centrifuged, frozen, and lyophilized. Written consent from all donors was obtained to use their blood samples to be used in the research study (ethical approval No. 6-2/10/53). PRF was prepared by centrifugation, and 1 ml of liquid PRF was used to form each PRF sample. For PRF/FU_CS µPs composites, 1 ml of PRF was mixed with 10 mg of FU_CS µPs using a spatula and allowed to coagulate prior the characterization. All synthesized samples were characterized by SEM (Fig.1) and rheology, evaluated the release kinetics of bioactive agents. In vitro cell viability was evaluated towards mouse derived pre-osteoblast cells (MC3T3-E1), human osteoblasts (hOB), and human mesenchymal stromal (hMSC) cells, and tested for osteogenesis in MC3T3-E1 cells.

RESULTS: The ELISA results showed distinct release profiles between pure PRF and PRF/FU_CS µPs over time, with pure PRF releasing higher levels of EGF, IL-8, and TGF-β1 than the PRF/FU_CS µPs composites. The FU_CS µPs particles maintained metabolic activity in primary hOBs and MSCs at 10 mg/mL, supporting their biological relevance. Alizarin Red S staining of MC3T3-E1 cells cultured with PRF, FU_CS µPs, and PRF/FU_CS µPs extracts at days 7, 14, and 21 showed enhanced calcium deposition with the composite. While PRF induced gradual mineralization, PRF/FU_CS µPs promoted earlier and stronger mineralization at all time points, indicating enhanced osteogenic differentiation.

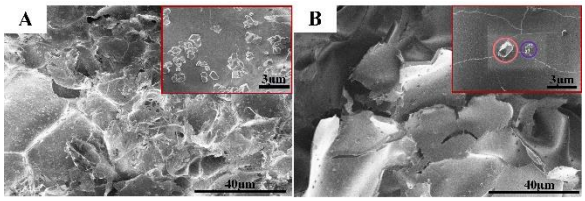

Fig. 1: SEM images of PRF matrice (A) and PRF/FU_CS µPs matrice (B).

DISCUSSION & CONCLUSIONS: FU_CS µPs constitute a distinct microparticulate platform that modulates the presentation of PRF-derived molecules through controlled physicochemical properties, enabling staged and biomimetic growth-factor release with prolonged bioactivity. The system supports osteogenic responses while maintaining cytocompatibility in relevant cell types, highlighting its potential as a tunable, bioactive biomaterial for regenerative applications.

ACKNOWLEDGEMENTS: The authors acknowledge financial support from the European Union's Horizon 2020 research and innovation programme under the grant agreement No. 857287 BBCE and 1.1.1.9 Research application No 1.1.1.9/LZP/1/24/088 of the Activity "Post-doctoral Research" "Development of *in vitro* model for bone substitute material cellular response evaluation (VIBE)".

31. Modelling diabetic wound healing *in vitro* for biomaterials research

K.Kajander[1], T.J.Heino[1]

[1]*Institute of Biomedicine, Faculty of Medicine, University of Turku, Finland*

INTRODUCTION:
Diabetic wounds represent a serious complication of diabetes and are frequently accompanied by infection. Bioactive glass (BG) S53P4 is known to have antimicrobial properties, and it can also promote the function of many cell types involved in soft tissue healing. Our aim was to set up an *in vitro* skin model with human cell lines to test the potential of BG S53P4 dissolution products in an environment with diabetic features.

METHODS: Normal dermal human fibroblasts (NHDFs) or green fluorescent protein (GFP)-expressing human umbilical vein endothelial cells (HUVECs) were cultured in cell culture conditions mimicking some of the features observed in diabetic conditions. The cells were cultured either in normal glucose concentration (5.5 mM) or high glucose concentration (25 mM). The cell cultures were further supplemented with different concentrations (0-800 µM) of methylglyoxal (MGO), which *in vivo* is responsible for oxidative stress and formation of advanced glycation end products.

The feasibility of the model was first assessed by examining the proliferation rate of both NHDFs and HUVECs under diabetic conditions using the IncuCyte Live Cell Analysis System. Furthermore, the viability of the cells was determined with the alamarBlue assay. The wound closure capacity of fibroblasts cultured in the *in vitro* diabetic model was examined with a scratch wound assay utilizing the IncuCyte Scratch Wound Analysis Software module.

After the cell culture model optimization, it was used to assess the effects of BG S53P4 dissolution products on fibroblasts first maintained under diabetic conditions. For this, the proliferation assay, viability assay, and scratch wound assay were repeated with the addition of BG S53P4-conditioned media.

RESULTS: According to our results, both fibroblasts and endothelial cells show a dose-dependent response to MGO, with higher concentrations leading to decreased proliferation and viability. Notably, these effects were consistent across both high and normal glucose concentrations. In a scratch wound assay, fibroblasts demonstrated enhanced wound closure in normal glucose environment compared to high glucose.

BG S53P4 conditioned medium appeared to promote fibroblast motility even in high glucose environment. Interestingly, combination of BG and MGO slightly impaired fibroblast migration. It also seems that BG S53P4 dissolution products in the concentration used in the current study could not reverse the harmful effect that MGO had on fibroblast proliferation and viability.

DISCUSSION & CONCLUSIONS: It is possible to develop *in vitro* models that include relevant human cell types and disease specific conditions for the testing of biomaterials. The models can be especially useful, if commonly used animal models differ greatly from humans. For example, the major mechanisms of wound healing are different between mouse and human, thus elucidating the molecular mechanisms of wound healing in a reductionist model can be valuable.

In our cell culture model, we were able to demonstrate the effects of hyperglycaemia and oxidative stress on some of the functions of fibroblasts and endothelial cell. Further research is still needed to conclude if the positive effects of BG S53P4 reported elsewhere could also be established in a diabetic environment.

ACKNOWLEDGEMENTS: This research is funded by Business Finland (T.J. Heino).

32. IMPACT OF INJECTABLE PLATELET-RICH FIBRIN HANDLING ON BIOLOGICAL PROPERTIES

Lauma Ievina[1,2], Karina Egle [1,2], Elena Della Bella[3], Lana Micko[2,4,5], Ilze Salma[2,4,5], Arita Dubnika[1,2 *]

[1]Institute of Biomaterials and Bioengineering, Riga Technical University, Riga, Latvia; [2]Baltic Biomaterials Centre of Excellence, Riga, Latvia; [3]AO Research Institute Davos, Davos Platz, Switzerland; [4]Institute of Stomatology, Riga Stradins University, Riga, Latvia; [5] Department of Oral and Maxillofacial Surgery, Riga Stradins University, Riga, Latvia.

INTRODUCTION: Injectable Platelet-rich fibrin (i-PRF) is a protein matrix with growth factors and immune cells extracted from venous blood via centrifugation [1]. Although widely used, results from studies using this autologous material are still unpredictable. This is at least due to the unexplored nature of i-PRF interactions [2]. Storage conditions and combination with materials can affect the biological properties of this blood derivative; thus, the goal was to identify how handling conditions influence the biological properties of i-PRF.

METHODS: i-PRF was isolated from healthy donor blood by centrifugation (5 and 3min, 700 rpm) and tested for growth factor release after multiple handling procedures: combined with materials - collagen (Collacone, Biotiss), bone substitute/ collagen (Bio-Oss, Geistlich), and hydroxyapatite/ βtricalcium phosphate (CeraForm, Teknimed) scaffolds by impregnation; frozen in -80 °C or flash frozen by N_2. The cytokine release from these i-PRF samples was measured over 10 days in α-MEM using ELISA. Fresh and frozen i-PRF samples were tested for viability with live/dead staining using Ethidium homodimer (MedChemExpress, New Jersey, USA) and Calcein-AM (Sigma-Aldrich, Saint Louis, MO, USA).

RESULTS: Although material impregnation with i-PRF does not prolong the growth factor release compared to pure i-PRF, the contact with materials can induce high concentration pro-inflammatory cytokine release, especially with collagen-containing materials, reaching up to 37.5-fold increase in cytokine concentration (Fig. 1). i-PRF freezing also significantly reduces the viability of cells contained in i-PRF, as after only 1 week of storage, the samples show a low or no viability. The growth factor release was also affected. After 7 days, TGF-β1 release decreases by up to 50 % from frozen samples than from fresh ones. Notably, IL-8 is only detectable in fresh i-PRF samples and is undetectable in cryopreserved samples.

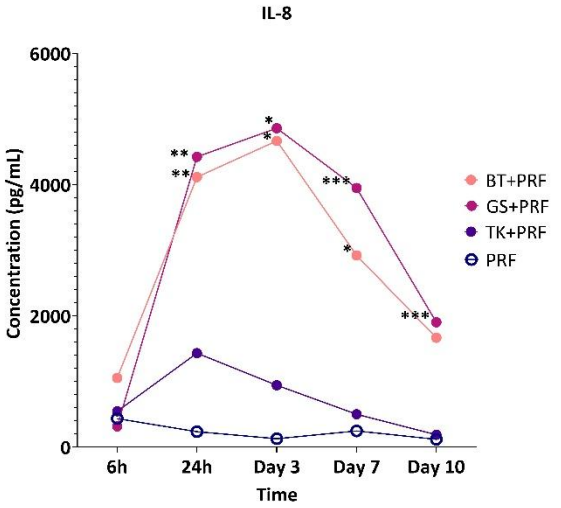

Fig.1: IL-8 release over 10-day period. BT- Biotiss, Collacone, GS – Geistlich, Bio-Oss® Collagen, TK– Teknimed, CeraForm. $p < 0.05$ (*), $p < 0.01$ (**), $p < 0.001$ (***) compared to i-PRF.

DISCUSSION & CONCLUSIONS: The impact of handling conditions on i-PRF properties remains largely unexplored, despite their potential influence on both clinical and experimental outcomes. The choice of material combination with PRF can affect the growth factor release properties. i-PRF storage conditions affect the viability of this material, thus impacting the biological properties. These results prove that additional studies exploring different i-PRF handling procedures should be conducted to fully predict the i-PRF outcomes.

ACKNOWLEDGEMENTS: This project has received funding from the European Union's Horizon 2020 research and innovation programme under grant agreement No 857287 and by the EU RRF within project No 5.2.1.1.i.0/2/24/I/CFLA/003 academic doctoral grant, ID 1023

REFERENCES: 1. Pavlovic et al, *Open Med., 2021,* 16, 446–454. 2. Ghanaati S. et al, *Oral Implantol*. 2018; 44: 471–92

33. Optimised Voronoi Lattices as Bone Surrogates

L.Gargan[1], R.Hewson[2], R.Murphy[3], M.Bryant[1], R.M.Hall[1]

[1]School of Engineering, University of Birmingham, Birmingham, UK [2]Department of Aeronautics, Imperial College London, London, UK [3]Dyson School of Design Engineering, Imperial College London, London, UK

INTRODUCTION: Characterisation of orthopaedic implants is typically completed using cadaveric bone due to its similarity to human bone *in vivo*. However, cadaveric bone is highly variable with physiological factors leading to large uncertainties in test results. Artificial bone surrogates capable of replicating the behaviour of human bone are an attractive alternative to relieve some of the complications associated with cadaveric bone. Whilst porous models, such as polymer foams, have been used extensively, replication of the full range of mechanical performance of human bone using artificial materials is yet to be achieved due to its complex hierarchical structure. As an alternative, optimisation of these porous models, such as Voronoi-based lattices, to match specific mechanical properties could allow for models that replicate the complex mechanical behaviour of human bone whilst maintaining a more consistent representation of its architecture. Whilst previous studies have favoured parametric testing, evaluating a limited number of discrete parameters and selecting the best-performing option for individual mechanical requirements, this work utilises a formal optimisation framework capable of exploring a large continuous design variable space to satisfy specified mechanical objectives and produce structures that mimic both the mechanical and morphological properties of human trabecular bone. This work aims to demonstrate the potential of a gradient-based formal optimisation framework for production of mechanically suitable trabecular bone surrogates.

METHODS: The computational framework presented in this work utilises the python package Firedrake for production and characterisation under the finite element method of Voronoi-based geometries. Optimisation is completed using the Interior Point Optimiser (IPOPT) integrated with HSL (formerly the Harwell Subroutine Library). Results for this work were generated by optimising under compressive loading the classification of geometry as plates or rods at each element, as well as the associated thickness. An initial rod-dominated structure was produced with 18 Voronoi cells. Optimisation tests were run with tight volume bounds of ±5% of initial BV/TV for a maximum of 30 iterations at a resolution of 24^3 due to current computational power constraints. Post-optimisation, structures were reproduced at a resolution of 128^3 for visualisation only.

RESULTS: The gradient-based optimisation algorithm explored a design space of 31,250 variables, converging within 30 iterations to achieve an improvement of 7.3% in global stiffness. Total BV/TV of the structure increased by 5% with successful redistribution of available material for mechanical performance demonstrated in Figure 1.

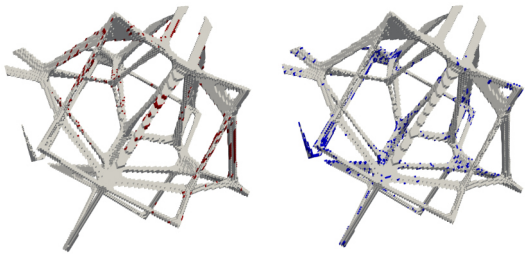

Fig. 1: Voronoi Structures with material added during optimisation in red (left) and material removed in blue (right).

DISCUSSION & CONCLUSIONS: The results presented in this work demonstrate the feasibility of this computational framework for optimisation of Voronoi lattices, with successful exploration of a large design variable space leading to the potential for improved structures over the previously favoured parametric method. Furthermore, due to the development of this framework from the ground up, complete control over each stage of the design and optimisation process is possible, affording feasible applications across orthopaedic research where microarchitecture is influenced by mechanical loading requirements. Whilst further work is required to refine this framework and evaluate its full potential, initial work demonstrates significant applications in design and evaluation of mechanically suitable orthopaedic implants.

ACKNOWLEDGEMENTS: This work was supported by the UKRI Engineering and Physical Sciences Research Council [grant number EP/W00709].

34. Epigallocatechin-3-Gallate Bioactive Coatings on Piranha-Treated Titanium Implants Limit Early Oral Biofilm Formation.

L. Virto[1], P. Nuevo[1], J. Gil[2] M. Sanz[1]

[1] ETEP (Etiology and Therapy of Periodontal and Peri-Implant Diseases) Research Group, University Complutense (UCM), Madrid, Spain, [2] Technological Health Research Center, Biomaterials of the Faculties of Medicine and Dentistry, International University of Cataluña, Barcelona

INTRODUCTION: Immobilizing functional molecules is a key strategy to enhance dental implant biofunctionality. This study aims to develop bioactive coatings using Epigallocatechin-3-gallate (EGCG), a flavonoid with antimicrobial, antioxidant, and anti-inflammatory properties (1), on piranha-treated surfaces (2).

METHODS:
Piranha-passivated titanium dental implants were coated with polydopamine (PDA), amino-terminated polyethylene glycol (aPEG), and EGCG. A multispecies *in vitro* dynamic biofilm model was established using a Robbins device under oral-mimicking anaerobic conditions. The inoculum consisted of *Streptococcus oralis, Veillonella parvula, Actinomyces naeslundii, Fusobacterium nucleatum, Aggregatibacter actinomycetemcomitans*, and *Porphyromonas gingivalis*. Biofilms were allowed to form for 6 hours on coated and uncoated (control) surfaces. Subsequently, DNA was isolated, and bacterial quantification was performed by qPCR using species-specific primers and probes targeting the 16S rRNA gene. Statistical differences were assessed using a general linear model ($p<0.05$).

RESULTS: Quantitative qPCR analysis revealed that EGCG-functionalized surfaces effectively inhibited bacterial adhesion compared to piranha-treated controls after 6 hours. While a consistent reduction in bacterial counts was observed across all tested strains, the coating displayed a particularly marked inhibitory effect against *A. naeslundii* and *A. actinomycetemcomitans*.

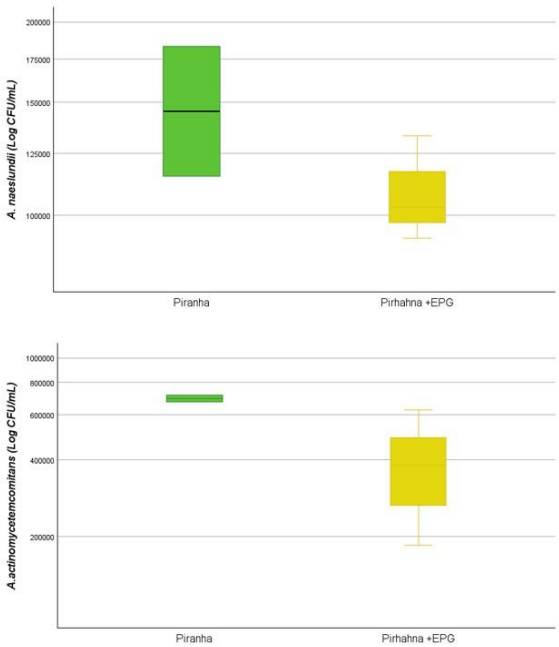

Fig. 1: Antibacterial effect of EGCG-coated, piranha-passivated titanium dental implants after 6 hours of biofilm development.

DISCUSSION & CONCLUSIONS: Overall, EGCG-functionalized titanium surfaces significantly reduced early multispecies biofilm formation under dynamic oral-like conditions. These coatings appear to be a promising strategy to improve dental implant biofunctionality and reduce the risk of peri-implant infections.

REFERENCES: 1 Higuchi M, Abiko Y, Washio J, Takahashi N. Antimicrobial effects of epigallocatechin-3-gallate on periodontal bacteria. Arch Oral Biol. 2024;167. **2** Nuevo P, Virto L, Ribeiro-Vidal H, Gil J, Sanz M. Piranha-passivated dental implant surface against oral biofilm formation. Clin Oral Implants Res. 2025.

35. Room-temperature Consolidated Amorphous Calcium Phosphate Bioceramics as Drug Delivery Systems

L.Dauge[1,2], J.Locs[1,2]

[1] *Institute of Biomaterials and Bioengineering, Riga Technical University, Riga, LV,*

[2] *Baltic Biomaterials Centre of Excellence, Headquarters at Riga Technical University, Riga, LV*

INTRODUCTION: Drug delivery for treatment of bone ailments carries numerous challenges. Slow tissue absorption and quick clearance lead to low therapeutic efficacy and increased risk for systemic side effects. Using localized drug delivery systems (DDS) helps increase the therapeutic efficiency. Various DDS vehicles for bone tissue have been explored, like calcium phosphate containing hydrogels, calcium phosphate cements and ceramic granules. Burst release of drugs is a mayor issue for ceramic DDS – the high processing temperatures only allow for them to be adsorbed on the surface of the finalised ceramic material. Encapsulation of drugs in the entire volume of a ceramic DDS would provide a much more sustained release profile.

METHODS: Room temperature consolidation (RTC) is a novel ceramic monolith production method, enabling low-energy, rapid creation of dense materials. Differing from the heat-dependent ceramic technology, high-pressure-driven RTC allows for non-crystalline or low crystallinity particle adjoining through dissolution-precipitation processes. E.g., amorphous calcium phosphate (ACP)'s metastability renders it impossible to sinter at elevated temperatures, but the hydrated structure and particle susceptibility to deformation make ACP a great candidate for RTC.

Strontium ranelate (SrRan) has been chosen as a model drug. It has proven its efficacy for treating post-menopausal osteoporosis in various clinical trials, but its oral bioavailability is low, and the therapeutical process is lengthy, with risks of serious systemic side effects.

RESULTS: At low drug concentrations and higher RTC pressures these ceramic DDS exhibit no burst release (Table 1), which can be attributed to the incorporation of the drug in the entire DDS volume (Fig. 1).

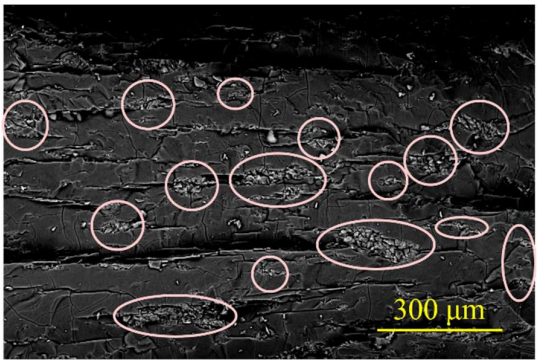

Fig. 1: SrRan dispersion in ACP bioceramics.

Table 1. Release duration of 50% of theoretical SrRan amount, depending on drug content and RTC pressure.

	1000 MPa	1100 MPa	1200 MPa
2.5 w/w% SrRan	30 days	33 days	33 days
5 w/w% SrRan	26 days	20 days	28 days
10 w/w% SrRan	5 days	9 days	20 days

DISCUSSION & CONCLUSIONS: The obtained results suggest that RTC approach has great potential in creating sustained release calcium phosphate bioceramic DDS for long term therapy. Further research should be done, using diverse medicinal compounds to test the benefits and limitations of this technology.

ACKNOWLEDGEMENTS: The authors acknowledge support from the European Union's Horizon 2020 research and innovation programme under the grant agreement No. 857287 (BBCE – Baltic Biomaterials Centre of Excellence).

The authors acknowledge support from European Regional Development Fund and state funded project No. 1.1.1.8/1/24/I/007 grant agreement No. 8012.

36. Cobalt-Doped Hydroxyapatite and Silicophosphates Bioceramics: Dual-Material Strategy for Enhanced Bone Regeneration and Angiogenic Support

Ł. Pajchel[1], W Gregorowicz[2], J. Kolmas[1]

[1] Department of Pharmaceutical Chemistry and Biomaterials, Faculty of Pharmacy, Medical University of Warsaw, [2]Students Scientific Group NANODRUG, Faculty of Pharmacy, Medical University of Warsaw

INTRODUCTION: Bone regeneration is a complex biological process requiring both osteogenic and angiogenic support. Hydroxyapatite (HA) and Silicophosphates (SP) ceramics, while established osteoinductive biomaterials individually, have limited intrinsic angiogenic capacity. Recent evidence demonstrates that cobalt ions (Co^{2+}) play a pivotal role in promoting vascularization through hypoxia-inducible factor (HIF) pathway activation, enhancing endothelial cell proliferation and VEGF expression. Strategic incorporation of cobalt into HA and SP matrices separately offers a rational approach to enhance the pro-angiogenic potential of these ceramics while preserving their osteogenic properties. This dual-material strategy addresses the critical need for biomaterials that simultaneously support bone formation and vascularization essential for successful regeneration of large bone defects. The present study investigates Co-doped HA (Co-HA) and Co-doped SP (Co-SP) ceramics as advanced bioceramics for enhanced bone regeneration [1].

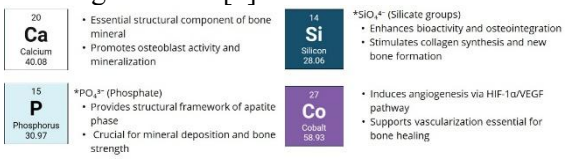

Fig. 1: The role of ions in biomaterials.

METHODS: Co-HA was synthesized using a well-established wet chemical method with varying cobalt concentrations [2]. Co-SP were prepared via a novel two-stage synthesis combining previously known techniques, optimized to achieve controlled cobalt incorporation [3]. Materials were characterized using X-ray diffraction (PXRD), Fourier-transform infrared spectroscopy (FT-IR), scanning electron microscopy (SEM), transmission electron microscopy (TEM), and Raman spectroscopy to assess phase composition, surface morphology, and structural properties. Elemental composition and Co^{2+} content were determined using atomic absorption spectroscopy (AAS) and energy-dispersive X-ray spectroscopy (EDS). *In vitro* biological studies were conducted using MTT and NRU assays to evaluate cell viability and biocompatibility. Results were compared between Co-doped and undoped control materials.

RESULTS: Synthesis of both cobalt-doped materials was successfully confirmed. Co-SP ceramics are presented in Fig. 2, demonstrating progressive color changes with increasing cobalt content. Contrary to previous reports on cobalt toxicity, appropriate Co^{2+} concentrations did not induce negative effects in MTT and NRU assays, demonstrating good biocompatibility.

Fig. 2: Synthesized Co-SP with increasing cobalt content. Visual appearance reflects varying degrees of Co^{2+} incorporation into the SP matrix structure.

DISCUSSION & CONCLUSIONS: Co-doped hydroxyapatite and Silicophosphates ceramics demonstrate significant potential for future clinical applications in bone regeneration and tissue engineering requiring angiogenic support.

ACKNOWLEDGEMENTS: Studies were supported by the National Science Center (Opus UMO-2023/51/B/NZ7/00555) and Medical University of Warsaw grant number: FW232/1/F/GW/N/22.

REFERENCES:

1.Gregorowicz, W.; et al. The Role of Cobalt Ions in Angiogenesis—A Review. *Int. J. Mol. Sci.* **2025**, 26(15), 7236.

2.Pajchel, Ł.; et al. Revisiting Physicochemical and Biological Properties of Zn^{2+}-Enriched Hydroxyapatite. *Nanotechnol. Sci. Appl.* **2025**, 18, 515–530.

3.Najafinezhad, A.; et al. A comparative study on the synthesis mechanism, bioactivity and mechanical properties of three silicate bioceramics. *Ceram. Int.* **2017**, 43(1), 919–932.

37. Proline-Rich Peptide–Enriched Hyaluronic Acid Gels Modulate Inflammation and Regeneration Markers Comparable to Enamel Matrix Derivative in a Porcine Wound Model

M. Santacroce[1], T. El Khassawna[2,3], C. De Luca[4], S.P. Lyngstadaas[1], H.J. Haugen[1]
1: Department of Biomaterials, Institute of Clinical Dentistry, University of Oslo, Oslo, Norway
2: Experimental Trauma Surgery, Faculty of Medicine, Justus Liebig University Giessen, Giessen, Germany
3: Faculty of Pharmacy, University of Jordan, Amman, Jordan
4: Department of Biomedical and Dental Sciences and Morphofunctional Imaging, University of Messina, Italy

INTRODUCTION: The study aims to evaluate whether proline-rich peptides (P2 and P6) enriched cross-linked HA exhibit comparable effects to Enamel Matrix derivative (EMD) on soft tissue wound healing in a porcine model.

METHODS: Twenty-two circular full-thickness skin wounds were created on the dorsal surface of six pigs. Five experimental groups were established based on the biomaterials used: **HA+P2**, **HA+P6**, **EMD**, **HA** and a **sham** group (no biomaterial applied). Each group consisted of four wounds. Two additional wounds served as indicators to monitor healing progress. When the indicator wounds reached 50% of their original diameter, tissue samples from all groups were collected for **histology**, **immunohistochemistry (anti-IL-10, anti-CD206, anti-CD163, anti-CD80 and anti-TNFα)**, and **proteomic analyses**. (Fig.1)

RESULTS: Proteomic analysis revealed a downregulation in the HA+P2 group versus EMD of IL-8 and complement fragments, with no significant changes in IL-1α/β ($q = 0.356$ and 0.362). In contrast, group HA+P6 displayed a significant downregulation of IL-1α and IL-8 ($q < 0.01$). IL-11 and TGFBR1 were significantly upregulated in both treatment groups compared with EMD (group HA+P2: $q = 0.0016$ and 0.0079; HA+P6: $q = 0.0158$ and 0.022), while TGFB1 showed an increase in HA+P2 ($q = 0.055$) and in group HA+P6 ($q = 0.020$). In both treatment groups, HA+P2 and HA+P6, Ameloblastin was upregulated compared with SHAM ($|logFC| = 0.26$ and 0.68, respectively). By immunohistochemistry, no statistically significant differences were detected among the groups in the signal intensities of IL-10, CD206, CD164, CD80, and TNF-α.

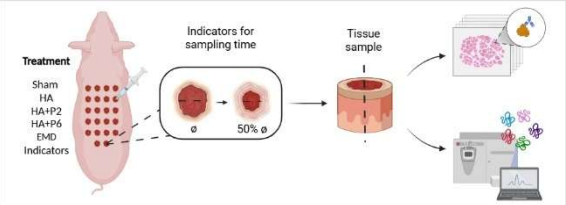

Fig. 1: Graphical overview of the experimental design

DISCUSSION & CONCLUSIONS: HA+P2 and HA+P6 promoted comparable expression of proliferation proteins and, at the same time, a stronger anti-inflammatory response when compared to EMD. Proteomics also revealed Ameloblastin (AMBN) expression in both groups, findings consistent with an enhanced regenerative response.

ACKNOWLEDGEMENTS: I would like to thank the UiO and its staff for their valuable support and collaboration.

CONFLICT OF INTEREST: IPR. The rights to the consensus peptides (US Patent US8367602B2 and related titles) belong to Industrie Biomediche Insubri SA (Switzerland). Corticalis AS holds a patent for combining hyaluronic acid with proline-rich peptides, with SPL as the inventor. HJH and SPL are shareholders of Corticalis AS. The other authors declare no conflicts of interest.

38. Boosting Serotonin Stability via Conjugation to Carboxymethyl Dextran

Maria Maniati [1], Athina Samara [1,2]

1 Departmentof Biomaterials, Institute of Clinical Dentistry, University of Oslo,
2 FUTURE, Center for Functional Tissue Reconstruction, University of Oslo, Oslo, Norway

INTRODUCTION: Serotonin (5 hydroxytryptamine; 5HT) is a bioactive amine with emerging applications in biomaterials and functional tissue reconstruction. However, its rapid oxidation and degradation under physiological conditions affect its stability and thus limit its use. Even more so in systems requiring sustained and prolonged bioactivity, such as 3D cell culture models. Here, we report the fabrication of a conjugate between 5HT and carboxymethyl dextran (CMD) to enhance serotonin stability. Beyond enhancing resistance to oxidative degradation, conjugation may influence receptor accessibility and activation kinetics, as macromolecular tethering can alter diffusion behaviour and effective ligand presentation at the cell surface.

METHODS: CMD was activated using EDC/NHS chemistry and reacted with 5HT. Residual NHS esters were quenched with ethanolamine. The resulting CMD–5HT conjugate was purified by acetone precipitation followed by dialysis. Successful conjugation was verified using Fourier-transform infrared (FTIR) spectroscopy. The degree of substitution was determined by UV–Vis spectrophotometry to be 27% relative to the total available carboxyl groups and the degradation of free serotonin in phosphate-buffered saline at 37 °C was monitored over 3 days via UV-Vis analysis.

RESULTS: FTIR analysis confirmed successful conjugation of 5-HT to CMD. The CMD–5HT conjugate exhibited the emergence of characteristic amide I (~1640 cm^{-1}) band, corresponding to C=O stretching of the amide carbonyl group, consistent with amide bond formation following EDC/NHS-mediated coupling (Fig. 1). Moreover, UV–Vis analysis of free serotonin in phosphate-buffered saline (PBS) at 37 °C demonstrated rapid oxidative degradation. A pronounced decline in absorbance at the characteristic peak (~275 nm) was observed within the first 24 h, with continued decrease over the 3-day monitoring period (Fig. 2), confirming the limited stability of unconjugated 5-HT under physiological conditions.

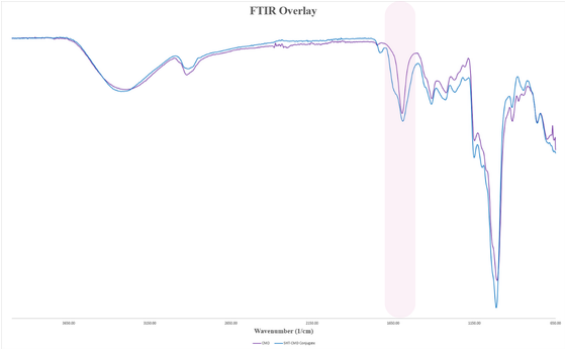

Fig. 1: FTIR comparison of pure CMD and the 5HT-CMD conjugate showing the emergence of characteristic amide I band following EDC/NHS mediated coupling.

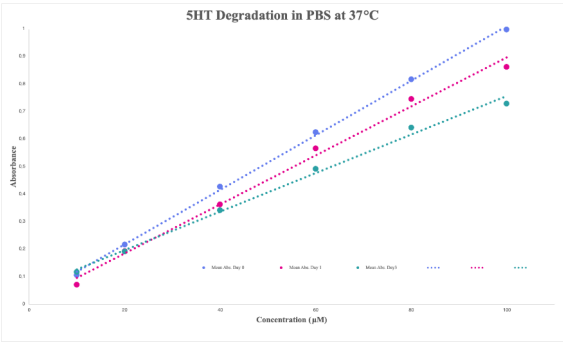

Fig. 2: Degradation of 5HT•HCl in PBS at 37°C, over 3 days measured by UV–Vis spectrophotometry.

DISCUSSION & CONCLUSIONS: Conjugation of 5-HT to CMD offers a strategy to mitigate oxidative degradation and potentially extend serotonin stability under physiological conditions. This approach provides a straightforward platform for stabilization of labile bioactive molecules, supporting future investigation of their functional properties and application in scaffold-based systems and three-dimensional (3D) tissue culture models.

ACKNOWLEDGEMENTS: MKM is supported by the Erasmus+ Programme of the European Union through the University of Patras.

39. Valorization of Eggshell Waste into Bioceramic-Coated Textile Scaffolds for Bone Tissue Engineering

J Bellvik[1], S Kopf[2], M Nakamura[3], A Zamani[2], M Persson[1]

[1] *Department of Textile Technology, Faculty of Textiles, Engineering and business, University of Borås, SE-501 90 Borås, Sweden*

[2] *Swedish Centre for Resource Recovery, Faculty of Textiles, Engineering and business University of Borås, Borås, SE-501 90, Sweden*

[3] *Medicity Research Laboratory, Faculty of Medicine, University of Turku Tykistökatu 6, 20520 Turku, Finland*

INTRODUCTION: Growing healthcare demands are driving the integration of bioeconomic principles into medical innovation. Biodegradable textile scaffolds fabricated from bio-derived poly(3-hydroxybutyrate)/poly(3-hydroxybutyrate-co-4-hydroxybutyrate) (P(3HB)/P(3HB-co-4HB)) offer a promising platform for bone regeneration. The use of eggshell-derived ceramic coatings provides a resource-efficient approach to enhance the material's osteoconductivity.

METHODS: Braided textile scaffolds were fabricated from melt-spun bio-derived P(3HB)/P(3HB-co-4HB) monofilaments[1]. Hydroxyapatite (HA) was synthesised from waste eggshells and applied as a surface coating onto the scaffolds. Scaffold morphology and coating coverage were examined by scanning electron microscopy (SEM). Human mesenchymal stem cells were seeded onto uncoated and HA-coated scaffolds to assess cytocompatibility. Cell viability was evaluated after 2 and 3 weeks of culture using a WST assay.

RESULTS: Braided P(3HB)/P(3HB-co-4HB) scaffolds were successfully fabricated, yielding uniform and reproducible architecture (Fig. 1 a-b). Eggshell-derived hydroxyapatite was homogeneously deposited onto the polymer fibres, as confirmed by SEM, which revealed a continuous ceramic coating and increased surface roughness compared to uncoated scaffolds (Fig. 1c-d). WST assays demonstrated sustained cell viability on both uncoated and HA-coated scaffolds after 2 and 3 weeks of culture (Fig 1 e). HA-coated scaffolds showed comparable or slightly enhanced metabolic activity relative to uncoated controls, indicating good cytocompatibility of the ceramic coating

DISCUSSION & CONCLUSIONS: Eggshell-derived hydroxyapatite was successfully deposited onto braided P(3HB)/P(3HB-co-4HB) scaffolds without compromising cell viability over 2–3 weeks. These results support the use of bio-derived polymer textiles and waste-based ceramic coatings as a cytocompatibility and resource-efficient platform for bone tissue engineering.

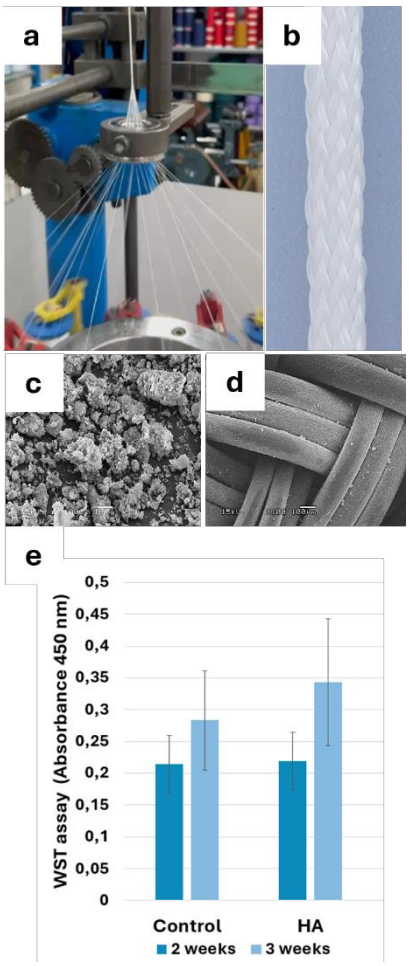

Fig. 1: (a–b) Braided P(3HB)/P(3HB-co-4HB) scaffolds. (c–d) SEM images of eggshell-derived HA-coated braided scaffold surface. (e) WST viability assay after 2 and 3 weeks.

REFERENCES:

Kopf et al. (2026) ACS Omega, doi.org/10.1021/acsomega.5c06548

40. The Impact of Collagen Source on Radiation-Induced Changes

M. Vopálková[1,2], T. Suchý[1,2], H. Chlup[2], M. Šupová[1], M. Šupolová[2], M. Braun[1], J. Kolář[2]

[1]Department of Composites and Carbon Materials, Institute of Rock Structure and Mechanics of The Czech Academy of Sciences, v. v. i., Prague, CZ, [2] Department of mechanics, Biomechanics and Mechatronics, Faculty of Mechanical Engineering, Czech Technical University in Prague, Prague, CZ

INTRODUCTION: Collagen, as a fundamental structural protein of the human body, has been extensively investigated for medical and biomaterial applications. Collagen isolated from different animal species may exhibit variations in physicochemical and mechanical properties despite belonging to the same collagen type (e.g., type I)[1]. These differences may be reflected in mechanical behaviour, response to cross-linking strategies, and minor compositional variations[2]. This study compares two sources of type I collagen (bovine and fish) with a focus on their mechanical response to □-radiation cross-linking. Complementary chemical and structural analyses were performed to enable a comprehensive evaluation of cross-linking effects with emphasis on interspecies differences.

METHODS: The study incorporated two sources of type I collagen (bovine and African catfish), prepared as hydrogels (8 wt%). Hydrogel strips were obtained by slow extrusion to prevent anisotropy arising from collagen bundle alignment. The prepared samples were then irradiated with □-radiation in a dose range of 1 to 25 kGy[3]. The mechanical properties were evaluated by means of tensile tests using the Zwick/Roell experimental system (Messphysik, Germany). In order to interpret irradiation-induced changes in relation to the collagen source, the samples were analysed using a range of complementary techniques. These included amino acid analysis to characterise the primary level of collagen structure, infrared spectroscopy to assess changes at secondary level (cross-linking, denaturation), and scanning electron microscopy to evaluate morphology associated with tertiary and quaternary structural organisation.

RESULTS: The tensile data reveal a pronounced difference between bovine and fish collagen in the non-irradiated state, which remains evident after irradiation at 25 kGy. Prior to irradiation, bovine collagen exhibited an ultimate tensile strength of approximately 6.8 kPa, compared to 1.1 kPa for fish collagen. After irradiation, the maximum stress increased to 228.7 kPa for bovine collagen and to 29 kPa for fish collagen. Irradiation affected the two materials to markedly different extents. At a strain of 0.05, bovine collagen showed a 1 985% increase in stress relative to the non-irradiated state, whereas fish collagen exhibited a 618% increase.

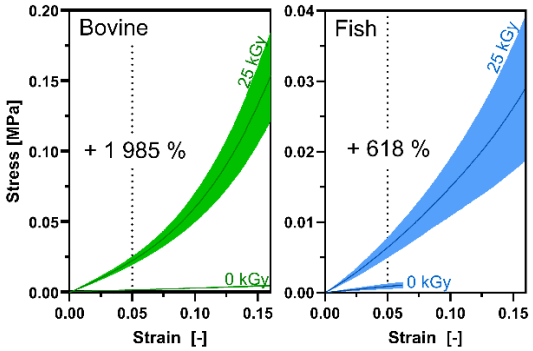

Fig. 1: Mean tensile stress–strain curves of bovine and collagen (0 vs. 25 kGy). Mean ± CI; percentage stress increase at 0.05 strain after irradiation is indicated.

DISCUSSION & CONCLUSIONS:
The mechanical behaviour of collagen strongly depends on its source, with different origins showing substantially different responses. Moreover, the effect of irradiation is not uniform: the same dose can lead to markedly different outcomes depending on the collagen source. The interpretation of these differences, based on comprehensive analyses across multiple levels of collagen structure, constitutes the focus of this contribution.

ACKNOWLEDGEMENTS: Supported by Ministry of Health of the Czech Republic, grant nr. NW24-02-00206.

REFERENCES: [1]H. Wang (2021) *Polymers*, **13**: 3868. [2]H. Liu et al. (2022) *Int. J. Food Sci.*, **58**: 1597-1610. [3]M. Šupová et al. (2023) *Int. J. Biol. Macromol.*, **253**:126989.

41. THE QUANTITATIVE MOLECULAR WEIGHT-ANTIMICROBIAL ACTIVITY RELATIONSHIP FOR CHITOSAN

Már Másson[a*] Sankar Rathinam[a] Amin Amani[a], Luca Protti[a]

[a] Faculty of Pharmaceutical Sciences, University of Iceland, Reykjavík, Iceland

*mmasson@hi.is

INTRODUCTION: The proceedings will be published as abstracts' collection in eCM conferences Open Access online periodical & eCM annual conferences (http://www.ecmconferences.org/). The present Microsoft Word file must be used as a template for the abstract production. The easiest way to use this abstract form is by cutting and pasting of unformatted text, to maintain the present format. This study aimed to investigate if literature data can be fitted to a QSAR equation that describes the relationship between antimicrobial activity and molecular weight.

METHODS:
Drawing inspiration from Kubiniy's bilinear quantitative structure-activity relationship equations [3], we formulated a bilinear equation to elucidate the molecular weight-antimicrobial activity association for chitosan and its derivatives.
To encapsulate the bilinear relationship between molecular weight and activity based on the measured minimum inhibitory concentration (MIC) of the polymer, we introduced Equation 1:

$$Log\left(\frac{1}{MIC}\right) = A_{max} + \frac{(A_{max} - A_{min})}{CMW} \times Mw - Log\left(\frac{10^{\frac{A_{max}}{CMW} \times Mw}}{10^{\frac{A_{min}}{CMW} \times Mw}} \quad \frac{10^{A_{max}}}{10^{A_{min}}}\right)$$

RESULTS:

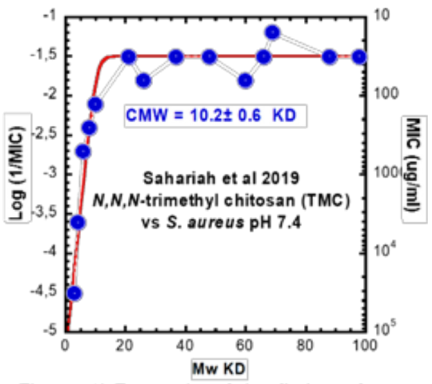

Figure 1) Example of the fitting of our published data to equation 1.

The shape of the graph described by the equation is governed by three constants. The CMW is the critical molecular weight for maximum activity, A_{max} (MIC_{min}) represents antimicrobial activity when Mw>CMW, and A_{min} (MIC_{max}) is the projected activity as Mw approaches zero.
Twenty-nine datasets from studies published between 1984 to 2019, providing MIC values for chitosan and its derivatives relative to MW, were used for the analysis. We used the KaleidaGraph Software for least-squares fitting, resulting in excellent conformity to the equations across datasets (Example shown in Figure 1 [4]). For datasets with suitable fits and at least three values on either side of CMW, CMW values ranged from 4 to 10 KD.

DISCUSSION & CONCLUSIONS: The study showed that there is a bilinear relationship between the molecular weight of chitosan and chitosan derivatives and antimicrobial activity. This type of relationship may exist for other biological properties of chitosan and may also apply to other polysaccharides.

ACKNOWLEDGEMENTS: Icelandic Technical Development Fund (Rannis Grant: 2112860-0611)

REFERENCES: [1] Sahariah et al. Int. *J. Mol. Sci*. **2019**, 20,1743
[2] M. Masson, Chitosan for Biomaterials iii: 2021, 131
[3] Kubiny. *J. Med. Chem.* **1977**, 20, 625
[4] M. Masson, Carbohyd. Polym. **2024**. 337, 122159

42. Ion-Based Strategies for Biological Optimisation of Angiogenesis-Osteogenesis Coupling in Large Bone Defects

M. Bayandori[1,2], M. Jafari Dargahlou[1], A. Nygård[1], G. Kohoolat[1], A. Shiralizadeh Dezfuli[1], H. Zhang[2], P. Uppstu[1]

[1] Laboratory of Molecular Science and Engineering, Faculty of Science and Engineering, Åbo Akademi University, Turku, Finland, [2] Pharmaceutical Sciences Laboratory, Faculty of Science and Engineering, Åbo Akademi University, Turku, Finland

INTRODUCTION: Large bone defects caused by trauma, tumour resection, or infection often fail to heal due to insufficient cellular recruitment, poor vascularisation, and limited biochemical signalling, while current clinical standards (e.g., autograft, Masquelet technique, distraction osteogenesis, free flaps) are constrained by donor-site morbidity, long treatment times, and patient burden [1]. Synthetic bone grafts and scaffolds are increasingly used but frequently lack the biological complexity and osteoinductive/angiogenic potency required for critical-sized defects [2]. Because angiogenesis and osteogenesis are tightly coupled and impaired vascular connectivity is a major cause of non-union, this study focuses on identifying optimal combinations of therapeutic ions and their temporal renewal profiles to achieve sustained, synergistic modulation of endogenous regenerative signalling (e.g., VEGF / BMP / PDGF related pathways) and promote coordinated vascularised bone regeneration. Compared with exogenous growth factors, therapeutic ions offer greater stability, lower cost, and easier incorporation into biomaterials [3]. These findings will be directly applied in later scaffold designs.

METHODS: Therapeutic ions (e.g., Ca, Sr, Mg, Zn, Cu, Co, B) and selected binary combinations will be systematically screened using coupled *in vitro* angiogenic and osteogenic models with cytocompatibility assays. Dose–response studies will define effective, non-toxic concentration windows, and temporal presentation regimes (single, repeated, renewal) will be compared. Angiogenesis–osteogenesis coupling will be assessed using co-culture and conditioned-media approaches with analysis of key cross-talk mediators (e.g., VEGF, PDGF-BB, BMP-related pathways) and targeted pathway perturbations. Prioritised ion combinations will be incorporated into 3D scaffold systems and evaluated in physiologically relevant 3D cultures.

RESULTS: We aim to find ion species and simple combinations that simultaneously enhance endothelial network formation and MSC/osteoprogenitor osteogenic differentiation within defined, non-cytotoxic concentration windows. We further aim to identify temporal ion presentation profiles that sustain bioactivity and determine synergistic or antagonistic ion–ion interactions associated with strengthened angiogenesis–osteogenesis coupling. In 3D scaffold contexts, we aim to verify retention of bioactivity and identify top-performing ion combinations for later scaffold incorporation.

DISCUSSION & CONCLUSIONS: Our findings are expected to demonstrate that optimised, dose and time-controlled ion cues can promote angiogenesis–osteogenesis coupling via endogenous signalling, offering a stable alternative to exogenous growth factors. This work is expected to provide a quantitative framework linking ion identity, combination, and renewal dynamics to coupled regenerative outcomes, enabling design and refinement of multifunctional scaffolds for vascularised bone regeneration and improved healing of large bone defects.

ACKNOWLEDGEMENTS: The authors would like to acknowledge the Finnish Cultural Foundation and the Lieto Savings Bank Foundation, for financial support. This study is part of the activities of the Åbo Akademi University Foundation (SÅA)-funded Centre of Excellence in Research "*Materials-driven Solutions for Combatting Antimicrobial Resistance* (MADNESS)".

REFERENCES:

1. 10.3389/fbioe.2020.00061.

2. 10.3390/jfb14020099.

3. 10.1016/j.biomaterials.2018.07.017.

43. Ion-Imprinted Layers as Calcium-Ion Carriers for Dental Applications: Spectroscopic Evidence, Morphology and Release Kinetics

M. Budnicka[1], M. Sobiech[2], K. Sieczko[1], P. Luliński[2]

[1]*Department of Pharmaceutical Chemistry and Biomaterials, Faculty of Pharmacy, Medical University of Warsaw, Poland,* [2] *Department of Organic and Physical Chemistry, Faculty of Pharmacy, Medical University of Warsaw, Poland*

INTRODUCTION: Durable sealing of the resin–dentin interface remains challenging. Supplying bioavailable Ca^{2+} locally may promote interfacial remineralization and improve longevity of adhesive restorations [1]. We designed thin ion-imprinted polymer (IIP) layers to bind and release Ca^{2+} ions, selecting 2-(methacryloyloxy)ethyl acetoacetate (M_1) as a functional monomer based on spectroscopy and molecular modelling, indicating the strongest, specific Ca^{2+} interactions among the screened monomers [2].

METHODS: Template–monomer interactions were assessed using ultraviolet−visible (UV−Vis) and proton nuclear magnetic resonance (^{1}HNMR) spectroscopies. Molecular modeling (Gaussian 16; BIOVIA Discovery Studio) was used to evaluate template–monomer complexation energies. Calcium-imprinted polymer (Ca-IIP) films were synthesized by thin-film photopolymerization using calcium chloride dihydrate as a template, 2-(methacryloyloxy)ethyl acetoacetate as a functional monomer, and ethylene glycol dimethacrylate as a cross-linker [2]. Morphology and elemental composition of Ca-IIP were examined by scanning electron microscopy (SEM) and energy-dispersive X-ray spectroscopy (EDS). Ca^{2+} release was quantified in water (pH=7.0), acetate buffer (pH=5.5), phosphate buffer (pH=7.4), and an artificial saliva model (pH=7.3). Data were fitted to Ho–McKay desorption kinetics and the Higuchi model.

RESULTS:
Spectroscopic analyses (UV-Vis, ^{1}H NMR) confirmed formation and stability of template–M_1 interactions in the pre-polymerization complexes. Molecular modeling identified the most favorable stoichiometry for Ca^{2+} coordination. SEM revealed an asymmetric surface with distinct porous domains, and EDS confirmed localized calcium retention in these regions. Release experiments showed medium-dependent desorption consistent with pseudo-second-order kinetics [2].

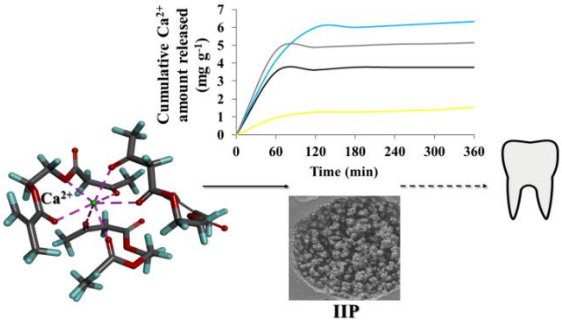

Fig. 1: Flowchart of the research concept.

DISCUSSION & CONCLUSIONS: There are only a few literature reports describing calcium-ion imprinting [3], and existing Ca-IIPs have primarily been explored as sorbents rather than as delivery systems. In this work, the combination of spectroscopic analyses and molecular modelling enabled the selection of a functional monomer that specifically interacts with Ca^{2+} ions, thereby allowing the synthesis of calcium-imprinted layers. The results demonstrate that these materials can release calcium in a medium-dependent manner—a feature not previously investigated for calcium-imprinted polymers. These findings expand the potential application of IIP materials toward dentistry, where controlled calcium release may support interfacial remineralization and improve the performance of adhesive systems.

ACKNOWLEDGEMENTS: National Science Centre, Poland (DEC-2021/05/X/ST4/00858), Medical University of Warsaw (FW232/1/F/MBM/N/21), and ICM, University of Warsaw (G68-2).

REFERENCES: [1]T. Baumann et al (2017) *Sci Rep*, **7**:12999. [2]M. Budnicka et al (2024) *Macromolecules*, **57**:5666–5678. [3]M. Budnicka et al (2022) *Trends Analyt Chem*, **156**:116711.

44. Bio-based, Compostable Printed Electrochromic Displays and Batteries from Quaternary Chitosan Derivatives

P A Parvathy[1], Sankar Rathinam[1], Yusuf Mulla[2], Ioannis Petsagkourakis[2], Mats Sandberg[2] and Már Másson[1].

[1]*Faculty of Pharmaceutical Sciences, School of Health Sciences, University of Iceland, Hofsvallagata 53, IS-107 Reykjavík, Iceland.*

[2]*PRISE Research Institutes of Sweden, Digital Systems, Smart Hardware, Printed, Bio- and Organic Electronics, SE-60221 Norrköping, Sweden.*

INTRODUCTION: The increased demand for sustainable electronics needs the development of **biodegradable**, **low-cost**, and **ecologically friendly materials**[1]. The current work explores the preparation of electrolytes, functional binders, and dendrite-suppressing agents, to develop bio-based batteries and printed electronic ink displays utilizing optimized quaternary chitosan materials. By leveraging the inherent bioactivity of chitosan, the developed devices are designed to be compostable, providing organic fertilizer at the end of their functional life cycle.

METHODS: Chitosan was chemically modified to N-alkyl and N-acyl derivative and refined using ion-exchange chromatography, diafiltration, and spray drying. The electronic ink (gel based) was prepared via UV curing of mixtures containing, UV-curable polymer precursor polyethylene glycol diacrylate (PEGDA) and N¹,N²-diethyl-1,2-ethanediamine (DA) (4:3) with modified chitosan.

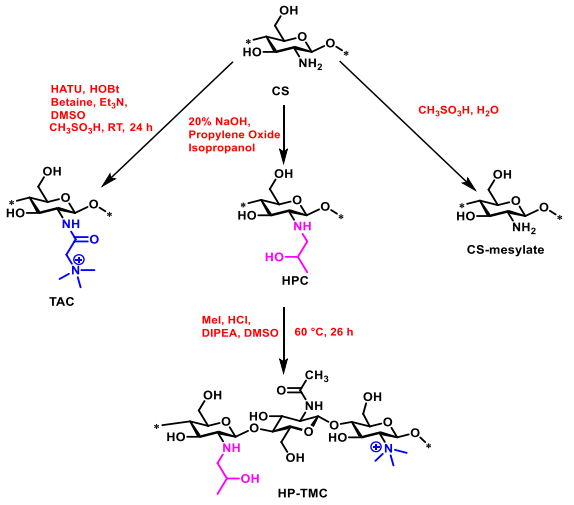

Scheme1. Synthesis of HP-TMC,Chitosan mesylate and TAC derivatives

RESULTS: The electrical characteristics of the materials were investigated with electrochemical impedance spectroscopy (EIS). The ink demonstrated both resistive and capacitive behaviour, with EIS indicating effective interfacial polarization and ionic relaxation. Efficient bulk ionic conduction at higher frequencies confirmed its viability for 3D-printed electrochromic display applications. Water hydration significantly improved ionic mobility in chitosan quaternary derivatives, resulting in lower impedance and better bulk ionic conduction

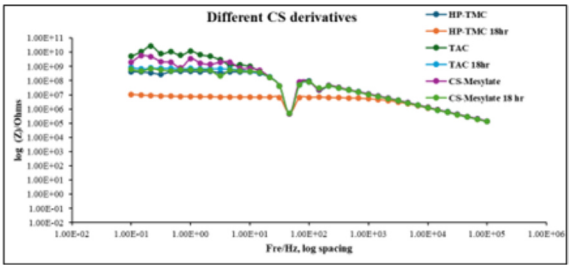

Figure1. Various chitosan derivatives with a 4:3 ratio of PEGDAand Base

DISCUSSION & CONCLUSIONS: Quaternary chitosan derivatives have been shown to be effective for printed electrochromic displays and biobatteries, with optimized formulations enabling compostable devices that support plant growth and sustainable printed electronics.

ACKNOWLEDGEMENTS: The authors gratefully acknowledge the support received under the ongoing Project 1225111 C-Bio-C-El - RannísTsþj.

REFERENCES:

1. López-Maldonado, E. A., Mavaei, M., Dan, S., Banitaba, S. N., Gholamhosseinpour, M., Hamedi, S., ... & Elgarahy, A. M. (2024). Diverse applications of versatile quaternized chitosan salts: A review. International Journal of Biological Macromolecules, 281, 136276., 2. Zhou, Y., Zhang, Y., Nie, Y., Sun, D., Wu, D., Ban, L., ... & Pan, X. (2025). Progress in Materials Science, 101460.

45. Centre of Excellence in Materials-Driven Solutions for Combatting Antimicrobial Resistance (MADNESS)

P. Uppstu[1], X. Wang[2,3], K.K. Bansal[1,2], S. Lafond[4], T. Viitala[2], C.-E. Wilén[1], C. Xu[3], H. Zhang[2], I. Porres Paltor[4], J.M. Rosenholm[2]

[1]Laboratory of Molecular Science and Engineering, Åbo Akademi University, Turku, Finland, [2]Pharmaceutical Sciences Laboratory, Åbo Akademi University, Turku, Finland, [3]Natural Materials Technology, Åbo Akademi University, Turku, Finland, [4]Information Technology, Åbo Akademi University, Turku, Finland,

INTRODUCTION: Antimicrobial resistance (AMR) poses a serious threat to public health, as it makes it difficult or even impossible to treat infectious diseases, and the World Health Organization listed AMR among top 10 global health threats. Furthermore, biofilm-forming bacteria pose significant challenges and are associated with the majority of chronic and device-related infections. Development of new antimicrobials is not a top priority for the pharmaceutical industry as it requires enormous economic and labour investment with uncertain commercial return. Thus, alternative approaches are urgently sought to combat AMR. Our Centre of Excellence (CoE) in Materials-driven Solutions for Combatting Antimicrobial Resistance (MADNESS; www.abo.fi/madness) at Åbo Akademi University was established to generate alternative solutions for AMR, by joining expert forces from the fields of pharmacy, materials chemistry, and artificial intelligence (AI).

METHODS: We employ several methodologies to create novel materials that are either inherently antimicrobial or have been loaded with drugs. The approaches we use:

1. Integration of AI in materials design for predicting and maximizing the antimicrobial activity and to shorten the design life cycle.

2. Nanoparticles (NPs) based on – (a) Woody polyphenols as inherently antimicrobial NPs, (b) Functional polymeric NPs as antimicrobial drug carriers, and (c) Inorganic NPs as carriers for genetic constructs.

3. Developing antimicrobial textiles for AMR therapy utilising flexible cellulose nanofibers with polypyrrole nanocoatings.

4. Development of antimicrobial, functional composite materials and 3D-printed templates for tissue regeneration.

5. Implementing new real-time label-free analytical methods for measurements of bacterial adhesion and biofilm growth kinetics via surface plasmon resonance.

RESULTS: Throughout the study, we will deepen our knowledge on the impact of distinct materials on AMR. We expect to create a "toolbox" for treating infectious diseases and other medical conditions where traditional antimicrobials are ineffective (Fig. 1).

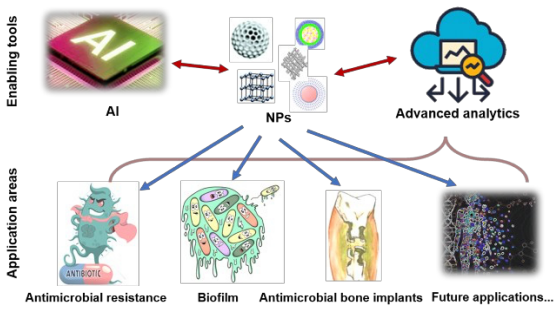

Fig. 1: Assisted by AI and advanced analytics, we develop NPs that are applied to overcome biofilm-forming resistant microbes in diseases as well as in wounds and in tissue defects.

DISCUSSION & CONCLUSIONS: We envision to create highly specialized solutions that have great potential for practical implementation and can have an impact on the pharmaceutical industries, while creating opportunities for entrepreneurs. In future, we believe to aid people in managing prevalent microorganisms in a financially viable manner.

ACKNOWLEDGEMENTS: The authors thank the Åbo Akademi University Foundation for funding the CoE for 2024–2028.

46. Thermosensitive Amniotic Membrane Hydrogel for Diabetic Wound Repair

P. Jaipal[1], S. Gujjar[1], S. Ranjan[1], M. Kumari[1], B. N. Panda[1], S. Mathapati[1*]

[1]*BRIC-Translational Health Science and Technology Institute, Faridabad-121001, Haryana, India*

INTRODUCTION: Decellularized extracellular matrix (ECM) hydrogels are promising regenerative biomaterials due to their ability to mimic the native tissue microenvironment. Human amniotic membrane (AM) is an abundant, ethically acceptable source enriched with wound-healing ECM components. This study developed and characterized thermosensitive hydrogels from decellularized AM ECM and evaluated their therapeutic efficacy in diabetic wound healing.

METHODS: Native AM was decellularized using a detergent–enzymatic protocol to remove cellular components while preserving key ECM proteins. The acellular ECM was lyophilized, cryo-milled, and enzymatically digested with pepsin under acidic conditions at three concentrations. Pregel solutions were neutralized and thermally gelled at 37 °C to form injectable, thermosensitive hydrogels. Physicochemical characterization included gelation kinetics, swelling ratio, porosity, mechanical stiffness, and enzymatic biodegradation. *In vitro* biocompatibility was assessed in fibroblasts, keratinocytes, and endothelial cells using live/dead staining, metabolic (MTS) assay, intracellular ROS, apoptosis, cytoskeletal organization, and cell migration assays. Proteomic analysis was performed to identify retained ECM proteins. *In vivo* efficacy was evaluated using a diabetic mouse full-thickness wound model.

RESULTS: AM ECM hydrogels demonstrated rapid and stable gelation, high water retention, and an interconnected porous microstructure. Mechanical strength and resistance to biodegradation increased with hydrogel concentration. All formulations showed strong cytocompatibility with fibroblasts, keratinocytes, and endothelial cells, with no detectable induction of intracellular ROS or apoptosis. The hydrogels promoted cytoskeletal organization and enhanced fibroblast migration. Proteomic profiling confirmed preservation of key matrisome proteins linked to epithelial differentiation, angiogenesis, and tissue regeneration. In diabetic mouse wound models, AM ECM hydrogels significantly improved wound closure rate, re-epithelialization, neovascularization, and collagen remodeling.

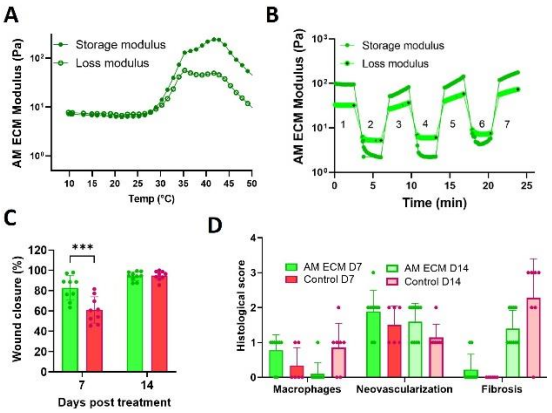

Fig. 1:(A) Temperature-dependent viscoelastic properties of AM hydrogel at temperature range of 10 to 50 °C. (B)Self-healing properties at alternating 7 strain cycles of 1% (low) and 100% (high) strain recovery at 10 Hz frequency. (C) Quantitative wound closure over a designated time. (D) Semi-quantitative histopathological scoring of inflammation and neovascularization.

DISCUSSION & CONCLUSIONS: The AM-ECM hydrogel provides a bioactive, thermosensitive, injectable scaffold that supports regenerative processes critical for diabetic wound healing. Its pro-migratory, cytoprotective, and pro-angiogenic effects highlight its translational potential as an advanced biomaterial for diabetic wounds.

ACKNOWLEDGEMENTS: THSTI core facilities and funding support from the Science and Engineering Research Board (Grant ID: SRG/2021/000420), India, and the Council of Scientific & Industrial Research (CSIR), India are gratefully acknowledged.

REFERENCES:

1. Jaipal, P. et. al. *ACS Biomater. Sci. Eng.* 2026
2. Gujjar, S. et. al. *Adv. Biol.* 2024

47. In vivo evaluation of an injectable dermal construct in a porcine wound model

R. Shamasha[1, 2], S. Kollenchery Ramanathan[3], N. Reustle[3], S. Frenger[2], E. Källåker[2], A. Starkenberg[2], J. Rakar[1, 2], G. Kratz[2,4], D. Aili[3], J. Junker[1, 2]

[1] Center for Disaster Medicine and Traumatology, Linköping University Hospital, Linköping, Sweden

[2] Experimental Plastic Surgery, Department of Biomedical and Clinical Sciences, Linköping University, Linköping, Sweden

[3] Laboratory of Molecular Materials, Division of Biophysics and Bioengineering, Department of Physics, Chemistry and Biology, Linköping University, Linköping, Sweden

[4] Anaesthetics, Operations and Specialty Surgery Center, Department of Hand and Plastic Surgery, Linköping University Hospital, Linköping, Sweden

INTRODUCTION: Severe burn injuries and full-thickness skin defects remain a major clinical challenge, largely due to limited availability of autologous donor tissue and the frequent development of fibrosis and scarring. Biofabricated, injectable dermal constructs represent a promising strategy to overcome these limitations by enabling minimally invasive delivery and in situ tissue regeneration. This study aimed to evaluate an injectable, fibroblast-laden granular hydrogel, termed µInk, in a clinically relevant porcine wound model. The objective was to assess its in vivo biocompatibility, biodegradation profile, and capacity to promote extracellular matrix (ECM) remodeling during dermal regeneration.

METHODS: µInk was fabricated by dispersing porous gelatin microcarriers (PGMs) within a hyaluronic acid–polyethylene glycol hydrogel network, resulting in a shear-thinning, self-healing construct suitable for extrusion-based application or direct wound injection. Autologous dermal fibroblasts were isolated and expanded from two adult pigs and seeded onto PGMs for 72 h prior to transplantation. Each animal received twenty full-thickness excisional wounds (2 cm diameter), which were treated with µInk either with or without fibroblasts. Wound biopsies were collected after 2, 4, 8, and 12 weeks for histological, gene expression, and protein analyses. Complementary in vitro studies were performed to evaluate fibroblast attachment, proliferation, and ECM protein synthesis on PGMs.

RESULTS: In vitro, fibroblasts exhibited robust adhesion to PGMs and produced key dermal ECM components, including collagen I, collagen III, and elastin. In vivo, PGMs were completely degraded within four weeks, indicating favorable scaffold biodegradability and tissue remodeling. Wounds treated with fibroblast-laden µInk demonstrated increased collagen deposition and distinct elastin-rich regions localized around the former microcarrier sites, compared to acellular controls, suggesting enhanced regenerative remodeling rather than fibrotic repair.

DISCUSSION & CONCLUSIONS: The µInk platform supports fibroblast viability, ECM deposition, and integration with host tissue in a large-animal wound model. These findings demonstrate the potential of injectable, biofabricated dermal constructs as a regenerative strategy for full-thickness skin repair and provide an important step toward large-scale preclinical and translational evaluation.

48. Fabrication of a Reusable Plate-Well Insert with a 3D-Printed Mounter and Hydrogel Scaffolds for 3D Cell Culture and Functional Assays

Saloua Saghir[1], Jana Hlinkova[2], Athina Samara[2], Giuseppe Schiavone[1]

[1]Department of Microsystems, Faculty of Technology, Natural Sciences and Maritime Sciences, University of South-Eastern Norway, [2]Department of Biomaterials, FUTURE, Center for Functional Tissue Reconstruction, University of Oslo, 0317 Oslo, Norway

INTRODUCTION: Three-dimensional (3D) cell culture systems better replicate native tissue environments than conventional two-dimensional models, yet widespread adoption remains limited by high costs, poor standardization, batch-to-batch variability, and incompatibility with common downstream analyses. Here, we present a reproducible, scalable protocol for fabricating reusable 24-well plate inserts combining a custom 3D-printed mounter with methacrylated hyaluronic acid (GMHA) hydrogel scaffolds, designed to integrate seamlessly with standard laboratory workflows and downstream functional assays.[1]

METHODS: Mounters were designed in Autodesk Fusion and printed in PLA (UltiMaker S5). GMHA hydrogels were synthesised by reacting hyaluronic acid with glycidyl methacrylate, UV-crosslinked (10 mW·cm^{-2}, 5 min), and lyophilised for storage at 4°C (up to 3 months). Prior to use, hydrogels were UV-sterilised and rehydrated in basal medium (DMEM/F12, 20% FBS) for 24–48 h. Human umbilical cord mesenchymal stem cells (UC-MSCs) were seeded at 50,000 or 100,000 cells per hydrogel and cultured for 7 days. Downstream analyses included LDH cytotoxicity assay, confocal immunofluorescence, and qPCR for nestin (NES) and beta-actin (ACTB), normalised to RPL19.

RESULTS: Mounters were reproducibly fabricated (bottom: 119.3 ± 17.8 mg; top: 179.1 ± 10.2 mg; n=9), and one 50 mL precursor batch filled two 48-well plates. UC-MSCs remained viable over 7 days in 3D culture. LDH release was lower in hydrogel versus glass controls at D5 and D7 ($p < 0.0001$), indicating reduced cytotoxic stress. NES expression was significantly upregulated in hydrogel-cultured cells at D7 ($p < 0.001$), consistent with maintenance of a progenitor-like phenotype (Figure 1).

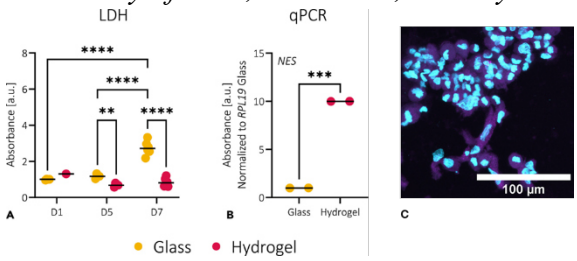

Fig. 1: a) LDH, b) qPCR, of UC-MSCs on glass vs. GMHA hydrogel and c) confocal imaging UC-MSCs in GMHA hydrogel.

DISCUSSION & CONCLUSIONS: The reduced LDH release and elevated NES expression confirm that the GMHA hydrogel matrix better preserves stem cell characteristics than rigid 2D surfaces. ACTB variability in hydrogel conditions highlights the importance of selecting mechanically stable reference genes for 3D systems. Key limitations include incomplete optical transparency and susceptibility to gel disturbance during media changes.

In conclusion, this protocol provides a reproducible, low-cost 3D culture platform fully compatible with standard 24-well plates and common downstream assays. Its open-source, modular design supports adaptation across cell types and experimental contexts, offering a practical alternative to disposable commercial scaffolds.

ACKNOWLEDGEMENTS: The authors acknowledge funding from SpareBank1 Stiftelsen BV; the EU CHIPS JU Horizon 2020 (grant no. 101112347, NerveRepack); and the Research Council of Norway (NORFAB IIIb, project no. 322552).

REFERENCE:

1. Saghir, S., Hlinkova, J., Samara, A., and Schiavone, G. (2025). Protocol for fabricating a reusable plate-well insert with a 3D-printed mounter and hydrogel scaffolds for 3D cell culture and functional assays. STAR Protocols *6*, 104014. https://doi.org/10.1016/j.xpro.2025.104014.

49. Bioactive glass scaffolds loaded with Superparamagnetic Iron Oxide Nanoparticles (SPIONs): a multifunctional approach for bone regeneration and hyperthermia in bone cancer treatment

S. Giacobbi[1], V. A. Gobbo[1], M. Miola[2], E. Verné[2], J. Massera[1]

[1]*Faculty of Medicine & Health Technology, Tampere University, Finland*

[2]*Department of Applied Science and Technology, Institute of Materials Physics and Engineering, Biomaterials Laboratory, Politecnico di Torino, Turin, Italy*

INTRODUCTION: Conventional therapies for treating bone cancer are often associated with side effects and recurrence, other than the presence of critical size bone defects, in case of surgical removal [1]. Magnetic hyperthermia has emerged as a possible alternative therapy because of its tissue-specificity and ability of reaching bone structures in depth without being invasive [2]. In bone tissue engineering, bioactive glass (BAG) 1393B20 represents a good candidate for bone regeneration, since it overcomes the crystallization tendencies of traditional silicate glasses, while promoting angiogenesis and osteogenesis *in vitro*, and mineralization and collagen formation *in vivo* [3]. This study focuses on combining magnetic hyperthermia and bone tissue engineering, to process multifunctional 3D printed magnetic scaffolds, able to repair critical bone defects while eradicating residual cancer cells. The scaffolds were composed of BAG 1393 B20 and Superparamagnetic Iron Oxide Nanoparticles (SPIONs), that act as heat sources for magnetic hyperthermia.

METHODS: SPIONs were synthesized via co-precipitation method and successively incorporated into an ink composed of 1393 B20 BAG powder and Pluronic F-127. The BAG/SPIONs ratios were 100:0 wt%, 95:5 wt% wet, 95:5 wt% dry, 90:10 wt% dry, with "wet" or "dry" indicating if SPIONs were introduced as a liquid solution or a dry powder. The impact of SPIONs addition was evaluated in the inks for 3D printing in terms of rheological properties with a rotational rheometer, and in the scaffolds in terms of mechanical properties, bioactivity, magnetic properties and heating capacity under alternating magnetic field exposure and cytocompatibility.

RESULTS: Manufacturing of porous cylindrical structures (h = 1 mm, ϕ = 5 mm) was successful for all compositions. The mechanical properties of the compositions 100:0 wt% and 95:5 wt% dry were close to the trabecular bone range, whereas the compositions 95:5 wt% wet and 90:10 wt% dry showed lower results, comparable to each other. The scaffold exhibited superparamagnetic properties and an increase of up to 10 °C was recorded under 10 min of exposure to an alternating magnetic field. All the compositions proved to be bioactive (precipitation of HA layer in SBF). Human adipose stem cells, cultured in direct contact with the scaffolds, exhibited a spread morphology. No significant impact on cell viability and proliferation was evidenced.

DISCUSSION & CONCLUSIONS: The lower mechanical properties for the compositions 95:5 wt% wet and 90:10 wt% dry were mostly due to the presence of SPIONs aggregates within the glass matrix that acted as impurities. The developed scaffolds enabled increasing the temperature of the medium within a range suitable for hyperthermia treatment. The presence of the SPIONs didn't interfere both with the bioactivity of the scaffolds and with cell viability and proliferation, indicating promising cytocompatibility. This study represents an innovative step towards the possibility of offering new, multifunctional treatments able simultaneously repair bone while preventing cancer cells proliferation and migration. Such material could potentially reduce cancer recurrence post-surgery.

ACKNOWLEDGEMENTS: This research has received funding from the Research Council of Finland (MAXHEAL project #361159).

REFERENCES: [1] American Cancer Society, «Surgery for Bone Cancer». 2024 [Online]. https://www.cancer.org/cancer/types/bone-cancer/treating/surgery.html

[2] Yazdanpanah, A., et al., *Nano Select*, 2023. https://doi.org/10.1002/nano.202300008.

[3] A. Szczodra et al., Acta Biomater., 2024. https://doi.org/10.1016/j.actbio.2024.07.053

50. Bioactive glass cements as a platform for the delivery of light-responsive riboflavin

Sarah Larroudé[1], Marjo Ala-Rämi[1], Eloïse Dondoua[1], Jonathan Massera[1]

[1]*Faculty of Medicine & Health Technology, Tampere University, Finland*

INTRODUCTION: Bioactive glasses are attractive for bone regeneration, especially borosilicate glasses such as 13-93B20 which offer fast dissolution with demonstrated pro-angiogenic and pro-osteogenic properties [1]. Combining bioactive glass with chitosan, a biocompatible polymer known to support osteoblast activity, may further enhance regenerative performance [2].
A major challenge in bone repair, especially in dental applications, is infection, often associated with prolonged antibiotics. Antimicrobial photodynamic therapy (aPDT) provides a promising alternative by using light-activated photosensitizers to generate reactive oxygen species and eliminate pathogens [3]. Riboflavin (RF or vitamin B2) is a safe, effective photosensitizer responsive to UV A and blue light, making it a strong candidate for integration into regenerative biomaterials [4]. In this context, bioactive glass - chitosan cements loaded with RF could serve as multifunctional platforms for on-site light-activated drug delivery and bone regeneration.

METHODS: In this study, RF photochemical behavior and its release dynamics, from 13-93B20 bioactive glass cements, under controlled environmental conditions were assessed. Initially, serial dilutions of RF, in TRIS buffer solution, were prepared and their absorbance spectra between 300 and 600 nm were recorded. RF solutions were exposed to blue light for 0-20 min, and absorbance spectra were recorded. TRIS buffer solution was conditioned with BG powder at 37ºC for 24h and RF solutions were exposed to light at RT or 37ºC for 0-20 min to evaluate changes in absorbance due to either pH and/or temperature. 13-93B20 bioactive glass was synthetized from analytical-grade reagents using the melt-quenching technique and crushed into powder (Ø< 38 µm). RF-cements were prepared by mixing BG powder and RF (0.04 mg/mL) with a 2wt% chitosan-20wt% citric acid solution.
Release tests were performed by immersing RF-cements in TRIS buffer solution (kept in the dark, continuously illuminated, alternating light/dark cycles (20 min) for up to 100 min). Absorbance spectra (300-600 nm) of the immersion solution at each time point were measured. The ionic composition of the immersion fluid was quantified using ICP-OES.

RESULTS: The results demonstrated that RF undergoes degradation under blue light irradiation, leading to the formation of photoproducts such as lumichrome and lumiflavin. In contrast, riboflavin remained stable under dark conditions and elevated temperatures but exhibited sensitivity to variations in pH. Furthermore, RF-loaded cements showed the ability to sustainably release the drug, achieving complete release within 24 hours. Importantly, the bioactive glass cements exhibited a protective effect on riboflavin: while the compound in solution was light-sensitive, the RF embedded within the cements and exposed to light in air showed no signs of degradation nor transformation into photoproducts.

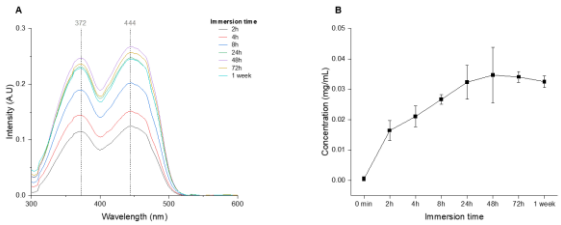

Figure 1: A) Immersion of RF-cements up to 1 week; B) [RF] release in TRIS buffer solution

DISCUSSION & CONCLUSIONS: Overall, this work introduces a novel light-responsive drug delivery platform that combines the bioactivity of bioactive glass cements with the antimicrobial properties of riboflavin. This promising and versatile approach shows significant potential for tissue engineering applications.

REFERENCES:

[1]A. Szczodra *et al. Acta Biomater.*, vol. 186, pp. 489–506, Sep. 2024. [2]J. Venkatesan and S.-K. Kim, *Mar. Drugs*, vol. 8, no. 8, pp. 2252–2266, Aug. 2010. [3]G. Amendola, M. Di Luca, and A. Sgarbossa, *Int. J. Mol. Sci.*, vol. 26, no. 16, p. 7993, Aug. 2025. [4]B. A. Buehler, *J. Evid.-Based Complement. Altern. Med.*, vol. 16, no. 2, pp. 88–90, Apr. 2011.

51. Antibacterial Chitosan-*graft*-Polyaniline/Hydroxyapatite Biocomposites for Bone Tissue Engineering Applications

S.¥ousefiasl[1,2], HJ. Haugen[1], E. Nazarzadeh Zare[3], Mojgan Alaeddini[2]

[1]*Department of Biomaterials, Faculty of Dentistry, University of Oslo, Oslo 0455, Norway,*
[2]*Dental Research Center, Dentistry Research Institute, Tehran University of Medical Sciences, Tehran, Iran.* [3]*School of Chemistry, Damghan University, Damghan, 36716-45667, Iran.*

INTRODUCTION: Bone has inherent regenerative capacity; however, in cases of critical defects and fractures, additional interventions are needed to enhance tissue regeneration. The limitations of autografts, allografts, and xenografts have encouraged the development of synthetic bone substitutes. Since bone is a natural composite primarily made of hydroxyapatite (HA), scaffolds that mimic this structure can better support regeneration. In this study, HA nanoparticles were incorporated into a chitosan matrix during the in situ copolymerization of aniline. This strategy combines the biocompatibility and osteoconductivity of HA and chitosan with the antibacterial and electrically conductive properties of polyaniline to create a multifunctional biocomposite scaffold for bone regeneration.

METHODS: Biocomposites of Chitosan-*graft*-polyaniline/hydroxyapatite (CS-*g*-PANI/HA) were fabricated using an in-situ copolymerization method with different concentrations of HA (5 wt.% and 10 wt.%). Briefly, chitosan was dissolved in acetic acid, followed by the addition of HA nanoparticles. An APS initiator solution was added dropwise, and aniline monomer was introduced, and the mixture was stirred overnight. The reaction was neutralized with NaOH, precipitated in ethanol, washed with Dimethylformamide to remove ungrafted PANI, then rinsed with acetone and vacuum-dried at 50 °C to obtain CS-*g*-PANI/HA *(Fig. 1)*. The physicochemical properties of the composites were characterized using FTIR, XRD, SEM, and EDS, followed by evaluation of their biocompatibility and antibacterial activity.

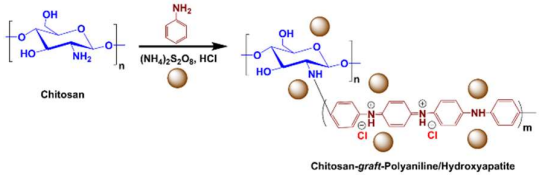

Fig 1: Schematic illustration of chitosan-graft-polyaniline/hydroxyapatite biocomposite fabrication.

RESULTS: Physicochemical analyses confirmed the successful synthesis of the CS-g-PANI/HA biocomposites. The cytotoxicity investigations indicated that HA and the biocomposites did not show significant toxicity toward the cultured cells (*Fig. 2*).

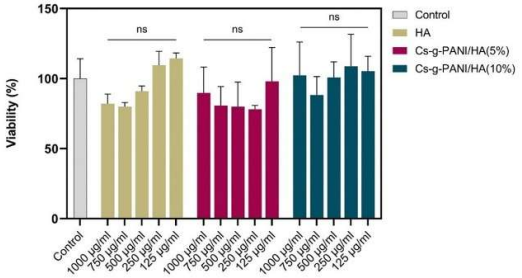

Fig. 2: Graph showing cytotoxicity analysis results of HA and biocomposites cultured with PDLSCs. (ns.: not significant).

The HA sample did not exhibit antibiotic activity against E. coli and S. aureus over the investigated concentration range. The MIC *and MBC* of biocomposites against *E. coli* and *S. aureus are* demonstrated in *Table 1*.

Table 1. MIC and MBC of samples at the final concentration of 4 mg/ml.

Bacteria	Sample	MIC (mg/mL)	MBC (mg/mL)
E. coli	HA	-	-
	Cs-*g*-PANI/HA(5%)	1.0	2.0
	Cs-*g*-PANI/HA(10%)	0.5	1.0
S.aureus	HA	-	-
	Cs-*g*-PANI/HA(5%)	1.0	2.0
	Cs-*g*-PANI/HA(10%)	0.5	1.0

DISCUSSION & CONCLUSIONS: CS-*g*-PANI/HA biocomposites were successfully synthesized and demonstrated favourable biocompatibility, comparable to HA. In contrast to HA, the composites exhibited antibacterial activity against *E. coli* and *S. aureus*, attributed to the presence of chitosan and polyaniline. These results suggest that the developed biocomposite augments the antibacterial properties of the osteogenic potential of the HA, which is advantageous for bone tissue engineering applications.

58. Development of Laponite Doped Injectable Dextran Hydrogels for Bone Tissue Engineering

Sharun Khan[1], Amitha Banu Shajahan[1], Stelios Alexandris[2], Ruiqi Jing[3], Thorbjørn Terndrup Nielsen[3], Kim Lambertsen Larsen[3], Cristian Pablo Pennisi[1]

[1]*Department of Health Science and Technology, Aalborg University, Denmark*
[2]*Department of Materials and Production, Aalborg University, Denmark*
[3]*Department of Chemistry and Bioscience, Aalborg University, Denmark*

INTRODUCTION: Bone defects that compromise structural integrity remain a significant clinical challenge in orthopaedic surgery, often resulting in fractures, prolonged healing times, and a reduced quality of life. Injectable bone fillers are commonly used to fill irregular bone voids and cystic lesions; however, conventional materials lack adaptability, bioactivity, and adequate integration with host tissue, which can limit bone remodelling and lead to adverse clinical outcomes. To address these limitations, we developed an injectable, dextran-based supramolecular hydrogel for bone tissue engineering. The hydrogel system is based on dynamic host-guest interactions between cyclodextrin- and adamantane-modified dextran, enabling the formation of an adaptable network.

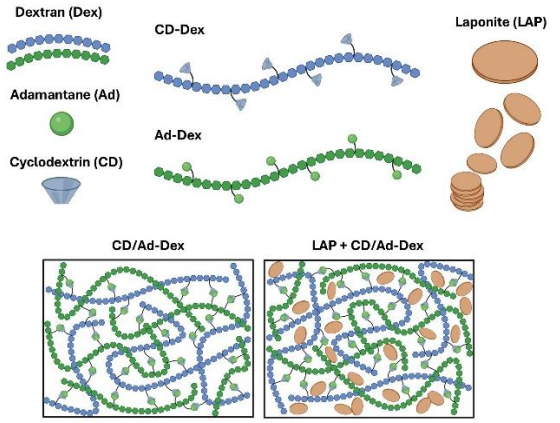

Fig. 1: Laponite-doped CD-Dex and Ad-Dex modified dextran leveraging supramolecular host-guest interactions.

METHODS: Laponite nanoclay was incorporated to enhance the mechanical properties and injectability of the hydrogel. Key formulation parameters, including dextran molecular weight, degree of substitution, host-to-guest anchor-point ratio, and laponite concentration, were systematically varied to fine-tune the rheological and mechanical properties relevant for injectability and structural support. A higher anchor-point ratio was employed to generate vacant cyclodextrin host sites, enabling future functionalization with bioactive cues and facilitating drug-loading and controlled-delivery applications. Hydrogel candidates meeting the criteria for injectability and stiffness, including a shear-thinning ratio below 0.5 and compressive stiffness within the range of 1 to 20 kPa, were selected for further evaluation. Biocompatibility was evaluated using a fibroblast viability assay in combination with haemocompatibility assessment.

RESULTS: Increasing dextran molecular weight enhanced mechanical strength, driven by longer polymer chains and increased network entanglement. The incorporation of laponite further improved the mechanical properties in a concentration-dependent manner, introducing pronounced shear-thinning behaviour and significantly enhancing injectability. The stiffness of the hydrogel formulations increased significantly with increasing laponite concentration from 0 to 3%, accompanied by a corresponding reduction in mesh size. Furthermore, the laponite-doped hydrogels demonstrated superior biocompatibility and haemocompatibility, indicating their suitability and safety for biological applications.

DISCUSSION & CONCLUSIONS: An injectable dextran-based supramolecular hydrogel with tunable stiffness and shear-thinning behaviour was developed by modulating polymer characteristics and laponite content. Laponite significantly enhanced mechanical strength and shear-thinning behaviour. The selected hydrogel candidates demonstrated good *in vitro* biocompatibility, supporting their potential for further evaluation.

ACKNOWLEDGEMENTS: This research was funded by the European Union's Horizon Europe programme through a Marie Skłodowska-Curie Postdoctoral Fellowship (Grant agreement ID: 101207455) for the project "BONEGEL: Development of a novel bone-adapting injectable smart hydrogel for bone tissue engineering."

53. Rheological design of dextran-based hydrogels for bioprinting urethral tissue constructs

Stelios Alexandris[1], Ruiqi Jing[2], Thorbjørn Terndrup Nielsen[2], Kim Lambertsen Larsen[2], Nele Pien[3], Sandra Van Vlierberghe[3], Jesper de Claville Christiansen[1], Cristian Pablo Pennisi[4]

[1]Department of Materials and Production, Aalborg University, Denmark; [2]Department of Chemistry and Bioscience, Aalborg University, Denmark; [3]Department of Organic and Macromolecular Chemistry, Ghent University, Belgium; [4]Department of Health Science and Technology, Aalborg University, Denmark

INTRODUCTION: Bioprinting urethral grafts aims to produce cell-laden constructs with mechanical properties that match the delicate, compliant corpus spongiosum surrounding the male urethra. This requires bioinks that are not only cytocompatible but also exhibit well-controlled viscoelasticity: pronounced shear-thinning for easy extrusion, sufficient yield stress for shape fidelity, and time-dependent stress relaxation within a physiologically relevant range. In this work, we present a material platform based on supramolecular dextran hydrogels designed for modular tuning of rheology and mechanics.

METHODS: A library of linear dextran polymers with varying molecular weights and degrees of substitution was synthesised. Dextran chains were functionalised with β-cyclodextrin (host), and different guest groups – benzophenone (Bzp), adamantane (Ada), and Ada-CH_2 were used to create dynamic host–guest interactions (Fig. 1). Parameters such as concentration, molecular weights of the components, and their degree of substitution (for a fixed anchor ratio) were varied according to an orthogonal design procedure to guide the selection of the most suitable hydrogel formulation. Small amplitude oscillatory shear measurements were performed to determine storage and loss moduli, linear viscoelastic limits, and the effects of frequency and temperature on gel formation. Flow curves and amplitude sweeps were used to quantify shear-thinning behaviour and yield stress, which are directly related to extrusion and shape fidelity during bioprinting. Time-dependent properties were investigated by stress-relaxation and creep–recovery tests, providing characteristic relaxation times and distinguishing between recoverable and permanent deformation.

RESULTS: The hydrogels exhibited shear-thinning behaviour, rapid stress relaxation primarily governed by host–guest content and polymer concentration, and thixotropic properties. The most important parameter that can be determined from the rheological data is the network mesh size, which must meet strict criteria based on the diffusion and proliferation properties of the cells to be introduced before bioprinting.

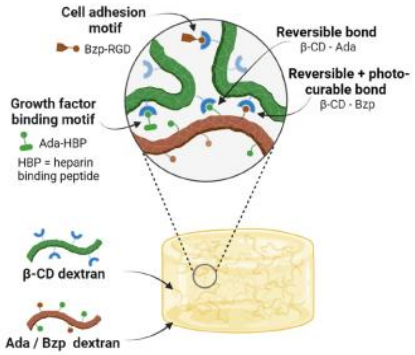

Fig. 1: Schematic diagram of dextran-based hydrogels

DISCUSSION & CONCLUSIONS: By systematically characterising the rheology of dextran hydrogel, we established a structure–property map linking molecular design (backbone, dynamic bonds, crosslink density) to printability and mechanical compatibility with urethral tissue. This rheological toolbox guides the selection of bioinks for urethral tissue constructs and provides general design rules for dynamic supramolecular hydrogels in extrusion bioprinting.

ACKNOWLEDGEMENTS: This research was funded by the European Union's Horizon Europe programme (STRONG-UR, grant agreement No 101191695). Views and opinions expressed are however those of the author(s) only and do not necessarily reflect those of the European Union or HaDEA. Neither the European Union nor the granting authority can be held responsible for them.

54. Dual-Energy–Assisted Material Segmentation in Contrast-Enhanced Micro-CT Imaging

T. Hildebrand[1], P. Moonen[2,3]

[1] Department of Biomaterials, Institute of Clinical Dentistry, Faculty of Dentistry, University of Oslo, NO; [2] Université de Pau et des Pays de l'Adour, E2S-UPPA, CNRS, LFCR, Pau, FR; [3] Université de Pau et des Pays de l'Adour, E2S-UPPA, CNRS, DMEX, Pau, FR

INTRODUCTION: Micro-computed tomography (micro-CT) enables three-dimensional imaging of biological samples but is limited in soft tissue visualization when relying solely on X-ray absorption. Contrast-enhanced micro-CT improves soft tissue contrast using heavy metal-based contrast agents, such as iodine [1]. However, segmentation remains challenging due to overlapping material attenuation. Dual-energy micro-CT provides additional energy-dependent attenuation information that enhances material discrimination and iodine-specific segmentation. This study investigates the distribution of iodine in rabbit bone and adjacent soft tissues during paraffin embedding to demonstrate enhanced segmentation using dual-energy–assisted contrast-enhanced micro-CT.

METHODS: Cylindrical femoral samples containing cartilage and bone marrow were harvested from 5-month-old New Zealand rabbits (N=10), fixed in 4% PFA, and decalcified in EDTA. Samples were either stored in PBS or contrast-enhanced with 1.5% Lugol's iodine, followed by ethanol dehydration and paraffin embedding. Spectral, dual-energy, and high-resolution micro-CT were performed to assess iodine distribution across different preparation states. Energy-dependent attenuation and clustering-based segmentation were applied, with classical histology used for validation.

RESULTS: Dual-energy micro-CT parameters were guided by spectral micro-CT pretests that provided iodine-specific attenuation information in selected planes. Although water-based Lugol's iodine was expected to improve contrast in laboratory dual-energy micro-CT, the resulting 3D datasets showed increased noise compared to spectral tomography. In contrast, paraffin-embedded samples exhibited reduced noise, enabling more robust material separation and improved segmentation despite a more confined iodine distribution. Surrounding materials were consistently separated in dual-energy grey-value space across all conditions.

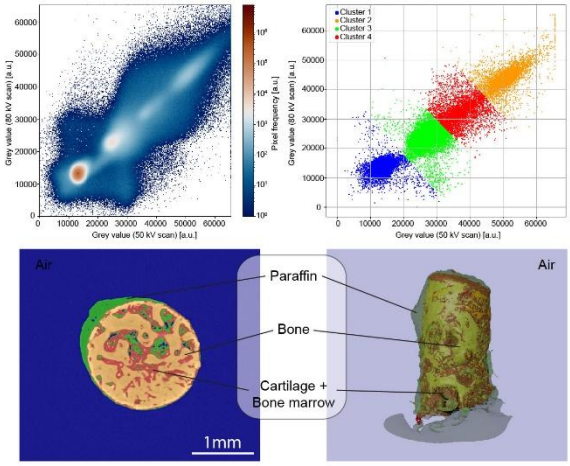

Fig. 1: Dual-energy–assisted segmentation of background (air), paraffin, bone, cartilage and bone marrow after iodine treatment.

DISCUSSION & CONCLUSIONS: Dual-energy–assisted contrast-enhanced micro-CT enabled reliable material segmentation across different preparation states, with paraffin embedding improving noise characteristics and segmentation stability in laboratory-based imaging. This approach allows non-destructive analysis of soft tissues and material interfaces while remaining compatible with standard histological workflows, making it a promising tool for advanced biomaterials characterization.

ACKNOWLEDGEMENTS: The authors gratefully acknowledge the staff at DMEX (Pau) for support during the spectral micro-CT measurements. Financial support enabling this work and the associated research visit was kindly provided by Håvard J. Haugen. The authors also thank Qianli Ma for assistance with sample acquisition.

REFERENCES: [1] Metscher BD. MicroCT for developmental biology. Dev Dyn. 2009.

55. Cobalt-containing hydroxyapatite as a new potential bone substitute material – synthesis and physicochemical characterization

W Gregorowicz[1,2], Ł. Pajchel[1], J. Kolmas[1]

[1] Department of Pharmaceutical Chemistry and Biomaterials, Faculty of Pharmacy, Medical University of Warsaw, [2]Students Scientific Group NANODRUG, Faculty of Pharmacy, Medical University of Warsaw

INTRODUCTION:

Hydroxyapatite (HA; $Ca_{10}(PO_4)_6(OH)_2$) is a well-known calcium phosphate widely used in regenerative biomaterials. In this work, cobalt was introduced into the hydroxyapatite HA structure by partially substituting Ca^{2+} ions. The resulting materials were extensively characterized and evaluated as bioactive HA-based biomaterials. Their potential to support bone tissue regeneration and formation is attributed to the pro-angiogenic effects of Co^{2+} ions [1]. The materials were synthesized via a wet-chemical route under controlled pH and temperature, yielding a series of samples with systematically varied cobalt incorporation levels, expressed as the molar fraction of cobalt substituting for calcium in the HA structure (x = 0.05; 0.1; 0.2 and 0.4) [2].

METHODS:

The powders were characterized by FT-IR and Raman spectroscopy to identify the main functional groups. Powder X-ray diffraction (PXRD) was used to determine the crystalline phases and their crystallinity. The elemental composition, including cobalt content, was measured by atomic absorption spectroscopy (AAS), while particle morphology and elemental distribution were studied using scanning electron microscopy (SEM). The morphology of the crystals was further investigated using transmission electron microscopy (TEM). Cytotoxicity tests were additionally carried out to assess the safety of these materials for potential biomedical use.

RESULTS:

The results show that this synthesis route produces homogeneous products with high chemical purity. Importantly, despite cobalt introduction, the materials obtained across the investigated concentration range are still hydroxyapatites, with cobalt incorporated into the HA structure rather than forming separate unwanted phases. Introducing Co^{2+} in the investigated range, modifies the crystal structure but does not induce cytotoxic effects, as confirmed by MTT and NRU cell viability assays.

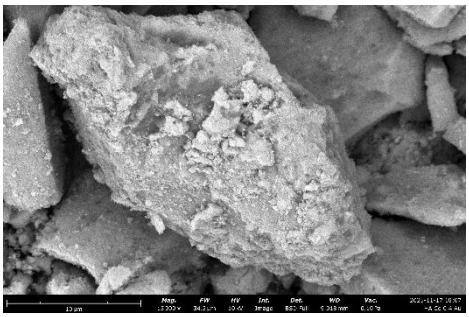

Fig. 1: Morphology of Co-doped hydroxyapatite powder (HA–Co 0.4) observed by SEM (15,000×, 10 kV)

DISCUSSION & CONCLUSIONS:

Results demonstrate that the proposed synthesis approach enables effective cobalt incorporation into hydroxyapatite and reliable tuning of its physicochemical properties within the investigated range. Importantly, this modification did not compromise basic in-vitro safety under the tested conditions. The obtained results show that it is possible to obtain HA-based biomaterials which could potentially serve not only as a bone-substitute scaffold but also as an active platform capable of modulating biological processes. Nevertheless, further in-depth studies in relevant biological systems are required to fully elucidate the impact of cobalt incorporation on bone healing and regeneration.

ACKNOWLEDGEMENTS:

Studies were supported by the National Science Center (Opus UMO-2023/51/B/NZ7/00555)

REFERENCES:

[1] Gregorowicz, W.; Pajchel, L. The Role of Cobalt Ions in Angiogenesis—A Review. *Int. J. Mol. Sci.* 2025, *26*, 7236.

[2] Kolmas, J.; et al. Magnesium Ion Substitution in Various Calcium Phosphates: A Way towards Bone Regeneration. Ceramics International 2025, 51, 1153–1160

56. BACTERIAL CELLULOSE AND KERATIN REINFORCED PAM HYDROGELS FOR DYE REMOVAL

Yu-Wen Tsai[1#], Prompong Khamwongsa[2#], Xuan-Ting Chen[1], Yu-Shan Lin[1], Zheng-Jie Lee[1], Sarute Ummartyotin[2*] and Yang Wei[1*]

[1]*Department of Chemical Engineering & Biotechnology, National Taipei University of Technology, Taipei, 10608, Taiwan.*

[2]*Department of Materials and Textile Technology, Faculty of Science and Technology, Thammasat University, Patumtani, 12120, Thailand.*

INTRODUCTION: Hydrogels are widely studied for wastewater treatment due to their high water affinity and tunable porous structures. However, conventional polyacrylamide (PAM) hydrogels often suffer from limited mechanical stability and insufficient adsorption selectivity. To address these limitations, this study develops a sustainable composite hydrogel reinforced with bacterial cellulose (BC) extracted from *Nata de coco* and keratin intermediate filaments (KIF) recycled from human hair, aiming to improve structural stability and dye removal performance [1].

METHODS: Composite hydrogels were prepared by incorporating BC and varying contents of KIF (0–2 wt%) into a crosslinked PAM network. The resulting hydrogels were characterized by FTIR spectroscopy, scanning electron microscopy, swelling behavior, porosity, compressive strength, and point of zero charge (PZC). Batch adsorption experiments were conducted using methylene blue (MB, cationic) and methyl orange (MO, anionic) dyes under different pH conditions to evaluate adsorption capacity, selectivity, and adsorption mechanisms.

RESULTS: Figure 1 summarizes the hydrogel design concept, sustainable raw materials, and macroscopic appearance of BC/KIF/PAM composites prior to structural and adsorption characterization.

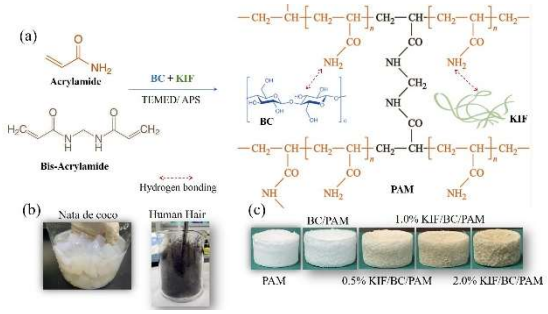

Fig. 1. BC/KIF/PAM hydrogel: formation, raw materials, and hydrogel samples.

Incorporation of BC and KIF reduced swelling while enhancing structural integrity and mechanical stability of PAM hydrogels. As shown in Fig. 2, dye adsorption exhibited clear pH-dependent behavior: adsorption of anionic MO correlated positively with swelling under acidic conditions (pH 3), whereas adsorption of cationic MB increased with decreasing swelling under basic conditions (pH 10), reaching ~60 mg/g for 2.0% KIF hydrogels, indicating enhanced and selective MB adsorption with increasing KIF content.

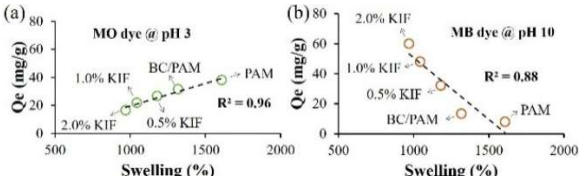

Fig. 2: Correlations between swelling ratio and dye adsorption capacity for MO at pH 3 (a) and MB at pH 10 (b) in BC/KIF/PAM hydrogels.

DISCUSSION & CONCLUSIONS: BC and KIF effectively reinforced PAM hydrogels, improving structural stability while enabling pH-dependent and selective dye adsorption. The reduced swelling and enhanced MB uptake at higher KIF contents highlight the role of keratin in promoting selective cationic dye removal, whereas limited MO adsorption confirms charge-dependent selectivity. These sustainable BC/KIF/PAM hydrogels demonstrate potential as tunable adsorbents for wastewater treatment applications.

ACKNOWLEDGEMENTS: This study was supported by a National Taipei University of Technology-Thammasat University Joint Research Program (NTUT-TU Joint Research Program NTUT-TU-113-03).

REFERENCES: [1] Tai, Y.-W. et al. Bacterial cellulose and keratin reinforced PAM hydrogels for dye removal. *Int. J. Biol. Macromol.* **308** (2025) 142458.

57. Biopolymer Hydrogels for Active Wound Healing

Z.¥íchová, S. Káčerová, O. Vašíček, J. Vícha, P. Humpolíček

Centre of Polymer Systems, Tomas Bata University in Zlín, Czech Republic

INTRODUCTION: Modern wound dressings are expected not only to protect injured tissue, but also to actively support all phases of the healing process, including inflammation control, cell proliferation, and tissue remodeling. Conductive hydrogels based on biopolymers represent a promising class of materials due to their ability to combine biocompatibility with bioactive and electroactive functions. In this study, composite hydrogels based on water-soluble partially re-acetylated chitosan and dialdehyde cellulose were developed and functionalized with polypyrrole nanoparticles to obtain multifunctional materials suitable for wound healing applications.

METHODS: Partially re-acetylated chitosan soluble at physiological pH was used as the main polymer matrix, while dialdehyde cellulose served simultaneously as a crosslinking agent and as a macromolecular anchor for pre-synthesized polypyrrole colloids. Hydrogels with different polypyrrole contents were prepared by simple blending followed by cast-drying. The materials were characterized in terms of chemical structure, morphology, viscoelastic behavior, swelling, and electrical conductivity. Biological performance was assessed in vitro using cytotoxicity, cell proliferation, migration, skin irritation, antioxidant activity, immunomodulatory response of macrophages and neutrophils, and antibacterial activity against *Escherichia coli* and *Staphylococcus aureus*.

RESULTS: The formation of a stable hydrogel network with uniformly distributed polypyrrole particles was confirmed, without particle aggregation or leaching. Covalent bonding between dialdehyde cellulose and polypyrrole significantly enhanced the mechanical integrity and allowed precise control over the conductive phase content. The prepared hydrogels exhibited conductivity values comparable to soft biological tissues and showed no cytotoxic or irritating effects. In vitro assays demonstrated enhanced cell migration (Fig. 1), effective scavenging of reactive oxygen species, modulation of inflammatory mediators, and pronounced antibacterial activity, particularly against *S. aureus*. The presence of polypyrrole substantially improved the overall biological performance of the materials compared to non-conductive reference hydrogels.

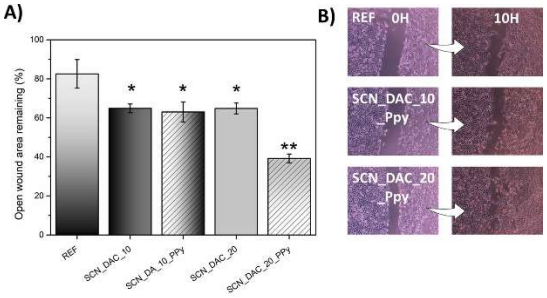

Fig. 1: All hydrogels accelerated wound healing in NIH/3T3 cells compared to the reference. The highest addition of PPy promoted wound healing most effectively by leaving only 39% of the wound area open after 10 hours.

DISCUSSION & CONCLUSIONS: The developed chitosan-based composite hydrogels combine conductivity, antibacterial action, antioxidant capacity, and immunomodulatory effects in a single biocompatible system. The use of dialdehyde cellulose as a multifunctional and low-toxicity component enables a sustainable synthesis route without the need for acidic conditions or toxic crosslinkers. These properties make the presented hydrogels strong candidates for next-generation active wound dressings with tunable physical and biological characteristics.

ACKNOWLEDGEMENTS: This work was supported by the Czech Science Foundation project 24-11534S and by the Ministry of Education, Youth and Sports of the Czech Republic – DKRVO (RP/CPS/2024-28/001).

REFERENCES: Káčerová, Simona, et al. "Chitosan/dialdehyde cellulose hydrogels with covalently anchored polypyrrole: Novel conductive, antibacterial, antioxidant, immunomodulatory, and anti-inflammatory materials." Carbohydrate polymers 327 (2024): 121640. Káčerová, Simona, et al. "Biocompatibility of colloidal polypyrrole." Colloids and Surfaces B: Biointerfaces 232 (2023): 113605.

58. Evaluation of hydrogel wound dressing with covalently immobilized antimicrobial peptides for prevention of surgical site infection

Zeljana Sotra[1,2], Edvin Blomstrand[3], Annika Starkenberg[1], Johan P.E. Junker[1,2], Martin Andersson[4,5]

[1] Experimental Plastic Surgery, Department of Biomedical and Clinical Sciences, Linköping University, Linköping, Sweden, [2] Center for Disaster Medicine and Traumatology, Linköping University Hospital, Linköping, Sweden, [3] Amferia AB, Astra Zeneca BioVentureHub c/o Astra Zeneca, Mölndal, Sweden,

[4] Department of Chemistry and Chemical Engineering, Chalmers University of Technology, Göteborg, Sweden, [5] Centre for Antibiotic Resistance Research in Gotheburg (CARe), Gothenburg, Sweden

INTRODUCTION: Surgical site infection (SSI) occurs in roughly 3% of all surgical wounds. These events increase patient suffering, leading to prolonged hospital stay, antibiotic overuse and higher mortality rates. Our study aims to evaluate prevention of SSIs by covalently binding antimicrobial peptides (AMPs) to soft amphiphilic hydrogel dressings. Covalent attachment increases peptide stability and ensures no release of peptides into the wound environment, decreasing toxicity and risk of resistance development.

METHODS: A porcine *in vivo* contaminated wound model was used to evaluate antimicrobial efficacy of the dressing (Regional Animal Ethics Board approval: ID1418), by closely mimicking the development of surgical site infections. Skin was antiseptically prepared with ethanol and iodine prior to contamination with 10^4 colony forming units (CFU)/ml *Staphylococcus aureus* (ATCC 29213). Circular 10 mm Ø partial-thickness wounds were created and treated with either AMP-functionalized hydrogel dressings or commercially available dialkylcarbamoyl chloride (DACC) coated foam dressings for a total of 7 days. Dressings were placed on wounds on day 0 and changed on days 2 and 4. Biopsies were obtained on days 2, 4 and 7. Tissue infection was determined by quantitative bacterial cultures and immunofluorescent (IF) staining. Re-epithelialization was evaluated with routine histology on paraffin-embedded tissue biopsies.

RESULTS: Quantitative cultures revealed an inhibition of wound contamination during the first two days. A slight, however non-significant, reduction of bacterial load was evident on days 4 and 7 on wounds treated with AMP-functionalized hydrogels in comparison to the control. IF stainings corroborated these findings.

Interestingly, despite the wound bioburden, histology showed significantly higher re-epithelialization in wounds treated with AMP-functionalized hydrogels at the end of treatment. Moreover, the hydrogels promoted significant wound contraction over the treatment period compared to the control.

DISCUSSION & CONCLUSIONS: The findings suggest that covalent immobilization of AMPs onto hydrogel wound dressing could potentially prevent surgical site infection. Moreover, the structure of the soft amphiphilic hydrogel, providing both high water content and high adsorption, facilitated early wound healing. Further studies are warranted to explore long-term healing outcomes across various wound types.

ACKNOWLEDGEMENTS: This template was modified with kind permission from eCM conferences Open Access online periodical & eCM annual conferences.

59. Development of Hepatic Stellate Cell-Targeted Trimethyl Chitosan Nanocapsules for the Delivery of Anti-Fibrotic MicroRNA as A Treatment for Liver Fibrosis

YC. Chang[1], PF. Huang[2], KC Yang[3], YY. Lin[1]

[1]Genome and Systems Biology Degree Program, National Taiwan University and Academia Sinica, Taipei, Taiwan, [2]Department of Materials Science and Engineering, National Taiwan University of Science and Technology, Taipei, Taiwan, [3]Department of Dental Technology, Taipei Medical University, Taipei, Taiwan

INTRODUCTION: Liver fibrosis is a chronic and progressive condition triggered by ongoing injury and improper repair, leading to excessive extracellular matrix (ECM) deposition and structural remodeling, which can ultimately progress to cirrhosis and liver failure [(1)]. Activation of hepatic stellate cells (HSCs) is a critical factor in fibrogenesis, suggesting that microRNA (miRNA)-based therapies targeting HSCs could be a promising approach to modulating fibrosis-related pathways [(2)]. Systemic delivery of miRNA is challenging due to poor stability in circulation and insufficient accumulation in target cells. Accordingly, we developed an HSC-targeted nanocarrier platform for anti-fibrotic miRNA delivery to enhance cellular uptake and improve therapeutic potential for liver fibrosis.

METHODS: Trimethyl chitosan (TMC) was synthesized through the chemical modification of chitosan and used as the main polymeric carrier [(3)]. To enhance cell-specific targeting and reduce off-target effects, the HSC-targeted protein was conjugated to the surface of TMC nanoparticles (NPs). An activated HSC (aHSC) model was utilized to assess NP uptake, cytocompatibility, and the ability of anti-fibrotic miRNA delivery to modulate fibrotic gene expression and protein production.

RESULTS: The confirmation of successful TMC synthesis was achieved through analyses using NMR and FTIR. Subsequent assessments utilizing Zetasizer revealed that the synthesized TMC NPs possessed an appropriate size distribution and a positively charged surface, characteristics that enhance their suitability for cellular engraftment applications. Encapsulating miRNA within TMC NPs did not adversely affect their physicochemical properties, thereby maintaining NP integrity and functionality. The conjugation of HSC-targeted protein to TMC NPs was confirmed by FTIR analysis, which showed successful grafting. The resulting HSC-targeted protein-modified TMC NPs exhibited good biocompatibility. The HSC-targeted protein-modified TMC NPs effectively targeted aHSCs. Notably, delivery of anti-fibrotic miRNA to aHSCs using HSC-targeted protein-TMC NPs downregulated fibrotic mRNA expression and the corresponding protein products.

DISCUSSION: This study established a TMC NP platform for targeted delivery of miRNA to cells. By grafting HSC-targeted protein onto the TMC NPs, we enhanced the specific targeting of aHSCs. In vitro experiments showed that transfecting aHSCs with anti-fibrotic miRNA using HSC-targeted protein-TMC NPs reduced fibrotic characteristics, indicating the therapeutic potential of these NPs for treating liver fibrosis. Further in vivo evaluations will be conducted using histological staining, fluorescence-based biodistribution imaging, and biochemical assays to investigate the potential antifibrotic effects.

ACKNOWLEDGEMENTS: This study was supported by the National Science and Technology Council (NSTC 114-2311-B-002-004 and NSTC 114-2221-E-038-017).

REFERENCES:

1. J Clin Invest. 2005; 115(2): 209-218.
2. Pharm Res. 2015; 32(2): 341-61.
3. Carbohydr. Polym. 1998; 36(2-3): 157-165.

60. Evaluation of Tazarotene Using an IL-1β-Induced Chondrocyte Hydrogel Model of Osteoarthritis

H. Hamzehpour[1], G. Boretti[2], Ó.E. Sigurjónsson[2], H. Jónsson and B.S. Snorradóttir[1]

[1]Faculty of Pharmaceutical Sciences, University of Iceland, Reykjavik, Iceland, [2]School of Science and Engineering, Reykjavik University, Reykjavik, Iceland, [3]Faculty of Medicine, University of Iceland, 107 Reykjavik, Iceland

INTRODUCTION: Hand osteoarthritis (HOA) is a degenerative joint disease characterized by cartilage degradation, inflammation, pain, and reduced joint function.[1] Because articular cartilage has limited capacity for self-repair, current treatments primarily address symptoms rather than the underlying pathology.[2] Three-dimensional (3D) bioprinting combined with hydrogel-based bioinks offers a promising approach for developing physiologically relevant *in vitro* cartilage models that can be used to evaluate potential therapeutics like tazarotene.

METHODS: A gelatin-based cartilage bioink (GelXA Cartilage, CELLINK) was used to fabricate cell-laden constructs. The C20A4 human chondrocyte cell line was expanded and suspended in the bioink prior to extrusion-based printing to form three dimensional constructs. Printed structures were stabilized using a dual crosslinking approach consisting of photo-crosslinking followed by ionic crosslinking in $CaCl_2$ solution.

To induce an osteoarthritis-like inflammatory environment, constructs were treated with IL-1β at concentrations of 2.5 and 5 ng/mL. The anti-inflammatory effects of tazarotene were then evaluated at concentrations of 25 μM and 50 μM and compared to untreated controls. Cell viability was assessed using Live/Dead staining, while inflammatory responses were quantified by ELISA analysis of pro-inflammatory cytokines TNF-α and IL-6. The experiment was subsequently repeated using primary chondrocytes isolated from patients with HOA to confirm the translational relevance of the model.

RESULTS: Inflammatory stimulation with IL-1β successfully induced an osteoarthritis-like phenotype characterized by increased secretion of inflammatory cytokines. Treatment with tazarotene resulted in decreased levels of TNF-α and IL-6 compared with untreated controls, indicating a reduction in inflammatory signalling. A dose-dependent relationship was observed, with the higher concentration of tazarotene producing a stronger reduction in inflammatory markers.

These findings were reproduced in constructs using primary HOA chondrocytes, further supporting the validity of the model. Live/dead assay results demonstrated good cell viability, with no observable cytotoxic effects of tazarotene.

DISCUSSION & CONCLUSIONS: This study demonstrates the feasibility of using a gelatin-based cartilage bioink and extrusion-based 3D bioprinting to generate viable chondrocyte-laden constructs for evaluating therapeutics targeting osteoarthritis-related inflammation. The model enabled assessment of the anti-inflammatory effects of tazarotene, with results indicating a dose-dependent reduction in pro-inflammatory cytokine release, suggesting potential therapeutic relevance in osteoarthritis.

Overall, the 3D bioprinted cartilage model represents a promising platform for investigating disease mechanisms and screening candidate therapeutics for osteoarthritis. Future work will include gene expression analysis to further elucidate the molecular pathways underlying the observed anti-inflammatory responses.

ACKNOWLEDGEMENTS: This research was partially funded by the Technology Development Fund, grant number 2215525-0611.

REFERENCES:

1. Kloppenburg & Kwok, Nat Rev Rheumatol, 2012, 8:22–31.

2. Kroon et al., RMD Open, 2018, 4:e000734.